4-2016

Influence of the 3D microenvironment on glioblastoma migration and drug response

Ruth Marisol Herrera Perez
Purdue University

PURDUE UNIVERSITY
GRADUATE SCHOOL
Thesis/Dissertation Acceptance

This is to certify that the thesis/dissertation prepared

By Ruth Marisol Herrera Perez

Entitled
INFLUENCE OF THE 3D MICROENVIRONMENT ON GLIOBLASTOMA MIGRATION AND DRUG RESPONSE

For the degree of Doctor of Philosophy

Is approved by the final examining committee:

Jenna Rickus Chair	Karen Pollok
Sherry Voytik-Harbin	
Kari Clase	
Robin Bentley	

To the best of my knowledge and as understood by the student in the Thesis/Dissertation Agreement, Publication Delay, and Certification Disclaimer (Graduate School Form 32), this thesis/dissertation adheres to the provisions of Purdue University's "Policy of Integrity in Research" and the use of copyright material.

Approved by Major Professor(s): JENNA RICKUS

Approved by: Bernand Engel 04/25/16

Head of the Departmental Graduate Program Date

INFLUENCE OF THE 3D MICROENVIRONMENT ON GLIOBLASTOMA MIGRATION AND DRUG RESPONSE

A Dissertation

Submitted to the Faculty

of

Purdue University

by

Ruth Marisol Herrera Perez

In Partial Fulfillment of the

Requirements for the Degree

of

Doctor of Philosophy

May 2016

Purdue University

West Lafayette, Indiana

To Jairo and Clemita

ACKNOWLEDGEMENTS

First, I am greatly thankful to my advisor Professor Jenna Rickus for all her support in every single aspect of my professional and personal development. Thanks for allowing me to try new research approaches and for believing in my capabilities for accomplishing new goals.

Thanks to professor Sherry Harbin for all her guidance and insight about tissue engineering and 3D culture. Her passion and excitement for research inspired me countless times during these years.

To Professor Karen Pollok and the Brain Tumor Research group. They welcomed me into the field of glioblastoma and always provided me great advice and new perspectives to approach my own research. The opportunity to attend the group monthly meetings helped me every time to remind myself how much I like what I do.

Thanks to Dr. Timothy Bentley for always sharing with us his knowledge about brain tumors and to Prof. Kari Clase for valuable research discussions and advice.

Understanding cancer from more a biological perspective was possible thanks to Professor Melissa Fishel. Her rigorous eye and questions made me think hard and allowed me to expand my skills to new research areas.

For my first experiments in glioma cell culture I thank Tarun Madangopal and Jing Lu. From them I also learned thorough lab techniques, multiple ways to approach my research needs and a good sense of practicality for trouble-shooting.

At the same time that I joined the Rickus lab so did Jen Kahn and Leyla K. Jen's attention to details was fundamental to help me improve presentations and written documents. And Leyla, who has shared with me the cyclic happiness of research, has been motivational not only for her courage exploring new things in the lab but also for being one of the most skilled experimentalist that I know.

I am also very grateful to Soo Ha and Yi Li who always kept my spirit up and were always available for a nice conversation and science discussion.

For my initiation in 3D cell culture I thank Rucha Joshi, who patiently taught me every single detail of collagen preparation and was always willing to discuss with me both, research issues and life experiences.

Exciting discussions about integrins and extracellular matrices were possible thanks to Nimisha Bajaj. She was also my default consultant to solve many lab challenges and one of the people that I always enjoyed having a conversation with, especially in Spanish.

I also thank Kevin Buno for sharing with me his techniques to get such beautiful 3D vasculature networks and immunofluorescence images as well as for enjoyable conversations about life and research while doing confocal microscopy.

Special thanks also to Joon Park, Rachel Morrison, James Nolan, Priya Prakash, and Cynthia Alvarado for insightful discussions and contributions to my research.

This work was possible as well thanks to all the good energy of my family.

And finally, thanks to Jairo for always inspiring me to explore my research from different scientific perspectives, for sharing with me this journey and for being my motivation, happiness, and constant support.

TABLE OF CONTENTS

Page

Page

Page

Page

LIST OF TABLES

LIST OF FIGURES

Figure Page

Figure Page

ABSTRACT

Herrera-Perez, Ruth M. PhD, Purdue University, May 2016. Influence of the 3D Microenvironment on Glioblastoma Migration and Drug Response. Major Professor: Jenna L. Rickus, Department of Agricultural and Biological Engineering.

Glioblastoma (GBM) is a highly invasive brain cancer characterized by poor prognosis. Despite significant efforts by the basic and clinical research community our understanding of GBM progression and recurrence has been incremental. Improvements in therapeutic response have been dismal, and GBM continues to be the deadliest tumor of the central nervous system, with patient average survival rate of 12 months. Synergistic relationships that the tumor cells establish with the brain microenvironment have been proven fundamental for successful tumor progression and maintenance. Yet, many *in vitro* GBM studies are performed in formats that fail to recapitulate the most essential component of the tumor microenvironment.

In this work we aim to describe the influence of multiple features of the tumor microenvironment on GBM migration characteristics and response to drug treatment. Our approach involved the development of a 3D *in vitro* tissue model that recapitulates the cellular, chemical and mechanical features of brain microenvironment. To assess the influence of the physical properties of the extracellular matrix (ECM) on GBM migration

we developed a matrix of hyaluronan supported by collagen with embedded microfibers to simulate the composition of brain ECM and the topographical cues of vasculature. Comparison of this model with Matrigel and collagen type-I showed that GBM exhibits different migration modes such as collective expansion, multicellular strands, and single cell migration as a response to the ECM composition and stiffness. Further incorporation of brain stromal cells as astrocytes and endothelial cells into the model showed that presence of astrocytes increased the migration of all GBM cell lines studied, however presence of endothelial cells only increased the migration of glioblastoma stem-like cells. Evaluation of the cytotoxic effect of multiple drugs on GBM was performed using our 3D model. Presence of extracellular matrix and stromal cells reduced the sensitivity of stem-like GBM cells to drug treatments. Our specific focus was on anti-STAT3 therapy and data obtained in the 3D model showed that the microenvironment regulates STAT3 activation as well as response to STAT3 drug targeting.

This work supports the fundamental role of the 3D-microenvironment as a modulator of GBM behavior and provides a consistent and tunable *in vitro* platform to be used in GBM studies for a more realistic understanding of *in vivo* cancer progression and response to therapy.

CHAPTER 1. INTRODUCTION

1.1 Objective

This thesis aims to contribute to the understanding of the tumor microenvironment as a modulator of glioblastoma migration and drug response. To this end, we sought to bridge conventional cancer cell culture and animal models by developing a tunable 3D platform that recapitulates *in vitro* the physical, compositional and cellular components of glioblastoma microenvironment. This model offers a more realistic platform to study in controlled fashion the influence of some components of the glioblastoma microenvironment on tumor migration and survival after chemotherapeutic treatment.

1.2 Motivation

Glioblastoma (GBM) is the most common type of glioma and the highest grade. GBM is the type of cancer that former American Society of Clinical Oncology president George Sledge labeled as "smart", due to the vast mutations acquired during progression, and the ability to rapidly invade healthy brain parenchyma.[1] Advances in medical treatments have demonstrated only minimal improvement of GBM patient's survival. Usually, less that 5% of the patients reach a 5-year survival milestone.[2] Tumor heterogeneity, resistance to treatment and diffuse infiltration into healthy tissue are the most relevant factors involved in GBM resistance to treatment. Such aggressive characteristics are closely connected to a synergistic relationship between the tumor cells and the microenvironment that allows GBM to successfully adapt, grow and invade,

Failure to include important features of the tumor environment in early *in vitro* studies is a significant consideration of why *in vitro* results are rarely translational to *in vivo* outcomes. A critical barrier in GBM studies is the lack of *in vitro* platforms that effectively represent the complexity offered by the microenvironment in terms of dimensionality, physical, and cellular properties. Most cancer studies are performed in liquid platforms that do not represent multi-cellular, microenvironment-mediated responses and have limited predictive capability. Although, xenograft models have been preferred in advanced studies to offer *in vivo* characteristics, their complexity limits systematic interrogation and obstructs studies at the cellular level.

Tissue engineering is an excellent tool that provides a multidisciplinary approach for *in vitro* GBM studies. The use of tunable matrices that closely represent the main characteristics of tumor microenvironment, such as the presence of the extracellular matrix and stromal cells in controlled contextual situations can provide excellent platforms to better understand GBM hallmarks such as invasion/migration, and drug resistance.

1.3 Thesis Overview

This work focused on developing and implementing a controllable 3D *in vitro* platform similar to the GBM microenvironment to bridge existent traditional models and offer deeper insights into the overall influence of components of the microenvironment such as extracellular matrix and presence of stromal cells on fundamental aspects of GBM such as survival, migration and drug response.

The tumor microenvironment is a fundamental contributor to tumor initiation, proliferation, resistance and metastasis and is comprised by three main components: the extracellular matrix, stromal cells and tumor cells. The engineered *in vitro* 3D model developed recapitulates the brain tumor microenvironment by incorporating cell-matrix and tumor cell-stromal cell interactions as well as biophysical clues from tumor niche. By using the model as a tool, we focused on the influence of two major components of tumor microenvironment, namely, the extracellular matrix and stromal cells on GBM migration and drug response. The transversal contributions result of this work that are individually summarized as four chapters 1) An introductory background on GBM and the importance

of the tumor microenvironment, 2) The role of the physical properties of the extracellular matrix (ECM) during glioma migration, 3) Influence of extracellular matrix and stromal cells presence on GBM drug-response, 4) Influence of dimensionality and presence of stromal cells on GBM migration and 5) The effect the 3D GBM microenvironment as a regulator of STAT3 activation and response to drug inhibition.

The first chapter presents introductory background remarks on the characteristics of GBM, the importance of migration as a characteristic feature of GBM, the importance of tumor microenvironment as a modulator of tumor progression and a brief overview of the advances in the development of *in vitro* models that mimic the GBM microenvironment.

The second chapter sheds light onto the regulation of GBM stem cell migration characteristics by different properties of 3D extracellular matrix (ECM) such as composition and stiffness. The brain ECM differs from other organs in composition and mechanical properties due to absence of rigid proteins and high presence of hyaluronan. Given the fundamental role migration on GBM relapse, we determined how stiffness, composition and topography of the ECM alter 3D-migration of GBM stem-like cells (GSCs). The results revealed that GSCs exhibit different migration modes such as collective expansion, multicellular strands, and single cell migration as a response to the ECM composition and stiffness. The development and evaluation of a model of brain-like ECM model showed that increasing concentrations of hyaluronan reduce migration and presence of structural cues induce changes in migration mode of GSCs, therefore confirming the migration plasticity of GSCs when facing a heterogeneous environment.

The third chapter describes the influence of the microenvironment on survival of GBM after drug treatment. We increased the complexity of our previously developed 3D model of the GBM extracellular matrix by incorporating brain stromal cells such as astrocytes and endothelial colony forming cells (ECFCs). The model was used as a predictor of therapeutic response in various patient-derived GBM cell lines. Presence of the 3D extracellular matrix decreased the cytotoxic effect of multiple drugs on GBM stem-like cells compared to liquid culture. Also, presence of stromal cells into the 3D model decreased the effect of single and combination drug treatment on GBM stem-like cells, however their presence did not influence the sensitivity of non-stem GBM cells to the same extent.

In the fourth chapter we determined the effect of presence of extracellular matrix and stromal cells such as astrocytes and endothelial cells on GBM migration. We concluded that presence of stromal cells in the 3D environment increases the migration of GBM stem-like cells. However, only astrocytes and not ECFCs increase the migration of non-stem GBM cells.

The last research contribution described in Chapter 5 investigates the effect of the 3D microenvironment on the basal activation of STAT3, a master regulator of multiple oncogenic processes, and on STAT3 inhibition by the small molecule SH-4-54. Preliminary results show that presence of the 3D ECM induces basal activation of STAT3 in GBM, including cell lines that did not show basal activation when cultured in liquid platform. Also, the presence of the 3D brain-like ECM influences the effectiveness of STAT3 drug inhibition on reducing GBM survival and migration.

1.4 Introductory Remarks on Glioblastoma and the Tumor Microenvironment

1.4.1 Characteristics of Glioblastoma

Glioblastoma (GBM) is a malignant astrocytoma grade IV that presents a poor prognosis and overall median survival of 15 months.[2] GBM is characterized by diffuse and rapid infiltration across healthy brain parenchyma, neovascularization of the neighboring microenvironment and presence of necrotic sections within the tumor mass.[3] Almost invariably GBM reappears in surrounding tissue after treatment by surgical resection, radiation, and chemotherapy. Advances in medical treatments have demonstrated only minimal improvement in GBM patient's survival with less than 5% of the patients reaching a 5-year survival milestone.[2]

A common characteristic of GBM tumors is the rapid neovascularization reached through paracrine signaling with vascular endothelial cells and in some cases through direct differentiation of GBM stem-like cells into vascular cells.[4–6] GBM tumors are also characterized by presence of a hypoxic niche as a result of rapid proliferation of tumor cells. Although the dual presence of a perivascular and hypoxic niche seem contradictory, hypoxic signals prompt vasculature formation, however rapid vascularization is achieved by formation of blood vessels that provide irregular oxygen supply to the tumor, where hypoxic sections arise.

The rapid infiltration into healthy tissue and heterogeneity of recurrent GBM have been directly related to the presence of a subpopulation of tumor cells with stem cell-like

features termed glioblastoma stem cells (GSCs). GSCs are classified as cells that reside in tumor mass and share characteristics with normal neural progenitors cells such as expression of stem markers (mainly CD133-prominin), self-renewal abilities, formation of neurospheres, and ability to differentiate into all cells of neural origin (astrocytes, neurons and oligodendrocytes).[7] Although the concept of GSCs has been debated mainly due to the lack of reliable set of markers, studies have demonstrated that GBM is one of several cancer types with a relative consistent presence of cancer stem cells.[8] As few as 100 GSCs $CD133^+$ have the ability to repopulate a complete new tumor after transplantation into a host.[9]

Given the tumor reappearance both, in the vicinity and in distant locations of the primary mass, it is hypothesized that GSCs have a high migratory ability and greater intrinsic mechanisms to resist and adapt to chemo- and radio therapy compared to non-stem GBM cells.[4,10] Moreover, the plasticity of GSCs to undergo genetic changes and differentiate into multiple lineages cells[4,6,11,12] is associated with the creation of a special niche that harbors this population and acts as a feedback loop to provide the conditions required for stemness maintenance. Normal neural stem cells reside mainly in specific locations of the brain as the subventricular zone (SVZ) and the subgranular zone, that provide direct contact with multiple cells required to support their niche, particularly, vascular networks and mesenchymal cells.[13] In a similar fashion, GSCs require specific features in their microenvironment.

1.4.2 Migration as a Hallmark of Glioblastoma

Malignant gliomas as GBM present diffuse and aggressive invasion of healthy brain tissue. GBM can successfully and rapidly invade any part of the brain, regardless of the distance to the primary tumor, yet, unlike other cancers rarely intravasates and metastasizes to other organs. The infrequent cases of extracranial metastasis are usually observed in lungs, liver, lymph nodes and bone marrow and are associated with surgical intervention of the primary mass such as biopsy and resection. Occurrence of GBM metastasis without prior surgical intervention in the patient has been reported, however these cases are extremely uncommon.

Successful and directional migration of GBM has been associated with the ability of the tumor cells to recapitulate some migratory features of neural cell progenitors during cortical development.[13,14] GBM preferentially migrates along preexisting tracks such as myelinated axons in the white matter and the basement membrane (BM) surrounding the vasculature as histopathological examination has shown.[14] This pattern of invasion suggests the presence of productive infiltration mechanisms mediated by the brain specific microenvironment that foster tumor expansion and are rarely present in other organs.

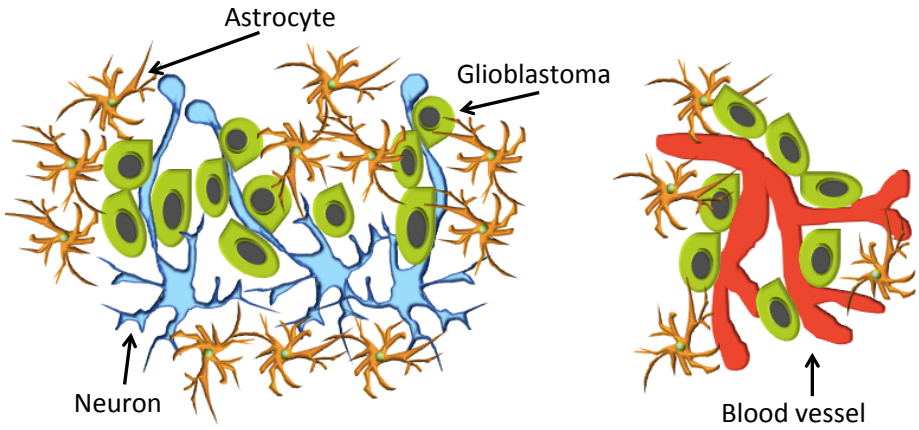

Figure 1.1 Main migration routes of glioblastoma (GBM) are axonal tracks and blood vessels

Cell migration requires a complex coordination of multiple processes that involve reciprocal signaling and communication with the microenvironment including the extracellular matrix, stromal cells and other components of the tumor mass. GBM directly remodels the microenvironment extracellular matrix by depositing glycosoaminoglycans, proteoglycans as well as other molecules that are not normally present in neural ECM. For instance, fibrillar collagen, absent in neural ECM has been detected in GBM both intra and extra-tumorally,[15,16] suggesting its deposition by tumor cells presumably to increase the stiffness of normal tissue as a way to facilitate migration. Similarly, the extracellular matrix of some high-grade gliomas such as GBM presents fibronectin, yet, similar to collagen; fibronectin is not a component of healthy brain ECM. Fibronectin deposition has been associated with increased activity transcription factor NF-kB in GBM cells through a process associated with uPA/uPAR activation[17] and associated with α5β1 integrin implicated in fibronectin fibrillogenesis.[18] Modification of

the extracellular matrix by glioma ultimately has the function of generating an environment more suited for the needs of the cancer cells such as migration and adhesion. Other components of the microenvironment such as stromal cells are also fundamental contributors of GBM migration. Paracrine signaling between tumor cells and stroma affect tumor migration, as has been thoroughly reviewed by Hoelzinger (2007) and Placone (2016). Additionally, recent studies have shown that microglia, the brain resident macrophages, contribute to tumor migration by both, increasing GBM expression of matrix metalloproteinases such as MMP-2[19] and secreting pro-inflammatory cytokine IL-18.[20] Secretion of glial-derived neurotrophic factor (GDNF)[21] and TGF-β by astrocytes triggered by interaction with tumor cells has also been shown to increase GBM migration.

Beyond the widely studied role of paracrine signaling GBM migration, physical contact between tumor and stroma also has a profound impact on the ability of tumor cells to successfully migrate. Physical interaction between tumor cells and vasculature in a process denominated vessel cooption is one of the earliest mechanism by which the tumor cells reach "vascular highways" to migrate. During co-option GBM cells target pericytes on the existing vessels by developing specialized protrusions called flectopodia. The physical communication established between the two cell populations is transient and occurs prior tumor neovascularization.[22] Similarly, increased expression of the gap junction protein connexin-43 in glioma cells has been linked to increased migration mediated by intercellular gap junction communication between the tumor and astrocytes as well as intercellular transference of microRNA-5096 and microRNA-4519, both implicated in tumor migration.[23,24]

The relationship between migration and microenvironment is reciprocal and dynamic. Along with interactions tumor-stroma and the effect of glioma on remodeling the extracellular matrix, the existing microenvironment also modulates the migration strategies adopted by cells. The adaption of cancer cell migration mode in response to different microenvironments has mainly been observed in 3D *in vitro* constructs. Observations of breast cancer cells switching from collective spheroids in basement membrane-like matrices to mesenchymal single migration in collagen matrices[25] or GSCs switching from single cell migration in collagen to a multicellular stream migration when faced with topographical clues that mimic blood vessels[26] are examples of the influence of the physical microenvironment on motility. Despite great advances understanding the influence of diverse physical cues on migration, how biological and physical factors interplay to determine a preferential migration strategy remains to be understood. Previous studies have linked the ECM properties like matrix elasticity with the polarization of regulators of cell migration such as Rho family GTPases. Petrie (2012) showed that elastic behavior of the ECM, induces specific polarization patterns of the Rho GTPases Rac1 and Cdc42 governed by RhoA, ROCK or myosin II activity.[27] Recently, Mertsch (2013, 2014)[28,29] showed that ROCK1 mediates substrate-dependent GBM migration and its inhibition decreases the ability of GBM to recognize different types of ECM and show preferences for specific ECMs to migrate.

The specific role of the multiple physical and chemical signals that the brain microenvironment provides to brain tumors (and vice versa) to trigger migration is still in

its infancy. However, elucidating such interactions is fundamental to understand the dynamics of brain cancer progression.

1.4.3 Role of the Tumor Microenvironment in Glioblastoma Progression

The influence of the microenvironment as a regulator of cell response has been increasingly recognized. Cell behavior is not only dependent of genetic instructions but is equally modeled by the external signals from the microenvironment. Specifically in cancer, such regulation reaches a higher level of complexity and reciprocity due to the active remodeling exerted by the cancer cells on the microenvironment. Cancer cells modify factors such as pH and nutrients availability and recruit supporting stromal cells[30] to recreate a new niche commonly referred as tumor microenvironment that works as a support network to foster tumor survival and resistance. Tumor microenvironment is comprised by three main components: tumor cells, extracellular matrix and surrounding stromal cells.

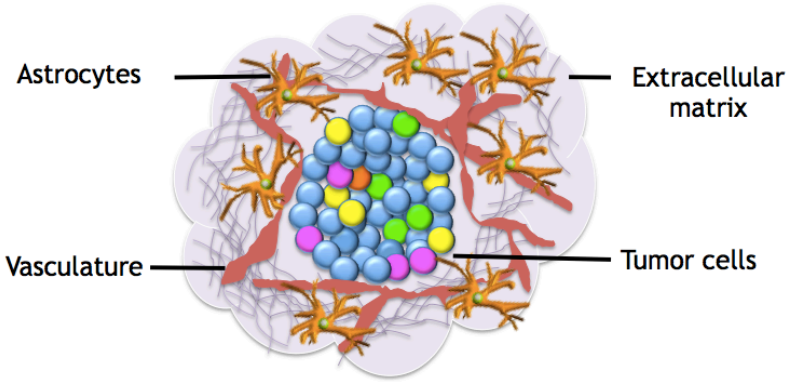

Figure 1.2 Components of the glioblastoma tumor microenvironment. Other cells native to brain tiusse and also associated to the tumor microenvironment such as oligodendrocytes, neurons, pericytes, microglia and others are not depicted.

The normal brain microenvironment presents distinctive characteristics compared to the majority of other tissues. Brain ECM is a low stiffness, loosely connected network mainly comprised of hyaluronan, a non-sulphated glycosoaminoglycan with high water-binding capacity, proteoglycans and Tenascin R and has no presence of rigid proteins such as type I collagen or fibronectin.[31] Other fundamental differences of brain microenvironment that contribute to the uniqueness of brain cancers as GBM are: the presence of a different immune defense comprised mainly by microglia, that is also recruited to help tumor survival,[32] and the existence of the blood brain barrier (BBB), formed by astrocytic end-feet lining the surface of the blood vessels, which prevents larger, hydrophilic or large molecules including chemotherapy agents to successfully reach the brain parenchyma.[33] Additional to the unique features of brain ECM, GBM dynamically remodels the native ECM to better suit the needs of the tumor during progression generating an extracellular matrix distinctive to the tumor that differs in composition and mechanical properties to the healthy brain ECM.

Stromal cells present on the surrounding or specifically recruited by the tumor are another important component of the tumor microenvironment and well-established modulators of cancer growth. One of the most studied stromal cells present in GBM microenvironment are endothelial cells, recruited by GBM to vascularize the tumor and contribute to both, maintenance and invasion.[4,7,34] Endothelial cells are recruited by GBM though a mechanism that involves the generation of a hypoxic niche, product of rapid and uncontrolled tumor proliferation, that releases proangiogenic signals and triggers the formation of new vasculature to supply the tumor.[35–37]New blood vessels present not only

a source of nutrients and oxygen but also a permissive route that guides migration and enhances the development of distant satellite tumors.

Likewise, astrocytes and microglia are important players during formation of GBM microenvironment. Astrocytes are the main non-neuronal cell of the brain and comprise nearly 50% of brain total volume.[38] Presence of GBM cells have shown to induce astrogliosis in astrocytes adjacent to the tumor,[38–40] by a process that recapitulates the astrocytic response to brain injury. Astrogliosis induced secretion of pro-inflammatory signals supports GBM migration and proliferation and acts as a protection barrier to immune surveillance, mainly by T-cells.[41]

Microglia are the immune cell residents of brain and account for nearly 10-20% of all the brain glia population. After injury or damage, microglia acquire an "activated phenotype" that corresponds to increase proliferation, migration, cytokine release and production of oxygen reactive species.[42] During formation of GBM microenvironment microglia heavily infiltrate the tumor mass and despite their role as macrophages do not contribute to reduce the tumor progression as it was initially hypothesized. Instead, an increasing number of studies suggest that microglia resident in the tumor microenvironment contribute to tumor maintenance and immune response suppression.[42] Tumor associated microglia can help ECM remodeling and tumor migration by secretion of matrix metalloproteinases and growth factors. Yet, tumor resident microglia have a reduced ability to induce anti-tumor T-cell response, likely due to tumor repression of microglia pro-immune processes as antigen presentation, phagocytosis inflammatory signals release.[42]

Finally, the third component of the tumor microenvironment are the tumor cells, and despite the plain relationship of tumor cells with the tumor microenvironment, is important to note that the heterogeneity of many GBM tumors and dynamic changes in tumor population are fundamental for the constant remodeling of the tumor microenvironment. The rapid development of new satellite tumors in GBM and resistant to treatment has directly related to the presence of a subpopulation of tumor cells with stem cell-like features termed glioblastoma stem cells (GSCs). GSCs are classified as cells from the tumor mass that share characteristics with normal neural stem cells such as expression of stem markers (mainly CD133-prominin), self-renewal abilities, formation of neurospheres, and ability to differentiate into all cells of neural origin (astrocytes, neurons or oligodendrocytes).[7] Although the concept of GSCs has been debated based on the lack of a reliable set of markers, studies have demonstrated that GBM is one of several cancer types with a relative consistent presence of cancer stem cells.[8] As few as 100 GSCs $CD133^+$ have the ability to repopulate a complete new tumor after transplantation into a host.[9]

Given the appearance of new tumors both, in the vicinity and in distant locations of the primary mass, it is hypothesized that GSCs have a high migratory ability and greater intrinsic mechanisms to resist and adapt to chemo- and radiotherapy compared to non-stem GBM cells.[4,10] Moreover, the plasticity of GSCs to undergo genetic changes and differentiate into multiple lineages cells[4,6,11,12] is associated with the creation of a special niches with the tumor microenvironment that harbor this population and acts as a feedback loop to provide the conditions required for stemness maintenance. In a similar fashion to neural stem progenitors, GSCs are thought to reside in locations similar to subventricular zone (SVZ) and the subgranular zone that provide direct contact with multiple cells required to support their niche, particularly, vascular networks and mesenchymal cells. [13]

GSCs require specific features in their microenvironment. A common characteristic of GBM tumors with presence of GSCs is the presence of a perivascular niche reached. Such vascular niche is product of the rapid neovascularization triggered by recruitment of vascular endothelial cells and in some cases by GSCs differentiation into vascular forming cells.[4–6] Tumor presenting GSCs also can contain a hypoxic niche as a result of rapid proliferation. Although the concomitant presence of a perivascular and hypoxic niche might seem contradictory, hypoxic signals prompt vasculature formation; yet, the rapid vascularization of the tumor results in leaking blood vessels and irregular oxygen supply giving rise to hypoxic sections within the tumor.

Given the reciprocal relationship between the tumor and its microenvironment, understanding GBM not as a sole aggregation of cells with certain genetic mutations but as a self-regulating entity comprised by multiple factors besides the tumor cells might offer new directions to target more effectively this disease.

1.4.4 3D *in vitro* Models of Glioblastoma Microenvironment

Regular studies of GBM are typically performed using 2D monolayer culture on surfaces such as glass or plastic, sometimes pretreated poly-l-lysine to increase cell adhesion or covered with a thin layer of collagen or laminin to incorporate certain components of the extracellular matrix during tumor culture. Studies using 2D liquid culture have contributed with seminal results in the overall understanding of GBM; yet, liquid culture has restricted versatility in terms of recapitulating the physiological features of the tumor microenvironment. One critical drawback of liquid culture to be used in tumor

microenvironment studies is the effect of a rigid planar surface on cell movement. First, because planar surfaces restrict the motility of cells to two dimensions and second, because allow the development of cell contacts with a substrate that much more rigidity and stiffness than any brain region. During 2D culture cells have a rapid and homogeneous accessibility to nutrients in the media. Contrastingly, in real tissues the presence of a 3D ECM generates a gradient of nutrients and oxygen that modulates tumor processes such as proliferation and recruitment of stromal cells.

Motivated by the need of better models to recapitulate the physiological conditions of GBM microenvironment, various authors have approached the generation of 3D culture platforms to recapitulate *in vitro* the GBM microenvironment. However, most of these studies have focused solely on the interaction glioma-ECM overlooking the importance of tumor-stroma interactions.

Diverse approaches have been developed to better simulate the tumor and tumor microenvironment, and can be classified into two main groups: scaffold-based and spheroid liquid-based 3D models. Controversy exists as to which recapitulates more precisely *in vivo* settings; yet, both approaches have advantages and disadvantages depending on the type of study performed. A combination of both, spheroids in scaffold-based platforms seem to be one of the best approaches, but can difficult the convenience for high-throughput studies.

Initial studies of GBM in 3D platforms were performed in collagen I or Matrigel matrices, however, a main drawback of in these models was the lack of similar composition to the extracellular matrix of glioma tumors as this is mainly comprised by hyaluronan. To

incorporate hyaluronan, Ananthanarayanan (2011)[43] and Pedron (2013)[44] developed chemically functionalized hyaluronan (HA) matrices to study GBM. Their data reflect similar responses to *in vivo* studies; yet, to achieve a crosslinking matrix, hyaluronan needs to be chemically modified and such modifications naturally absent *in vivo* can alter tumor-ECM interaction. Similarly, as a attempt to better recapitulate the presence of hyaluronan in glioma 3D models, Yang (2011)[45] and Rao (2013)[46] generated collagen-HA matrices, however, these studies used pepsin-treated collagen, a collagen that have lost the collagen telopeptides required to form covalent crosslinks and therefore does not reflect the architecture and mechanical properties of *in vivo* structures.[45–47]

New approaches to better mimic GBM microenvironment need to be developed. The work presented here aims to contribute to the field by introducing a tunable 3D model that recapitulates the composition of the GBM microenvironment and also incorporates stromal cell populations to generate a model physiologically more relevant for *in vitro* studies.

Still, many challenges lie ahead in order to have a better approximation the *in vivo* tumor microenvironment. Among the more relevant tasks is the incorporation of tissue compositional and physical heterogeneities present in different regions of the brain. Also, the ability to generate a model with similar cell density and number of cell types as the tumor microenvironment as well as cell-ECM ratio similar to native tissues. Currently, 3D matrices present limitations in the cell number possible to incorporate due the matrix retraction and deformation caused by cell forces. The use of spheroids within 3D ECM as structures dimensionally similar to the tumor mass has several advantages especially in

the formation of oxygen and nutrient gradients. Nevertheless, accurate assessment of metabolic rate and survival can be challenging in these models especially in the event of using these models as high-throughput platforms for drug analysis.

CHAPTER 2. GRATION OF GLIOBLASTOMA STEM CELLS IS MODULATED BY THE PROPERTIES OF THE EXTRACELLULAR MATRIX

2.1 Introduction

Glioblastoma (GBM) is a highly invasive and lethal brain cancer. GBM resistance, rapid growth and propagation have been linked to the presence of a subpopulation of tumor cells with stem cell-like features termed glioblastoma stem cells (GSCs).[8,48–52] Given the aggressiveness of GSCs, it has been hypothesized that these cells drive the invasion into healthy brain tissue and contribute to regrowth of a new heterogeneous tumor.

It is now well established that tumor cell invasion and maintenance of tumor stem cells are processes regulated by the microenvironment and involve specific interactions with the extracellular matrix (ECM).[53–55] Healthy brain ECM has a distinct composition relative to other tissues and organs. It represents a low stiffness, loosely connected network comprised mainly of hyaluronan.[31,56] In cases such as glioma development, tumor cells actively remodel their microenvironment by depositing its own ECM, including type-I collagen as a component of the tumor tissue, the surrounding peritumoral environment,[15] and the GSCs niche.[57] GBM can successfully invade any part of the brain, yet, unlike other cancers rarely metastasizes to other organs. During invasion, migratory GBM cells preferentially use existing tracks such as myelinated axons in the white

matter and basement membrane (BM) surrounding blood vessels.[14] Such specific invasion pattern suggests the existence of productive infiltration mechanisms mediated by the brain specific microenvironment that foster tumor expansion.[31,58]

Despite the well-known characteristics of brain microenvironment and glioma invasion routes, there is still a lack of understanding about the mechanistic migration processes exhibited by GBM cells and specifically by GSCs.[59] A critical barrier in the cancer field is that most of the invasion and migration studies are conducted using 2D substrates that fail to recapitulate the dimensionality, composition and physical properties of brain tissue.[60] Consequently, 3D *in vitro* models that mimic multiple features of the tumor microenvironment and allow the study of important cancer cell subpopulations such as GSCs, are required to complement *in vivo* models and histopathological analysis.

In this study we recreated the one of main features of the GBM microenvironment, the extracellular matrix, by developing a tunable 3D matrix with similar composition to GBM ECM with incorporated topographical tracks that simulate the brain vasculature, to study over time the migratory behavior of GSC neurospheres by using the GBAM1 ($CD133^{+}$) cell line. The composite matrix consisted of a hyaluronan network structurally supported by a customizable collagen-oligomer fibril matrix embedded with BM-coated microfibers to provide alternative migratory paths as occurs *in vivo*. For comparison, we generated reconstituted matrices from the most common 3D cell culture substrates, type-I collagen monomers and Matrigel. To account for differences in molecular composition and fibril-matrix formation capacity of different type-I collagen formulations, we

prepared matrices with diverse structural and mechanical properties using commercial monomeric collagen (BD Biosciences), atelocollagen and oligomeric collagen. We cultured the GSCs (GBAM1) neurospheres in the different matrices and monitor overtime how fundamental migratory behavior such as migration mode, velocity, maximum distance and morphology exhibited by GSC neurospheres was regulated by the compositional and physical properties of the different matrices.

2.2 Experimental Section

2.2.1 Maintenance of GBM cell line

GBM cells isolated from human surgical tumor specimens sorted by FACS for CD133 expression (GBAM1) were kindly provided by Dr. Phillip Tofilon and the Moffitt Cancer Center. GBAM1 cells were maintained in stem liquid media DMEM/F12 supplemented with B27 without vitamin A (Life Technologies, Carlsbad, CA) and with growth factors EGF, bFGF (50 ng/ml each, Peprotech, Rocky hill, NJ), at 37°C in an atmosphere of 5% CO_2. Cells were propagated in T25 or T75 flasks and fed with complete media every other day. Neurospheres were disaggregated with TrypLE (Life Technologies, Carlsbad, CA) and passaged every 7 days.

2.2.2 Synthesis of collagen matrix

3D collagen matrices were generated using rat tail type-I collagen monomers from BD Biosciences (San Jose, CA), pig skin type-I collagen oligomer,[61] and pig skin type-I atelocollagen. All collagens were adjusted to desired concentration and polymerized by

neutralization with 10X PBS (1X PBS has a 0.17M total ionic strength) and 0.1N sodium hydroxide to reach pH 7.4. During and after neutralization all reagents were maintained at 4°C, the neutralized collagen solutions were pipetted at volumes of 100 µl in 96 multi-well plates and polymerized at 37°C during 30 min.

2.2.3 Development of a brain-like extracellular matrix

To generate the composed oligomer-hyaluronan matrices, sodium hyaluronate of molecular weight between 351-600 KDa (Lifecore Biomedical, Chaska, MN) was dissolved in 10X PBS and added during neutralization of the oligomer to attain final concentrations of 2 mg/ml oligomer and 2, 5 and 10 mg/ml hyaluronan. To mimic the topography generated by the blood vessels in the brain parenchyma, pseudo-vessels were recreated using sterile rods of PDS II- polydioxanone of diameter 100-150 µm (Ethicon, Blue Ash, OH) coated with Matrigel by immersion. The coated rods were incubated at 37°C for 30 min and immersed in the oligomer-hyaluronan matrix prior polymerization.

2.2.4 Cell culture in 3D matrices

GBAM1 cells were cultured in complete liquid media for 4 days. Neurospheres were embedded in each of the matrices (Matrigel from BD Biosciences, collagen and collagen-hyaluronan) prior polymerization to achieve a density of 1-2 neurospheres per 100 µl of polymeric suspension. Volumes of 100 µl of cell-matrix suspension were platted into 96 well plates. The matrices were polymerized at 37°C for 30 minutes and 100 µl of complete liquid media was added. Cells were cultured at 37°C in an atmosphere of 5% CO_2.

2.2.5 Analysis of mechanical properties

Rheological properties of the matrices were measured by oscillatory shear in a stress-controlled AR2000 rheometer (TA Instruments, New Castle, DE, USA) using a parallel plate geometry (40 mm diameter). Each sample (1 ml) was polymerized at 37°C on the rheometer during 30 min, the geometry was set at 725 μm gap distance and humidity was maintained by a solvent trap as previously described.[61] The viscoelastic properties, shear storage modulus (G') and shear loss modulus (G'') were determined by a strain-stress sweep from 0.01 to 0.4% at 1 Hz (this range was chosen from predetermined linear-viscoelastic response regions). All measurements were conducted on at least three independent samples.

2.2.6 Immunofluorescence staining

For detection of N-cadherin in Matrigel matrices, neurospheres were fixed with 4% glutaraldehyde, permeabilized with 0.5% triton X-100 (Sigma-Aldrich, St. Louis, MO), blocked with 5% BSA (Life Technologies, Carlsbad, CA) in PBS and incubated with primary N-cadherin antibody (Santa Cruz Biotech, Santa Cruz, CA) (dilution 1:40) at 4°C for 12 h followed by washing and incubation with secondary antibody tagged to Alexa-488 (Life Technologies, Carlsbad, CA) (dilution 1:200) at 4°C for 6 h. Nuclei were counterstained with Hoechst 33342 (Life Technologies, Carlsbad, CA).

2.2.7 Laser scanning confocal and light microscopy

Images of neurospheres were taken every 24 h during 3 days using bright field and phase contrast in a CKX41 Olympus inverted microscope. All images were collected using an AmScope (10MP) camera. Confocal microscopy was performed using a Nikon A1R-MP confocal microscope with objectives Apo 40X (1.25 NA) and Plan Fluor 40X-oil (1.3 NA). Confocal reflectance microscopy was performed to analyze the structure of the collagen-hyaluronan matrices in their hydrated state. The images were obtained from three independent samples for each matrix at random positions using the objective Plan Fluor 20X (0.75 NA) in reflectance mode.

2.2.8 Analysis of morphology and migration

Bright field and phase contrast images were analyzed using the software ImageJ (NIH, Bethesda, MD). Migration distance was quantified as the distance from the initial perimeter of the neurosphere to the edge of the most external protrusion or migratory cell.[47,62] Average migration velocity was calculated by dividing the distance recorded by the time interval chosen (24, 48 or 72 h).

2.2.9 Statistical analysis

Quantitative data were compared by t-test (α=0.05), Mann-Whitney or ANOVA using the statistical software package SAS 9.3 (SAS Institute, Cary NC).

2.3 Results

2.3.1 GBAM1 presents stem-like characteristics

GBAM1 human patient-derived cells were previously sorted and isolated for $CD133^{+}$ expression. To corroborate that the cells met all criteria to be considered a stem-like population[9] we tested the formation of neurospheres during liquid standard culture, expression of the stem-like markers and ability to differentiate into glial cells. GBAM1 cultured in liquid platform formed non-adherent neurospheres in all stages of culture (Fig 2.1 A).

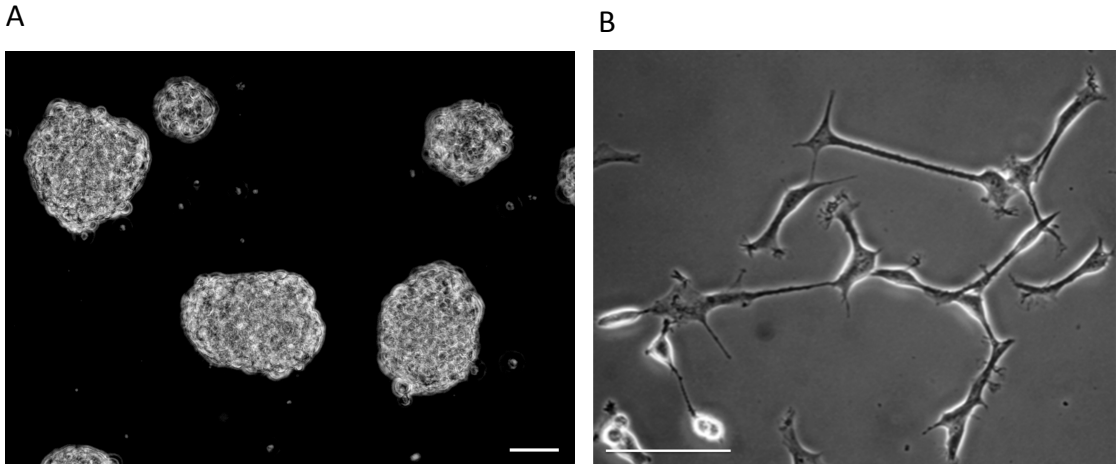

Figure 2.1 **A.** GBAM1 form non-adherent neurospheres in liquid culture. Bars 200 μm. **B** GBAM1 differentiate after 15 days of culture in differentiation medium. Bars 100 μm.

Immunofluorescence staining showed that neurospheres expressed the stem markers Sox2, Notch, and CD133+ and did not express the standard marker for reactive astrocytes GFAP (Fig 2.2 A). Contrary to GBAM1, human astrocytes did not express any of the

stem-markers, but expressed GFAP (Fig 2.2 B). Evaluation of the ability of GBAM1 to differentiate into glial cells after deprivation of growth factors and addition of FBS, resulted in visible morphological change, and gaining of adherence, all characteristics of differentiated brain cells in liquid culture (Fig 2.1 B).

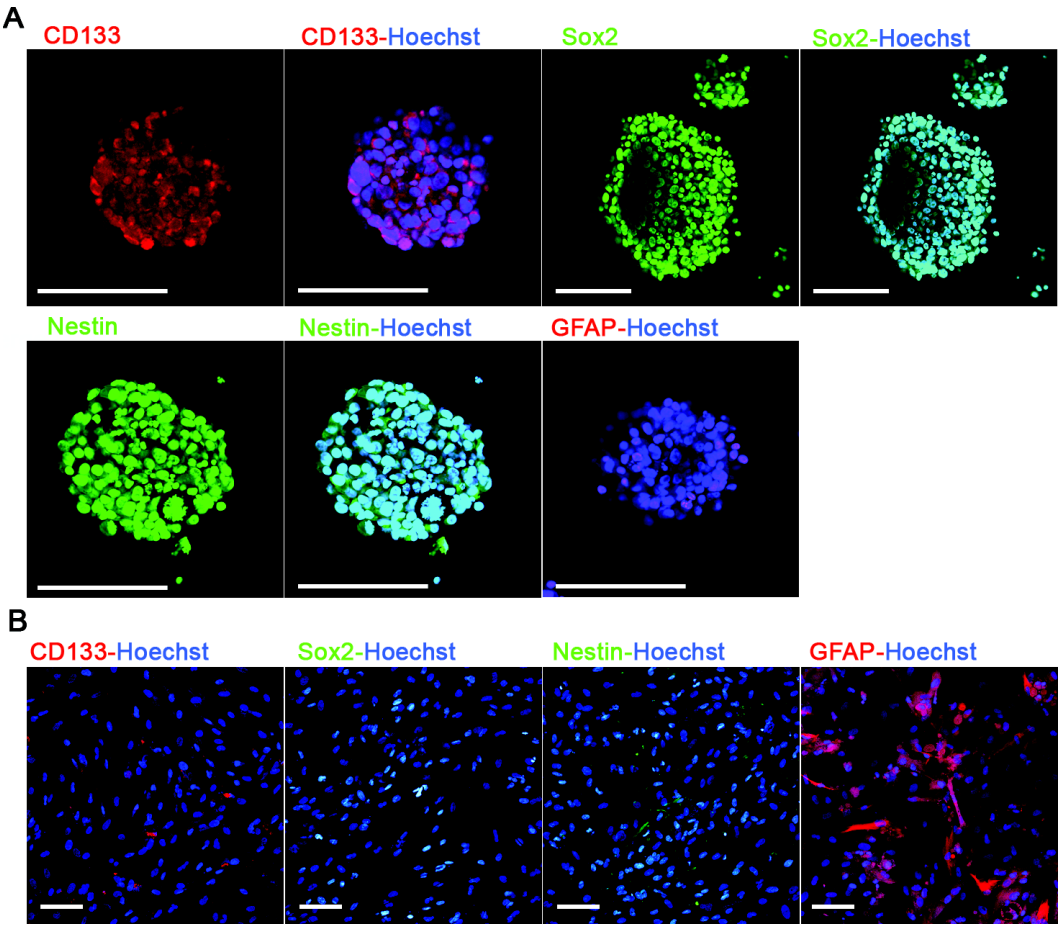

Figure 2.2 **A**. GBAM1 neurospheres (passages 17-23) exhibit markers of GBM cancer stem-like cells (CD133, Sox2 and Nestin) after 5 days of liquid culture. GFAP marker for differentiated astrocytes is not expressed. **B**. Human primary astrocytes do not express stem-like markers (CD133, Sox2 and Nestin), but are positive for GFAP expression. Bars 100 µm.

2.3.2 Modulation of GSC migration by Matrigel characteristics

Invasion of cancer cells has been traditionally studied in Matrigel matrices due to its similar composition to the basement membrane (BM), an *in vivo* type of ECM used by cancer cells for invasion.[55,63] To investigate the migration of GSCs in matrices of similar composition to BM, neurospheres were seeded in Matrigel (100%), Matrigel (75%)-DMEM/F12 (25% v/v) and Matrigel (50%)-DMEM/F12 (50% v/v) to monitor migration. During the first 24h neurospheres developed thin pseudopodia-like extensions that were more abundant and larger in Matrigel 50% compared to other Matrigel matrices. Subsequently, the extensions exhibited in Matrigel 75% and 100% disappeared, and cells continued expanding as a functional aggregate with spherical morphology resembling multicellular migration by expansive growth (Fig. 2.3).[(33)] Contrastingly, the initial pseudopodia developed in Matrigel 50% extensions were gradually replaced by large and wide protrusions with elongated tips that grew radially and remained in contact with the neurosphere.

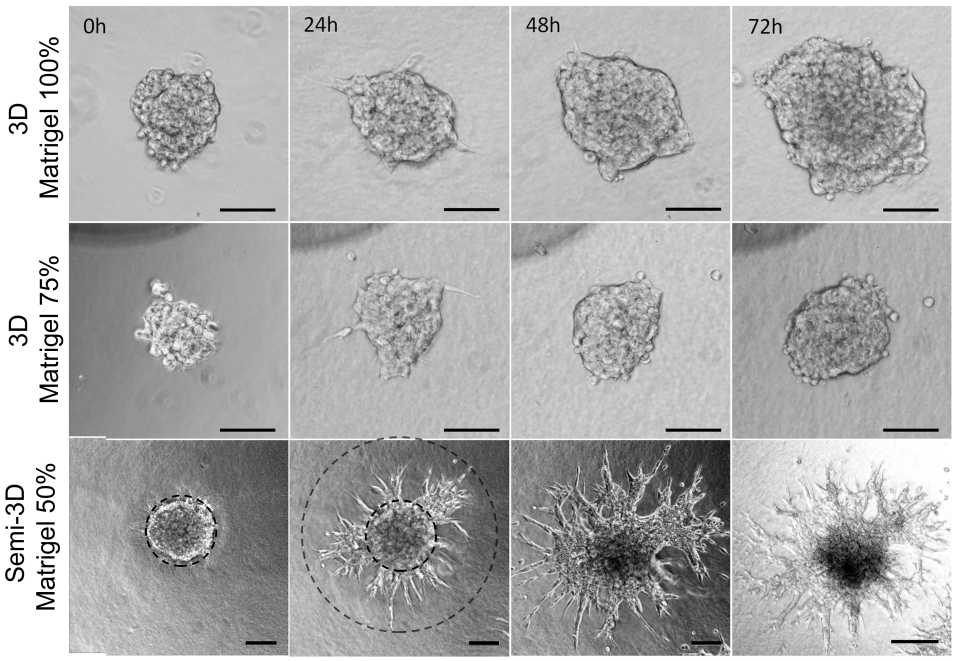

Figure 2.3 GSC neurospheres present different migration characteristics when seeded within Matrigel matrices of different concentration. Neurospheres exhibit migration by expansive growth when cultured in 3D matrices of Matrigel 100% and 75%, while in Matrigel 50% exhibit multicellular strand migration due to low stiffness of the matrix (semi-3D substrate). Bars 100 μm. Migration was determined as the distance from the initial perimeter of the neurosphere to the edge of the most external strand or migratory cell.

3D reconstruction from confocal microscopy images of neurospheres cultured in Matrigel 50% showed that the tips of the migratory strands were located on the same focal plane (Fig 2.4 A) suggesting that in contrast to the other 3D matrices, Matrigel 50% allowed the generation of focal contacts with the plate surface generating a semi-3D (or 2.5D) substrate.[64] It is possible at this Matrigel concentration, the material shear storage modulus became low enough (Table 2.1) for the neurospheres to settle and interact with the rigid surface of the 2D culture plate.

Table 2.1 Viscoelastic properties of the different matrices used for 3D migration studies of GSCs (n=3), mean ± SEM.

Matrix	Shear storage modulus G' (Pa)	Matrix	Shear storage modulus G' (Pa)
Matrigel 100%	56.5 ± 3.1	BD-Col 3 mg/ml	24.5 ± 0.3
Matrigel 75%	35.6 ± 0.8	BD-Col 1.5 mg/ml	6.5 ± 1.9
Matrigel 50%	17.9 ± 0.3	Atelocollagen 4 mg/ml	39 ± 2.1
Oligomer 3 mg/ml	885 ± 92.3	Atelocollagen 2 mg/ml	4 ± 1.3
Oligomer 2 mg/ml	397 ± 32.7	HA:2 mg/ml-Col:2 mg/ml	126.2 ± 14.6
Oligomer 1.5 mg/ml	225 ± 14.1	HA:5 mg/ml -Col:2 mg/ml	107.9 ± 19.6
Oligomer 1 mg/ml	90 ± 5.2	HA:10 mg/ml -Col:2 mg/ml	36.1 ± 0.6

Note: Stiffness of normal brain tissue ranges between 260-500 Pa.[65] Although given the heterogeneity of the organ there can be sections with lower of higher values.

To corroborate that multiple cells in contact formed the extensions we performed immunostaining to detect expression of N-cadherin. The results suggest maintenance of cell-cell contacts in both, the cells forming the neurosphere and the cells migrating as multicellular extensions (Fig 2.4 B). In comparison, GSCs in 3D Matrigel expanded into significantly smaller distances and with significantly slower velocities compared to the GSCs that were able to contact the rigid culture plate.

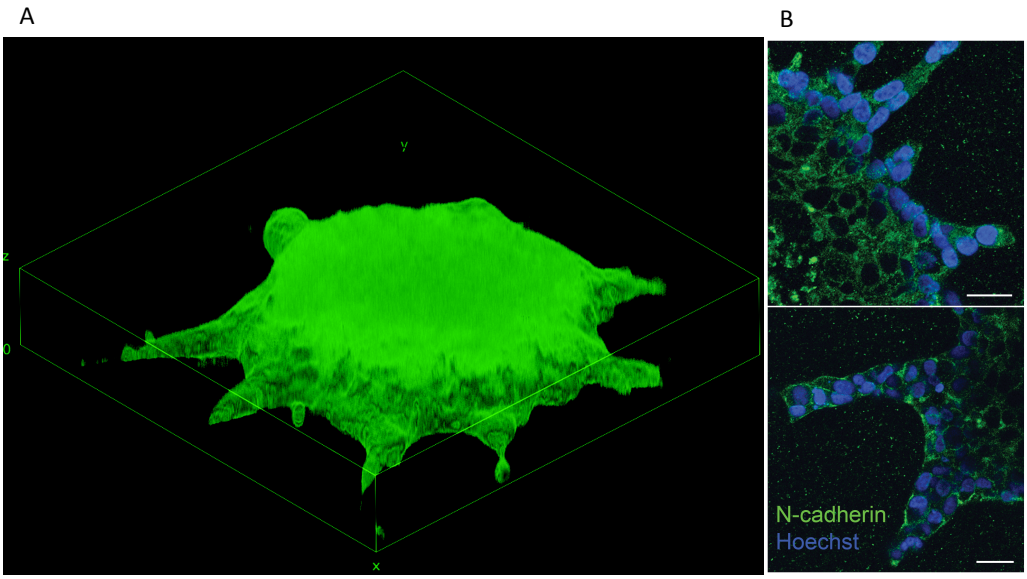

Figure 2.4 **A**. Z-reconstruction of GSCs migrating in Matrigel 50% after 24 h shows that collective migrating extensions are located in the same focal plane. **B**. GSCs cultured in Matrigel 50% develop contacts with rigid surfaces of the plate (semi-3D substrate) giving onset to wide, stable and long protrusions comprised of one or more cells with intact and stable cell-cell contacts. Neurospheres after 72h of culture were fixed and stained with Hoechst 33342 and N-cadherin-Alexa 488. Staining for nuclei was incomplete due to the high density of the neurosphere. Bars 25 μm

2.3.3 Type-I collagen matrices support single cell migration of GSCs regardless of collagen concentration or formulation

Fibrillar collagens are ubiquitous components of the ECM in the majority of tissues and organs and have been demonstrated to be present within glioma tissues and its surrounding ECM during tumor_progression.[16] To further explore the morphology and migration characteristic of GSCs, type-I collagen matrices with diverse characteristics were generated using type-I oligomers (Oli) isolated via acid-solubilization of pig skin, type-I atelocollagen from pepsin-treated pig skin (Atelo), and BD-Biosciences type-I collagen from rat tail (BD). Migration of GSCs in all collagen matrices occurred by

single cell migration (Fig 2.5) consistent with the migration mode presented by other glioma cells in commercial collagen.[47,62] Different concentration of collagen, absence of telopeptides (atelocollagen), or collagen source (commercial rat tail or pig skin) did not modulate the migration mode exhibited. Neurospheres cultured in collagen developed thin pseudopodia–like extensions with subsequent detachment of single cells from the neurosphere. Migration occurred in all directions with cells presenting a spindle-shape morphology resembling mesenchymal single-cell migration (Fig 2.5).

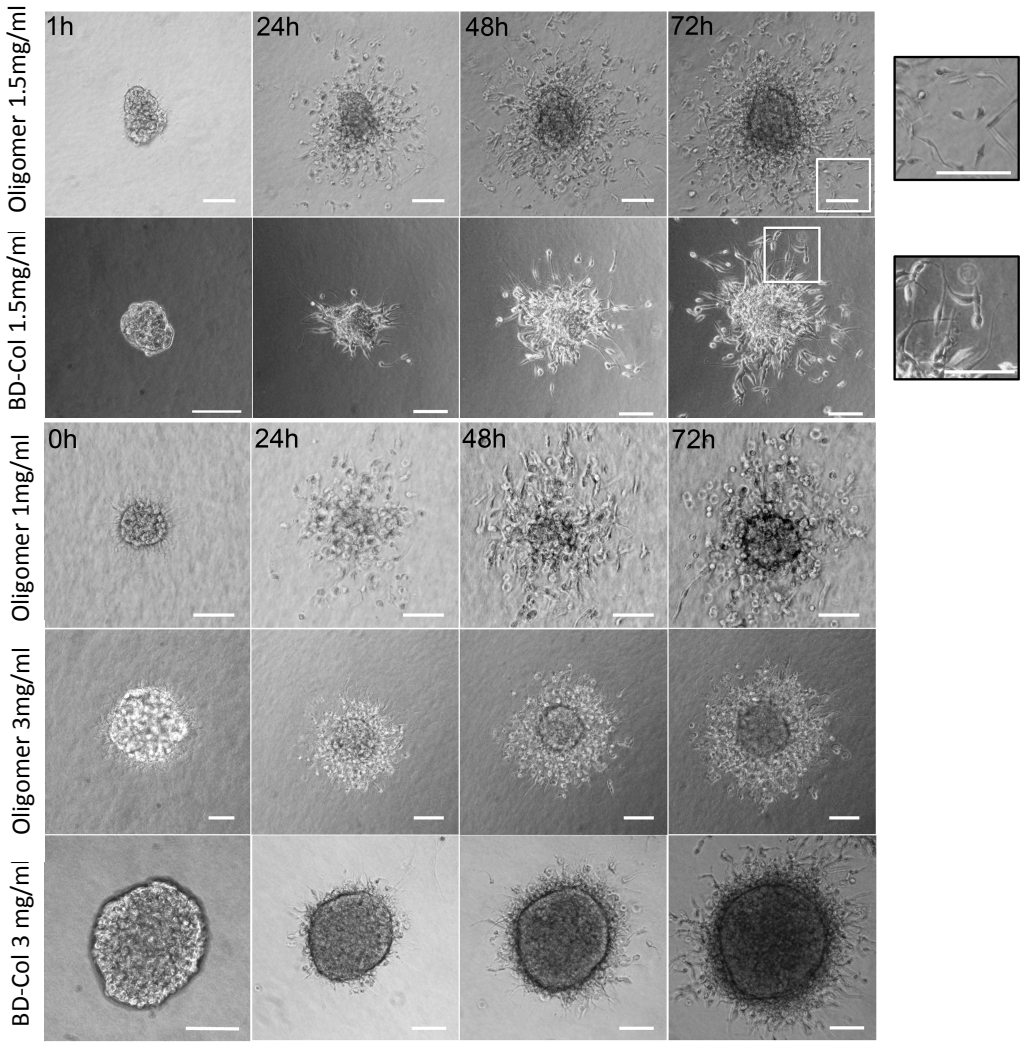

Figure 2.5 GSC neurospheres embedded in multiple types of collagen type-I matrices present single cell migration mode. Bars 100 μm.

2.3.4 Collagen formulation and concentration influence migration distance and velocity of GSCs

Parameters such as collagen source, isolation method, and polymerization reaction conditions dictate the mechanical and physical properties of self-assembled collagen matrices[61] and are expected to affect migration distance and velocity. While previous

studies have explored glioma migration in collagen, only standard commercial monomeric collagen was used to generate 3D matrices.[46,47,62] Unlike conventional monomer matrices, which represent entanglements of long fibrils, oligomers induce interfibril associations to yield branched fibril networks. Here, collagen matrices were prepared at concentrations ranging from 1-4 mg/ml, and GSCs migration distance and velocity were measured as a function of concentration, formulation and matrix stiffness.

Variation of collagen concentration affected the migration velocity of GSCs (Fig 2.6). The relationship between concentration and velocity was specific for each of the collagen formulations. Atelocollagen matrices, prepared from collagen molecules in which telopeptide regions have been enzymatically eliminated showed short migration distances and low matrix stiffness values (Fig 2.7 Table 2.1) along with low velocities that slightly increased with concentration (Fig 2.6). BD-collagen matrices also exhibited low stiffness and induced slightly higher although non-statistically different levels of invasion compared to atelocollagen. However, the velocity decreased moderately as the collagen concentration increased (Fig 2.6). In contrast to other formulations, oligomer presented the highest stiffness at the same fibril density (Fig 2.7 Table 2.1) and a broad range of migration distances as a function of collagen concentration.

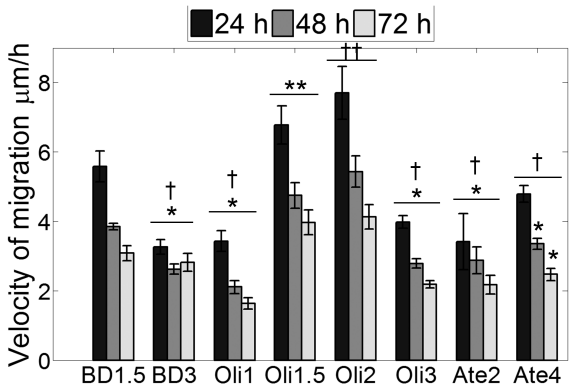

Figure 2.6 BD1.5 (BD-Col 1.5 mg/ml), Oli (oligomer), Ate (atelocollagen)**.** The highest velocity was reached in Oligomer 1.5 mg/ml and Oligomer 2 mg/ml, 2 mg/ml. Maximum velocity was reached during the first 24 h of culture and decreased subsequently. Values marked as * are statistically different from ** p-value<0.05, † are statistically different from †† p-value<0.05. n=9 (Oligomer), n>4 (BD-Col and atelocollagen), error bars indicate ± SEM

The velocity and distance increased with oligomer concentration until reaching a maximum in 2 mg/ml matrices, subsequently, velocity and distance decreased for matrices of higher concentration (3 mg/ml) (Fig 2.6). Interestingly, matrices such as BD-Col and Ate that represented the low-end of the matrix stiffness spectrum (4-39 Pa) supported low migration distances and velocities similar to those obtained in matrices as Oli-3 that represented the highest matrix stiffness (885 Pa) evaluated and exhibit higher cell-matrix contacts but reduced porosity. Analysis of oligomer matrices encompassing a wider range of stiffness values (90–885 Pa) suggested an optimum range where the maximum migration is reached (Fig 2.7). GSCs cultured within matrices Oli-1.5 and Oli-2 (225-397 Pa) of similar stiffness values to brain tissue (260-500 Pa)[65] supported the greatest migration.

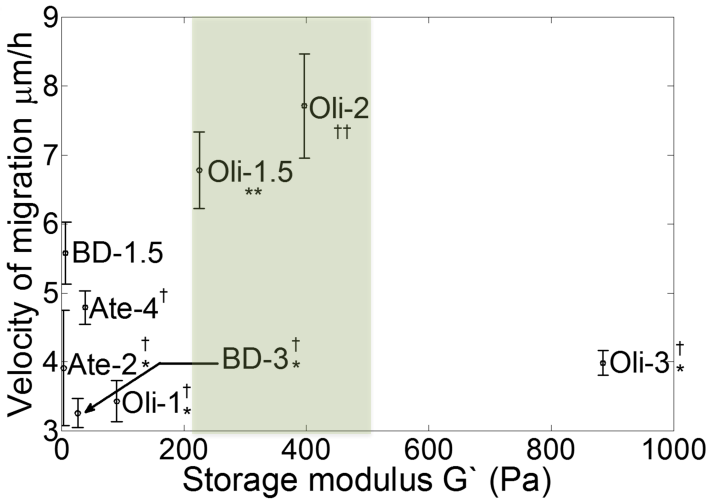

Figure 2.7 Optimal migration velocity of GSCs in collagen-I occurs at stiffness levels in the range found in normal brain (represented in green section).[65] Values marked as * are statistically different from **, † are statistically different from ††, p-value<0.05. Oligomer matrices with G' of 225 Pa (Oligomer 1.5 mg/ml) and 397 Pa (Oligomer 2.0 mg/ml) supported the greatest migration distance and velocity compared to other collagen matrices. Error bars indicate ± SEM

2.3.5 Presence of hyaluronan in composite matrices reduces GSC migration

To recreate some essential features of glioma ECM composition and study the migratory behavior of GSCs, composite matrices of hyaluronan (HA) and type-I collagen (Col) were generated with 0, 2, 5, and 10 mg/ml of HA and a constant oligomer concentration of 2 mg/ml. GSC neurospheres cultured in Col-HA matrices exhibited early pseudopodia extension followed by single cell migration similar to what was observed in collagen-only matrices. Nevertheless, increasing hyaluronan concentration proportionally reduced migration as well as the frequency of cell detachment from the neurospheres (Fig 2.8 A,B). Cells cultured in Oligomer 2 mg/ml exhibited the greatest migration distance, while cells in HA:2-Col:5 mg/ml and HA:2-Col:5 mg/ml presented a significant reduction of

migration compared to only oligomer matrices. The most drastic reduction was observed in HA:10-Col:2 mg/ml where very few cells detached from the neurosphere and migrated considerable short distances. Cells that left the neurosphere were able to increase the migration velocity over time different to what was observed for the other matrices (Fig 2.8 C). Additionally, presence of HA induced morphological changes of the migratory cells. Cells switched from an elongated morphology observed in the only-oligomer and HA:2-Col:2 mg/ml matrices, to a mixed population of elongated and rounded cells in HA:5-Col:2 mg/ml matrices, and to a mostly rounded morphology in HA:10-Col:2 mg/ml matrices.

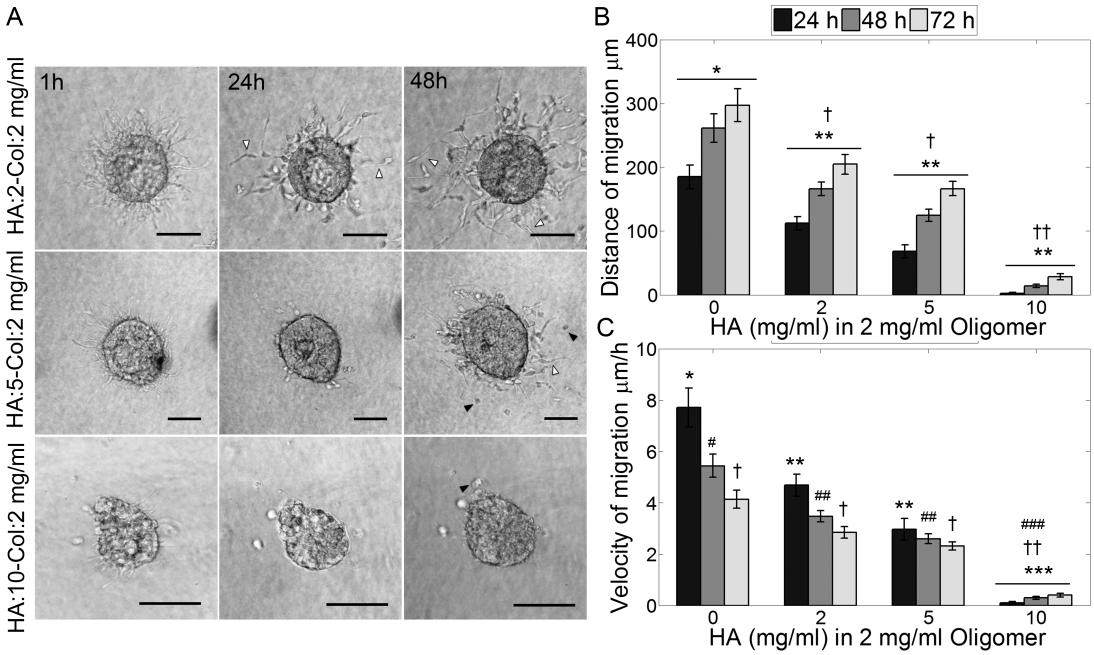

Figure 2.8 **A**. GSCs present single cell migration in composite Oligomer-hyaluronan matrices similar to only-oligomer matrices. Increasing concentration of hyaluronan decreases the number of migrating cells and alters the morphology of the migratory cells from elongated to spherical shape. White arrows point out elongated migrating cells, black arrows point out rounded migrating cells. Bars 100 µm **B.** Distance of migration is reduced with increasing presence of HA. All matrices present statistically different distance at all time points excepting HA:2-Col:2 and HA:5-Col:2 mg/ml **C.** Velocity decreased with time as observed with other matrix types, except HA:10-Col:2 mg/ml matrix where the velocity increased with time. Values marked as * are statistically different from ** p-value<0.05, † are statistically different from †† p-value<0.05, #, ## and ### are statistically different p-value<0.05. n=9, error bars indicate ± SEM.

2.3.6 Addition of hyaluronan modulates fibril microstructure and mechanical properties of oligomer matrices

To further analyze how the incorporation of hyaluronan altered the mechanical properties of the matrices and the migratory behavior of GSCs, we performed viscoelastic shear tests of the composite matrices. Increasing HA concentration reduced the storage and loss moduli while slightly decreasing the phase angle (δ) of the matrix (Table 2.2). The

greater values of the storage modulus compared to the loss modulus, indicate that the matrix dynamic response is mainly controlled by the elastic (solid) phase. Structural changes of the matrix caused by HA were examined by confocal reflectance microscopy (CRM) and suggest that hyaluronan incorporation does not affect fibril density, as was expected for matrices of the same collagen concentration, but disrupts the formation of interfibril associations reducing the fibril branching (Fig 2.8). Since collagen fibril branching is correlated with matrix stiffness,[66] the reduction of fibril associations caused by HA might have contributed to stiffness reduction.

Table 2.2 Viscoelastic properties of the composite matrices of oligomer collagen and hyaluronan (n=3), mean ± SEM. HA: hyaluronan.

Matrix	Viscoelastic Properties		
	G' (Pa)	G" (Pa)	δ (degrees)
HA:2-Col:2 mg/ml	126.2 ± 14.6	15.8 ± 0.4	7.2 ± 0.1
HA:5-Col:2 mg/ml	107.9 ± 19.6	13.4 ± 2.2	7.1 ± 0.1
HA:10-Col:2 mg/ml	36.1 ± 0.6	3.7 ± 0.1	5.9 ± 0.0

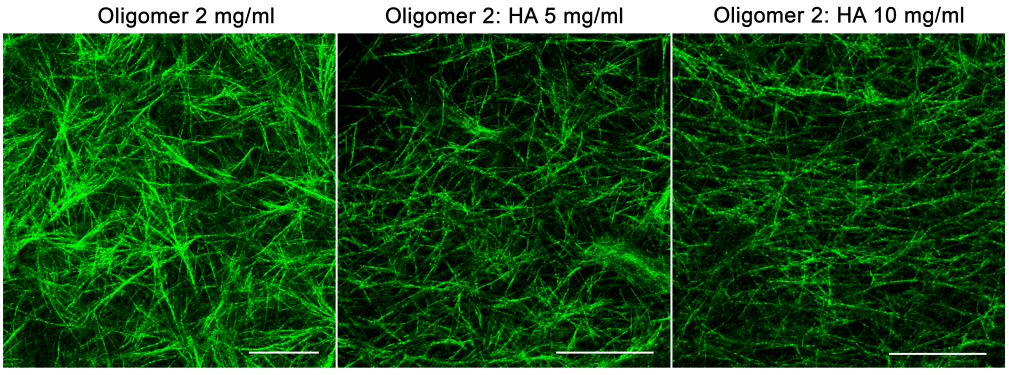

Figure 2.9 Confocal reflectance microscopy of oligomer matrices with varied concentration of hyaluronan. Hyaluronan presence altered the collagen interfibril associations. Bars 50 μm.

2.3.7 Glioblastoma stem cells (GSCs) exhibit multiple migration modes

We next asked what would be the overall migratory response of GSCs in a 3D *in vitro* microenvironment that mimics the composition and topography of the glioma environment in a single 3D construct. To address this question we cultured GSC neurospheres in a composite matrix of HA:10-Col:2 mg/ml with embedded Matrigel coated microfibers to imitate the structural tracts formed by the blood vessels thereby providing the cells diverse migratory paths. We observed that neurospheres located close to the fibers migrated towards the fiber and developed strand collective migration using the topographical cues as physical support (Fig 2.10 A). Cells migrating along the rods maintained cell-cell contacts during movement as was identified by the expression of N-cadherin and did not separate from the neurospheres, whereas cells facing the collagen-hyaluronan matrix directly (no rods nearby) detached from the neurosphere and exhibited single cell migration as was observed previously in only-collagen and collagen-hyaluronan matrices.

The velocity and maximum distance for collective migration along the rods (Fig 2.10 B, C) were comparable with the values obtained for single cell migration in oligomer 2 mg/ml matrices and are greater than the values obtained for migration in oligomer-hyaluronan matrices. The results indicate that multicellular strand migration exhibited during durotaxis, such as along the structural cues in composite matrices and in the semi-3D (Matrigel 50%) matrix, is the most productive and fastest migration mode as it favors the generation of combined motility force, and maintains important paracrine signaling.[53]

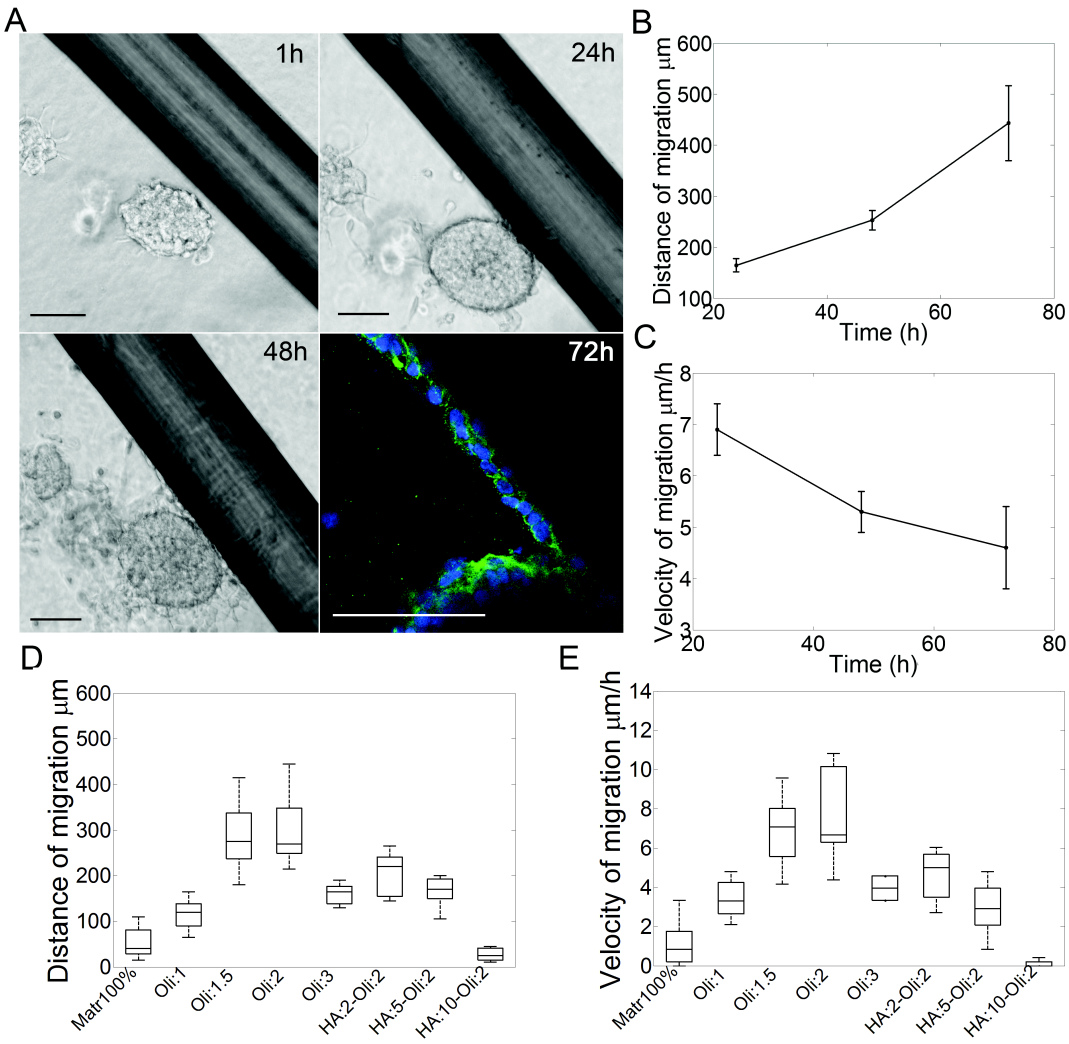

Figure 2.10 **A**. GSC neurospheres exhibited multiple migration modes in composite matrix as single cell migration mode across the 3D matrix and collective strand migration along the topographical cues present in the matrix. Immunofluorescence was used to detect N-cadherin. N-cadherin appears in green and nuclei in blue. Staining for nuclei was incomplete due to the density of the neurosphere. Bars 100 µm. **B.** Distance of migration along the rods increases with time and presents values comparable to those obtained during migration in Matrigel 50%. N=4, error bars indicate ± SEM. **C.** Velocity of migration along the rods slowly decreases with time presenting values comparable with other types of matrices such as Oligomer 2 mg/ml, n=4, error bars indicate ± SEM. **D.** Comparison of GSCs maximum distance of migration in different types of matrices at 72 hours, n=9. **E.** Comparison of GSCs velocity of migration in different types of matrices at 24 hours, n=9.

2.4 Discussion

Migration of glioblastoma stem cells (GSCs) has been linked to post-operative tumor recurrence. Nevertheless, the migratory characteristics of this cell population in diverse types of extracellular matrices, has not been previously studied in detail. Here, we used multiple 3D formats commonly used for tumor invasion studies such as Matrigel and type-I collagen as well as a novel composite *in vitro* model that mimics the ECM composition, physical properties, and topography of glioma microenvironment. Our results indicate that GSCs exhibit varied velocities and migration modes such as collective migration, expansive growth, single-cell migration and combined collective-single migration as a function of the composition and physical characteristics of the 3D microenvironment.

In 3D matrices of Matrigel, the neurospheres adopted a rounded morphology resembling expansive growth. Such morphology can be associated with the structural characteristics of the matrix. Matrigel presents different crosslinking patterns as well as larger pore sizes than native BM,[55,67] and does not confine or resist neurosphere expansion. As a consequence, cells tend to exhibit characteristics related to proteolysis-independent migration such as amoeboid morphology for single cells[68] or expansive growth,[25] consistent with the morphology observed in Matrigel 75% and 100%. Our results also suggest that reduction of matrix stiffness as in Matrigel 50% generates a semi-3D (or 2.5D) substrate where close contact between the neurospheres and the rigid surface of the culture plate allows the formation of focal contacts and stable multicellular strands supporting greater migration distances.

The drastic change of GSCs morphology to strictly elongated, mesenchymal-like, single migration in type-I collagen corroborates the relevance of the ECM properties on the regulation of cancer cell migration. Fibrillar collagen although non present in normal brain ECM, has been found in glioma tissues, surrounding ECM,[15] and as a component of the GSCs niche,[(16)] suggesting that glioma cells deposit it to support tumor migration. While previous studies have explored the migration of glioma cells in collagen matrices by using established cell lines and commercial collagen,[46,47,62] we focused on studying the invasiveness of GSCs due to their role in tumor migration and regrowth. Additionally, we generated matrices with oligomer collagen that as recent reports showed, offers a number of advantages over conventional monomeric collagens, including hierarchical collagen fibril assembly that recapitulates that observed *in vivo*, presence of tissue-specific intermolecular crosslinks, short polymerization time, and customization over a broad range of relevant physicochemical features.[61] GSC neurospheres exhibited single cell detachment and mesenchymal migration in all the types of collagen matrices studied, consistent with the migration mode presented by other glioma cells lines in 3D-collagen matrices.[47,62] The velocity and distance of migration were modulated by the concentration of the collagen as was expected due to changes in the fibril density and pore size of the matrix.[54,61] In atelocollagen matrices where no crosslinks are present, increasing concentration resulted in higher migration due to higher generation of cell-matrix contacts and proteolysis-independent migration. In covalently cross-linked matrices such as BD-collagen and oligomer, increasing collagen concentration reduces the pore size and the available space for cell movement; hence, migration relies on the ability of the cell to degrade and remodel the extracellular matrix, or to deform its body until reaching an

appropriate size to move through the pores.[69] Similarly, reduction of the collagen concentration and consequent increase of the pore size can also reduce migration due to the lack of structural support for the development of cell-matrix contacts and generation of traction force to propel movement. These differences in migration due collagen matrix concentration are similar to observations by other authors[62] and support the existence of an optimum collagen concentration range where the fibril density and pore size support the maximum cell migration.[70–72]

Hyaluronan enrichment of the ECM and overexpression of CD44 receptors have been associated with glioma invasion of brain parenchyma.[73–75] Interestingly, when increasing quantities of hyaluronan were incorporated to collagen matrices to resemble glioma microenvironment, the number of migratory cells and migration distance were reduced. Also, the cell morphology shifted to a more-rounded appearance. Previous studies of collagen-hyaluronan 3D matrices[43,45,46] have related increasing HA concentrations with matrix stiffness and subsequent reduction of cell migration with adoption of rounded morphology. Similarly, in PEG-HA matrices, increased stiffness has derived in changes of cell morphology.[76] Nevertheless, our results showed that incorporation of non-crosslinking hyaluronan decreases matrix stiffness (Table S1) but also induces adoption of cell-rounded morphology. As other studies of acid-solubilized collagen matrices have shown, HA incorporation increases interstitial fluid movement resistance without affecting fibril density.[(45)] Consistently, Col-HA matrices presented a similar fibril density upon HA addition, however the interfibrilar associations were disrupted. Therefore, we suggest that the stiffness reduction is linked to reduction fibrillar branching

caused by HA during matrix polymerization,[66] and the adoption of cell rounded appearance is mainly due to increased resistance of the interstitial fluid caused by hyaluronan hydration that opposes an additional barrier for cell deformation and movement.

It is accepted that GBM presents a rapid infiltration pattern with preference for myelinated axons and blood vessels.(14) Recently it was shown using *in vivo* xenograft models that GBM cells present directional and efficient migration (greater net distance and velocity) along blood vessels while migration through the parenchyma occurs by expression of multiple pseudopodia with constant changes in direction.[78] Certain GBM cell lines also presented a chain-like morphology when extending from the tumor to the blood vessels.[79] In line with such findings, our results, obtained using an *in vitro* composite matrix, suggest that GSCs detect the asymmetric rigidity gradient presented in the environment and develop different migration modes according to the mechanical properties of the structures to invade. Migration across collagen-hyaluronan matrix, which poses a low-stiffness environment triggers cell detachment and single cell migration with constant changes of direction; however, when rigid structures (as the microrods) are presented to the neurospheres, the cells develop collective strand migration along the directional tracts. Such migration mode by multicellular strands was present along rods regardless of the percentage of Matrigel coverage on the rod surface. Hence, we suggest that the rigidity of the topographical clue coupled with the proximity of the neurosphere to the clue induce durotaxis and formation of strand collective

migration, and that this type of collective migration is likely to be present not only along blood vessels but also along myelinated axons.[80,81]

2.5 Summary

In this study we describe a new composite tunable matrix that resembles important features of glioma microenvironment as ECM composition, mechanical properties and preexisting structural cues. This model can be used to dissect and increase our mechanistic understanding of the migratory behavior of GSCs in 3D environments. Furthermore, we analyzed multiple matrices of varied mechanical properties using Matrigel and diverse types of fibrillar collagen, to assess how the migratory characteristics of GSCs are affected by the physical properties of the matrix. Our results indicate that GSC neurospheres are able to exhibit multiple velocities and migration modes such as collective migration (expansive growth and strand)[82] and single cell migration (mesenchymal) as a function of the mechanical and compositional properties of the matrices. In a composite collagen-hyaluronan matrix, the migration of GSCs was reduced by the presence of hyaluronan; nonetheless, cells adopted a productive and fast migration as a collective strand by using the preexisting topographical cues presented as migratory paths. Taken together the results suggest that GSCs migration is not limited to a unique migration mode as is usually observed in *in vitro* studies, but are able to exhibit concomitantly multiple migration modes (collective and single) as a response to the heterogeneity of the environment. The recreation of additional characteristics of cancer environments such multiple cell co-culture and functional vascular networks in

controllable 3D-models is a powerful tool to study cancer development and progression. Additional efforts in this area will contribute to the elucidation of fundamental mechanisms such as how cell sensing of the microenvironment composition and mechanical characteristics induces the adoption of different migration mechanisms.

CHAPTER 3. INFLUENCE OF THE EXTRACELLULAR MATRIX AND STROMAL CELLS ON GLIOBLASTOMA DRUG RESPONSE

3.1 Introduction

Recognition of the tumor microenvironment as a biological regulator of GBM progression is critical not only to elucidate the biological mechanisms involved in tumor development and progression but also in the early stages of the development of drug treatments that effectively target the cancer cells and their supportive niche. Presence of the tumor microenvironment has been correlated with poor response of cancer cells to chemo- and radiotherapy as well as to inhibition of immune surveillance.[51,83,84] An appropriate example of the importance of the understanding the dynamic relationship tumor-microenvironment during drug development has been the development of anti cancer drugs such as Bevacizumab that target the interaction with tumor-microenvironment. Bevacizumab, an antibody that inhibits the vascular endothelial growth factor-A (VEGF-A) was approved for GBM treatment to directly inhibiting tumor angiogenesis.[85] Despite the overall dismal improvement that Bevacizumab has have on GBM patients,[86] recognition of the synergistic relationship tumor-microenvironment as a potential drug target has been a fundamental step in the development of more effective and specific treatment approaches.

Given the importance of tumor microenvironment during GBM drug response, a close representation of its multiple components during early stages of drug development is fundamental for the development of translational therapies. The use of *in vitro* platforms that represent more closely the *in vivo* settings of the tumor microenvironment has multiple advantages such as presence of cell-ECM interactions and existence of nutrient and oxygen gradients.[83,87] However the majority of these approaches are only focused on the recapitulation of the 3-dimensionality of the tumor and presence of ECM and very few have also considered the effect of stromal cells as components of the tumor microenvironment.

3D scaffold-based co-culture models are powerful tools to represent the tumor microenvironment since can incorporate the ECM, stromal and tumor cells and allow controlled analysis of the role of intercellular signaling on tumor behavior. Despite the great advantages that these models offer for initial drug screening of potential GBM treatments, a comprehensive 3D model of GBM microenvironment that accounts for ECM and tumor cell heterogeneity has not been yet developed. In this work we use a 3D *in vitro* tissue model that recapitulates the physical characteristics of GBM ECM with incorporated stromal cells as astrocytes and endothelial colony forming cells (ECFCs) to determine the role of both, extracellular matrix and stromal cells presence on the viability of GBM after drug treatment. To achieve a more comprehensive conclusion on the effect of microenvironment on GBM survival, we used multiple patient derived GBM cell lines, including stem-like and non-stem GBM cells. Furthermore, different drug treatments were tested such as temozolomide, Nutlin-3a and the STAT3 inhibitor SH-4-54.

Temozolomide is the standard chemotherapeutic agent for GBM treatment and acts by damaging (through methylation) the DNA and inducing cell death. Nutlin-3a acts as a MDM2 inhibitor, a negative regulator of p53 tumor suppressor and has shown very promising results for treatment of multiple cancers types, especially in combination with other treatments.[88,89] Lastly, we used a newly developed small molecule inhibitor of signal transduction and activator of activation STAT3 (SH-4-54), this drug acts by inhibiting the phosphorylation of STAT3 required for activation of genes involved in cancer associated processes as metastasis, proliferation and survival and has been proved to effectively reduce survival of brain tumor initiating cells (also called tumor stem-like cells).[90]

3.2 Experimental Methods

3.2.1 Cell culture in liquid substrates

GBM human–derived cell lines GBM10 and GBM43 were originally obtained from Dr. Jann Sarkaria (Mayo Clinic, Rochester, MN) and have been described elsewhere.[91] MHBT32 is a low passage primary patient line kindly donated by the Dr. Karen Pollok and Dr. Aaron Cohen at Indiana University and the Methodist Hospital of Indianapolis. All cell lines were maintained in high-glucose DMEM (Life Technologies, Carlsbad, CA) supplemented with 10% FBS. Cell line U87MG was maintained in IMDM (Life Technologies, Carlsbad, CA) supplemented with 10% FBS. GBM human cell line GBAM1 (CD133+ >98% from passages 22-25) provided by Dr. Phillip Tofilon and the Moffitt Cancer Center was maintained in DMEM/F12 supplemented with B27 without

vitamin A (Life Technologies, Carlsbad, CA) and with growth factors EGF, bFGF (50 ng/ml each, Peprotech, Rocky hill, NJ). Human primary astrocytes from ScienCell (Carlsbad, CA) were maintained according to vendor specifications. Endothelial umbilical cord blood ECFCs from EndGenitor Technologies (Indianapolis, IN) were cultured in collagen type-I coated T-75 flasks in EGM-2 medium (Lonza, Walkersville, MD). All cell lines were cultured at 37°C in an atmosphere of 5% CO_2, fed with complete media every other day and passaged at 70-80% confluence.

Table 3.1 Properties of human-derived GBM cell lines

Cell line	EGFR Amplification	PTEN status	p53 status	p16 deletion
GBAM1(CD133+)	-	-	-	-
GBM10	No	wt	wt	Yes
GBM43	No	wt	170 Phe>Cys	Yes
MHBT32	-	-	-	-

3.2.2 Cell culture in the 3D brain-like matrix

3D matrices of collagen-hyaluronan were generated using pig skin oligomer collagen (GeniPhys, Zionsville, IN) at concentration 2 mg/ml as described by Whittington (2013). Sodium hyaluronate (MW 351-600) KDa (Lifecore Biomedical, Chaska, MN) was dissolved in 10X PBS during collagen neutralization to attain a final concentration of 10 mg/ml of hyaluronan. GBM cells were suspended at the desired density in the 3D matrix prior polymerization at 37°C for 30 minutes. Complete media was added to the top of the matrix, and cells were cultured at 37°C in an atmosphere of 5% CO_2.

3.2.3 Drug treatments

GBM cells were cultured for 24 h (in liquid medium or within the 3D Col-HA matrix) in a 96-well plate at 5000 cells/well with 100 µl of complete media prior addition of one-time dosage of the drug treatments. Co-culture of GBM with with stromal cells was done at a ratio 1:1 or 1:1:1. The drugs Nutlin-3a, anti-STAT3 inhibitor SH-4-54 and Temozolomide (TMZ) (Sigma-Aldrich, St. Louis, MO) were dissolved in DMSO and added to a total of 200 µl of medium per well. Controls were treated with DMSO. Combination drug treatments of SH-4-54 at fixed concentration of 5 µM with varied concentration of Nutlin-3a (0 - 50 µM) were performed in liquid and 3D culture for GBAM1 and GBM10. Dual combination of Nutlin-3a (25 µM) and SH-4-54 (5 µM) or triple combination of Nutlin-3a (25 µM)+ SH-4-54 (5 µM)+TMZ (1050 or 750 µM) were tested both in liquid and 3D culture in GBAM1 and GBM10 cell lines.

3.2.4 Assessment of cell viability

Viability of GBM cells cultured as 2D monolayer or in 3D Col-HA matrix was assessed 72h or 120h after drug treatment using Alamar blue assay (ThermoFisher Scientific, Waltham, MA). Alamar blue solution was added to each well to reach 10%v/v; cells were incubated with the reagent for 3h at 37°C and fluorescence was measured (560 nm excitation - 590 nm emission). Readings were normalized to DMSO control to calculate viability percentages.

For assays involving co-culture of GBM with astrocytes and ECFCs the GBM cells were marked with CellTracker™ Green CMFDA dye (ThermoFisher Scientific, Waltham, MA) prior 3D culture and drug treatment. Viability was assessed using confocal microscopy

by treating the samples for 10 min with viability dye eFluor 660 (eBiosciences) 72h after drug treatment. Total GBM cells were detected by Celltracker green and dead GBM cells by colocalization of both dyes using ImageJ software.

3.2.5 Statistical analysis

All measurements are expressed as mean SD unless otherwise stated. Comparisons between treatments were made using two samples t-test or one-way analysis of variance (ANOVA) with Tukey-Kramer mean comparison. Analysis of effect of drug treatment and presence of other cells on GBM migration was made using two-way analysis of variance with Tukey-Kramer mean comparison. Statistical significance was evaluated at $\alpha = 0.05$.

3.3 Results

3.3.1 Effect of temozolomide (TMZ) treatment on GBM cell viability in 2D liquid culture

GBM cell lines were treated with varied concentration of temozolomide (TMZ) as a one-time dosage, and cell viability was evaluated 5 days after treatment using Alamar blue assay. The concentration range of treatment was chosen based on previous studies by collaborators for IC50 determination (data not shown). We observed that all the cell lines exhibited a weak response to low TMZ concentrations (Fig 3.1). TMZ IC50 for cell lines GBAM1, GBM10 and GBM43 was reached at 753, 1383 and 800 μM respectively; these

values were much higher than previously determined by our collaborators using a methylene blue proliferation assay (Table 3.2). TMZ IC50 for MHBT32 was reported at 5.8 μM (Table 3.2), however in our hands, this cell line showed low response to treatment and constant viability of 80% after TMZ treatment from 25 to 200 μM.

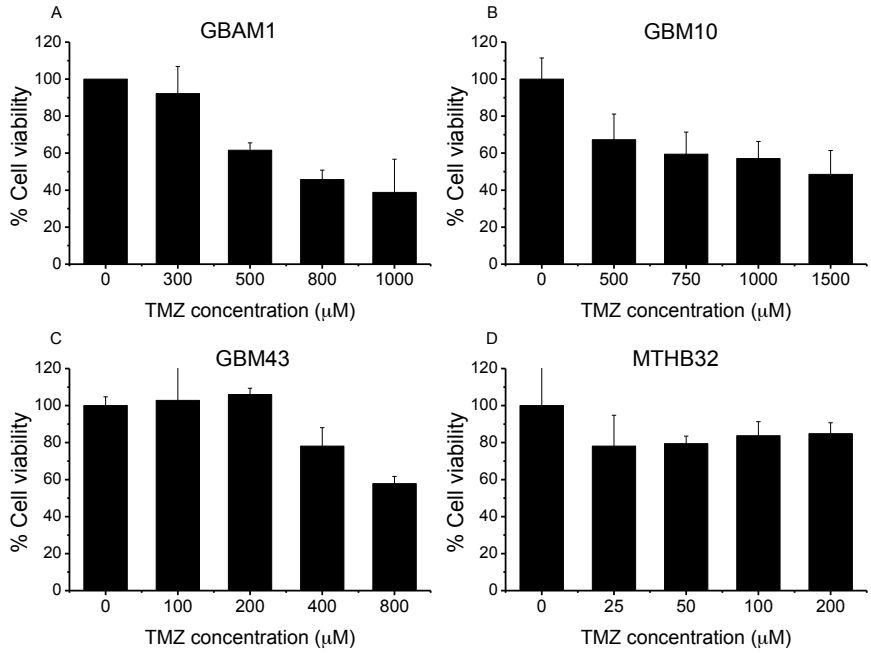

Figure 3.1 Patient derived GBM cell lines exhibit weak response to TMZ treatment in 2D liquid culture. MHBT32 cell line was resistant to increasing concentrations of TMZ. Data presented as Mean ± SD (n=>3)

Table 3.2 Comparison of GBM TMZ IC50 in 2D liquid culture. Relative IC50 calculated are higher than IC50 previously determined by collaborators.

	TMZ Reported (2D)	**TMZ Liquid (2D)**	**Nutlin-3a (2D)**
GBAM1	Unknown	735	110
GBM10	923	1383	40
GBM43	263	800	26
MHBT32	5.8	> 200	17

3.3.2 Effect of MDM2 and STAT3 inhibitors on GBM cell viability

Given the poor response to temozolomide exhibited by all GBM cell lines studied, we tested the effect on viability of the MDM2 inhibitor Nutlin-3a alone and in combination with SH-4-54, a newly synthesized STAT3 inhibitor. Cell viability was evaluated 72h after drug treatment with concentrations of Nutlin-3a ranging from 5 to 50 μM as single treatment or combined with a 5 μM of SH-4-54. Treatment with Nutlin-3a decreased viability in all cell lines (Fig 3.2). Concentrations of Nutlin-3a as low as 5 μM reduced viability of GBAM1, GBM10 and U87MG to 82%, 75% and 35% respectively. Yet, increasing Nutlin-3a concentration to 25 μM did not affect viability when compared to 5 μM. Further increase in Nutlin-3a concentration to 50 μM caused a drastic decrease in GBM viability, especially in GBM43 and U87MG than presented only 20% viability after treatment. Stem-like GBAM1 presented less sensitivity to Nutlin-3a than the other cell lines reaching 65% viability at maximum concentration studied (50 μM). Treatment with SH-4-54 reduced viability of stem-like GBAM1 when combined with 5 and 50 μM of Nutlin-3a, however combination treatment had no effect on GBM10, GBM43 or U87MG viability compared to single Nutlin-3a treatment.

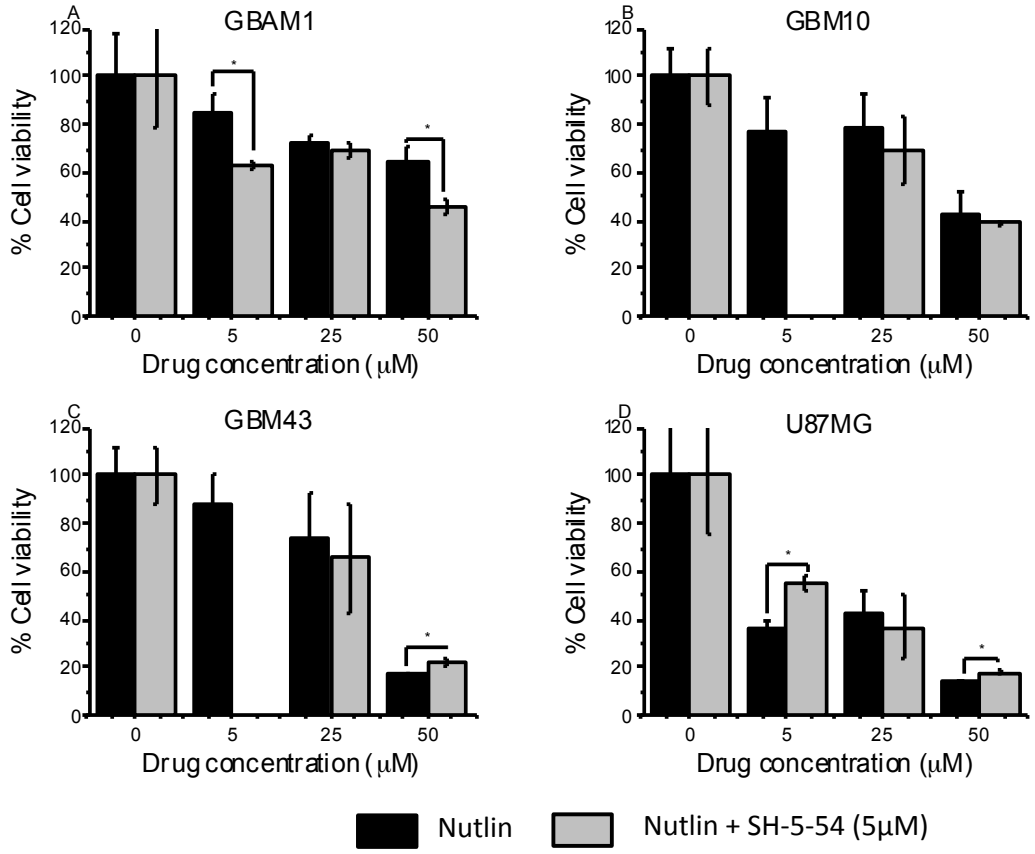

Figure 3.2 Nutlin-3a treatment decreases the viability of all GBM cell lines studied. Combination of Nutlin-3a with SH-4-54 further decreases viability in stem-like GBM cell line GBAM1 but does not potentiate the effect of Nutlin-3a in non-stem GBM cells. * Represents statistical difference at α=0.05.

3.3.3 Dimensionality influences GBM response to drug treatment

Since the cell lines GBM10 and stem-like GBAM1 presented similar responses to TMZ and Nutlin-3a but had very different responses to anti-STAT3 treatment, we evaluated the drug response of cells cultured both, in standard 2D liquid monolayer and in a brain-like 3D model of collagen-hyaluronan. GBM viability after drug treatment tends to be higher for cells cultured in the 3D model compared to 2D liquid, although in certain cases, for

instance when the drug effect is very low (SH-4-54 on GBM10) the difference in survival between 3D and 2D culture is not significant. Interestingly, GBM10 treatment with Nutlin-3a showed a very different tendency compared to other drugs and cell lines, in this particular case, viability during 3D culture was lower than in 2D liquid. In general, in contrast to 2D liquid culture, viability in 3D culture after treatment was greater than 75% despite the drug or concentration used, which likely suggests that dimensionality and presence of the extracellular matrix plays a role on GBM survival after chemotherapeutic treatment.

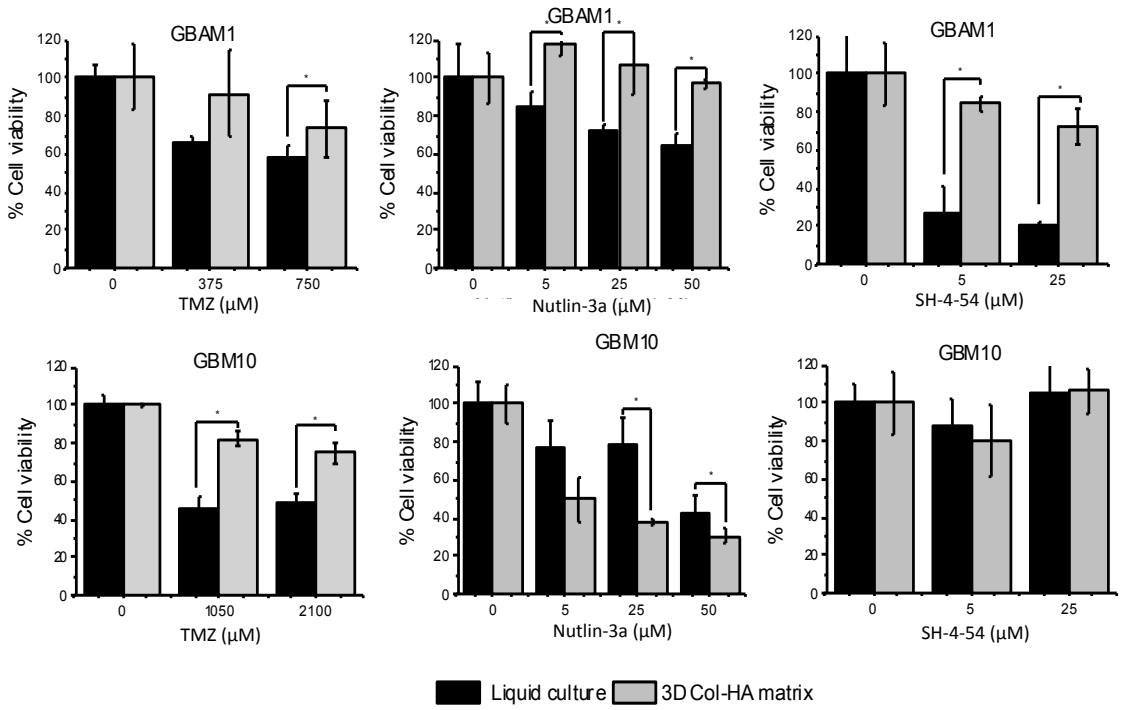

Figure 3.3 Differential effects on drugs on GBAM1 and GBM10. The presence of a 3D ECM reduces the cytotoxic effect of all drugs tested in GBAM1. However presence of the ECM has a differential effect on GBM10 viability. * Represents statistical difference at α=0.05.

3.3.4 3D co-culture with astrocytes increases viability of GBAM1 after TMZ treatment

Stromal cells present in the tumor microenvironment influence tumor progression. In the case of brain, astrocytes are the main non-neural cell type and comprise nearly 50% of total brain volume. To determine the influence of stromal cells in GBM drug response, we incorporated astrocytes along with GBM cells into the 3D model of collagen-hyaluronan to evaluate GBM survival after treatment with temozolomide. Incorporation of astrocytes significantly increased viability of the stem-like cell line GBAM1 after TMZ treatment compared to GBM 3D culture without astrocytes (Fig 3.4). In contrast, there was only a slight increase in GBM10 viability in presence of astrocytes. Presence of astrocytes in the 3D model increased viability of the stem-like cell line GBAM1 from 60% to 120% and from 59% to 72% in GBM10 after TMZ treatment when compared to 2D liquid culture, showing that combined factors such as presence of the ECM and brain stromal cells can act synergistically to decrease GBM sensitivity to drug treatment when compared to standard 2D liquid culture.

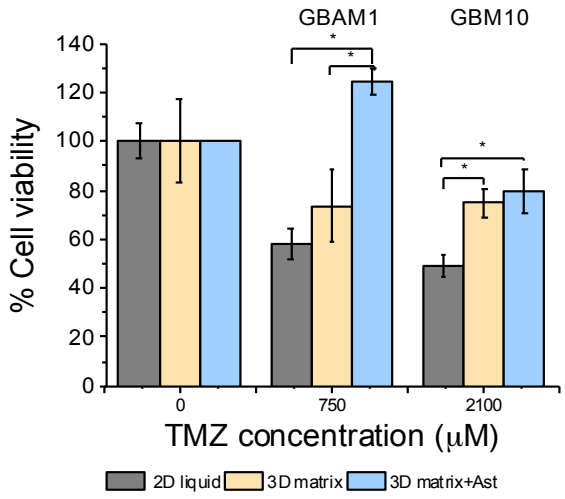

Figure 3.4 Astrocyte co-culture with GBM in 3D culture decreases the cytotoxic effect of temozolomide in GBAM1 compared to only-GBM 3D culture. * Represents statistical difference at α=0.05.

3.3.5 3D co-culture with ECFC and astrocytes increases viability of GBM after drug treatments

A hallmark of GBM is the ability to induce angiogenesis to support tumor growth. Vascular proliferation is a defining histological feature separating GBM from lower grades of astrocytoma. To address the importance of endothelial cells in the GBM microenvironment and therefore tumor drug response, we incorporated endothelial colony forming cells (ECFCs), able to form vascular networks, with astrocytes and GBM cells into the 3D model of GBM ECM. The multicellular 3D model was then treated with the STAT3 inhibitor SH-4-54, combination of Nutlin-3a (25 μM) – SH-4-54 (5 μM) and triple combination of Nutlin-3a (25 μM) – SH-4-54 (5 μM) - TMZ (750 μM for GBAM1 and 2100 μM for GBM10) to determine the effect of normal brain cells on

GBM survival. Presence of astrocytes and ECFCs increased GBAM1 survival to nearly 100% survival after treatment with SH-4-54 compared with 38% in 2D liquid culture, and 80% in 3D culture. GBAM1 viability after dual or triple drug combination was higher in co-culture with ECFCs and astrocytes compared to liquid culture but not significantly different than in 3D culture without stromal cells. Co-culture of astrocytes and ECFCs in the 3D GBM10 cultures increased survival following triple treatment from 35% in liquid culture and 25% in 3D culture without stromal cells to 75% in 3D co-culture.

Interestingly, GBM cells cultured in the 3D model with ECFCs and astrocytes exhibited an overall survival higher than 70% despite the drug combination that was applied. The effect of ECFCs and astrocytes on increasing GBM survival was especially evident after drug treatments that were very effective in decreasing survival in 2D culture such anti-STAT3 drug SH-4-54 for GBAM1 and triple combination of SH-4-54 - Nutlin-3a - TMZ for GBM10.

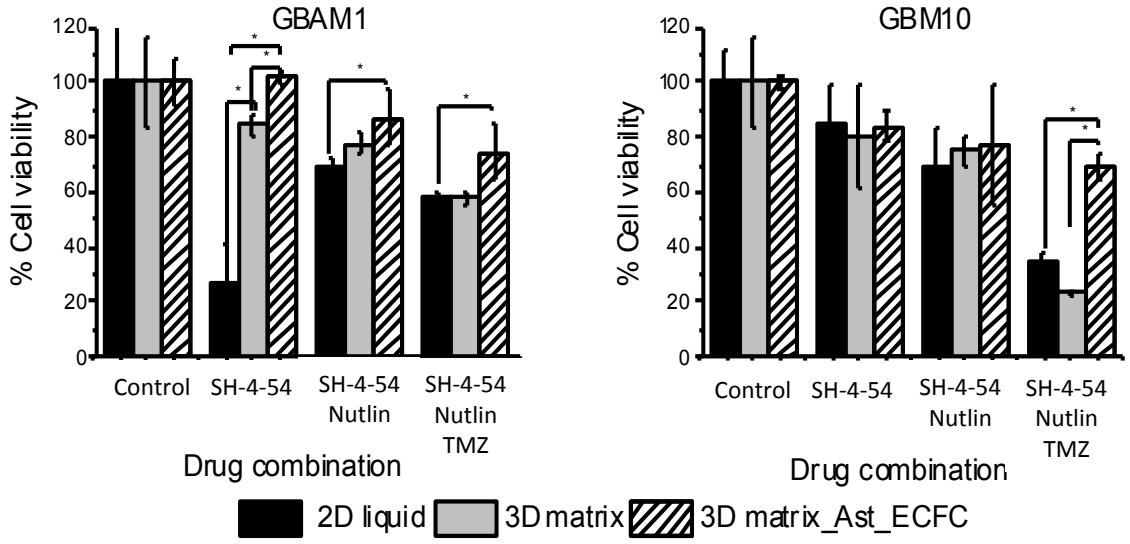

Figure 3.5 Presence of stromal cells in the 3D extracellular matrix drastically reduces the cytotoxic effect SH-4-54 STAT3 inhibitor on GBAM1 and the effect of triple drug combination of GBM10. * Represents statistical difference at α=0.05.

3.4 Discussion

Despite the widely recognized importance of the microenvironment as modulator of tumor behavior, current models for drug screening do not recapitulate the essential components of the tumor microenvironment like the presence of extracellular matrix and stromal cells. Previous studies have shown that cancer cells cultured in 3D environments can present either higher or lower sensitive to chemotherapeutic agents compared to cells cultured in standard 2D liquid culture.[92–97] Although assessment of drug response varies widely depending on factors such as cancer cell line studied, 3D-culture approach, drug evaluated or presence of non-tumor cells, it has become clear that many characteristics of the microenvironment play a role in how cancer cells respond to treatment. In this study

we evaluated the effect of the extracellular matrix and presence of brain stromal cells on survival of GBM after treatment with chemotherapeutic agents by using a developed 3D model that recapitulates the characteristics of the brain extracellular matrix and the presence of brain stromal cells. We observed that presence of a 3D extracellular matrix as well as astrocytes and ECFCs increases the survival of GBM stem-like cells after drug treatments compared to standard 2D liquid culture. Similarly, dimensionality and stromal cells affected viability of non-stem cells after treatment, however the drug effect was diminished or dependent on the drug tested when compared with GBM stem-like cells. Is important to note that GBM10 in 2D and 3D-matrix culture was relatively resistant to all treatments except to triple treatment, hence the effect of extracellular matrix and stromal cell on GBM10 viability was only well appreciated following triple drug treatment.

Evaluation of survival after drug treatment performed in 2D liquid culture showed that the GBM cell lines used in this study present low sensitivity to TMZ (IC50 values higher than 700 μM) as well as varied sensitivity to the MDM2 inhibitor Nutlin-3a and STAT3 inhibitor SH-4-54. Nutlin-3a treatment visibly reduced the viability of non-stem GBM cells lines GBM10, GBM43 and U87MG but had a lesser effect on viability on the stem-like cell line GBAM1. Sensitivity of the non-stem cell lines GBM10, GBM43 and U87MG to Nutlin-3a can be linked to p16 deletion in GBM10 and GBM43[91] and in U87MG. Given the decreased functionality of p16, that functions as an MDM2 negative regulator, we expected higher than normal MDM2 activity in these lines. Disruption of the MDM2-p53 interaction by Nutlin-3a and consequent reduction of p53 degradation will lead to decreased viability especially in cells with high activity of MDM2 as the non-

stem GBM lines studied. Effectively, Nutlin-3a reduced the viability of non-stem cell lines presenting mutations on p16 compared to the stem-like cell line GBAM1. Previous studies have recognized Nutlin-3a as an inducer of cell cycle arrest and apoptosis in wt-p53 GBM cell lines.[98] Interestingly, our results show that p53 mutants such as GBM43 respond to Nutlin3a treatment in a similar way than wt-p53 cell lines GBM10 and U87MG. When Nutlin-3a was combined with the anti-STAT3 inhibitor SH-4-54 as an attempt to decrease viability, only stem-like cells showed reduction in viability compared to only Nutlin-3a treatments. Our results are in concordance with previous studies that shown that inhibition of STAT3 function is detrimental for the proliferation and survival of stem-like brain cancer cells[90,99]. Studies by Rahaman (2002)[100] demonstrated that inhibition of constitutive expression of STAT3 is lethal for GBM cells. In our studies we did not observe such lethality, likely due to the fact that SH-4-54 inhibits phosphorylation and dimerization of STAT3 but does not deplete constitutively expressed STAT3.

Evaluation of the role of dimensionality on GBM viability was performed in GBM10 and GBAM1 by comparing viability after drug treatment in liquid culture and in the 3D model. Presence of ECM influenced viability of the stem-like line GBAM1 regardless of the drug treatment applied. In all cases presence of the 3D ECM reduced the effectiveness of the drug and increased GBAM1 cell viability. Previous assessment of the effect of dimensionality on stem-like GBM cells was done on collagen surfaces as semi 3D-culture platforms. Similar to our results GBM stem-like cells treated with other drugs like multikinase inhibitors exhibited increased viability in semi 3D platforms compared to liquid culture.[97]

The effect of the ECM on GBM10 viability differed depending on the treatment applied. Presence of the 3D ECM reduced the effectiveness of TMZ but increased the effect of Nutlin-3a. Viability after treatment with the inhibitor SH-4-54 was very similar in 2D and in 3D, likely due to poor effectiveness of the compound to decrease GBM10 viability or due to lack of STAT3 activity. Drug response has been previously evaluated in 3D platforms and compared to 2D liquid response in various cancer cell lines with mixed outcomes regarding the effect of the ECM on increasing or decreasing sensitivity of cells to treatment. For instance, chemotherapeutic agents such as doxorubicin, paclitaxel and tamoxifen were less effective in reducing viability of breast cancer cells in 3D matrices compared to liquid culture.[96,101] In contrast, other studies suggest that pancreatic and breast cancer cells cultured in 3D matrix presented increased sensitivity to drug treatment compared to liquid culture.[94,95]

Different to the effect of ECM, the role of stromal cells on cancer drug response has been less explored. Previous attempts to assess the effect of stromal cells on cancer viability after drug treatment were performed in 2D liquid culture or using cancer cell spheroids. In both studies it was observed that the presence of stromal cells such as astrocytes and fibroblasts reduced effectiveness of drug treatments in GBM and breast cancer respectively.[102,103] Still, to the best of our knowledge our 3D model for multiple co-culture of stromal and GBM cells is the first attempt to recreate an *in vitro* brain tumor microenvironment that combines dimensionality, similar GBM ECM and stromal cells for testing the effectiveness of drug treatment on GBM. Similar to the results obtained by Chen (2015),[103] which demonstrated that GBM and astrocytes co-culture at a ratio 2:1

decreased GBM apoptosis after TMZ or vincristine treatment, we observed that a protective effect of astrocytes. Presence of astrocytes at a ratio 1:1 to GBM cells decreased sensitivity of GBAM1 to TMZ compared to both liquid culture and 3D culture without stromal cells. In contrast, presence of astrocytes decreased sensitivity of GBM10 compared to liquid culture and not to the 3D culture without astrocytes.

Dual presence of astrocytes and ECFCs reduced the effect of drug treatments that were very effective in liquid culture in both non-stem and stem-like GBM cell lines. Interestingly, we observed that presence of stromal cells in the 3D microenvironment had a greater effect on protecting the stem-like cell line GBAM1 against chemo-agents compared to the non-stem cell line GBM10. The greater effect of the microenvironment decreasing the sensitivity of the GBM stem-like cells to drug treatments suggest that for cancer stem-like cells as for normal cell progenitors the microenvironment is a complex and dynamic entity that regulates, supports and protects stem cell function.

3.5 Summary

In this study we described the effect of different components of the tumor microenvironment such as dimensionality and presence of stromal cells on the sensitivity of GBM cells to various chemotherapeutics agents. To this end we generated a 3D model that represents the physical, compositional characteristics of GBM ECM as well as the presence of stromal cells astrocytes and vasculature-forming cells. Presence of a 3D matrix with similar composition to GBM ECM decreased the cytotoxic effect of TMZ,

Nutlin-3a and STAT3 inhibitor SH-4-54 on the stem-like line GBAM1 compared to standard 2D liquid culture; however had a varied effect in the non-stem line GBM10.

Incorporation of astrocytes within the 3D GBM ECM model further reduced the effect of TMZ on GBAM1 compared to liquid culture and GBM 3D culture without stromal cells. Astrocyte presence reduced sensitivity of the non-stem cell line GBM10 compared to liquid culture but had little effect compared to 3D culture without stromal cells, suggesting a possible greater protective effect of astrocytes on GBM stem-like cells. Combined presence of ECFCs and astrocytes into the 3D model decreased the toxicity of drug treatments on GBAM1 compared to liquid culture, and reduced the toxicity of STAT3 inhibition compared to 3D culture without stromal cells.

Presence of stromal cells had a lesser effect on GBM10 viability. Is important to note that GBM10 was isolated form a recurrent GBM patient and presented overall poor response to drug treatment. Therefore, the effect of the stromal cells on viability was only evident after aggressive treatment with triple combination of TMZ - Nutlin-3a - SH-4-54.

The recreation *of an in vitro* model of the tumor microenvironment offers a unique tool to study how different factors of the environment contribute to GBM response to chemo-agents in order to generate therapies potentially translational to *in vivo* settings.

CHAPTER 4. DIMENSIONALITY AND PRESENCE OF STROMAL CELLS INFLUENCE GLIOBLASTOMA MIGRATION

4.1 Introduction

Glioblastoma (GBM) is characterized by rapid infiltration across brain parenchyma. Prior to tumor surgical resection, cells from the primary mass leave the tumor and invade healthy brain tissue to form new satellite tumors that ultimately lead to patient relapse.[14] Synergistic relationships between tumor cells and the local microenvironment have been recognized as fundamental modulators of GBM migration and colonization strategies.[104–106] During GBM development, intercellular signaling between tumor cells and normal tissue constitutes one of the first steps towards the formation of a supportive microenvironment. Recruitment of supportive stromal cells such as vasculature forming cells during angiogenesis, and suppression of microglia and T-cells normal functions are essential for the maintenance of the tumor as a functional, self-regulating entity. [107]

Interactions of the tumor with its microenvironment and paracrine signaling with the supportive stroma promote GBM migration and are associated with the presence of similar migration patterns exhibited by the neural progenitors during early stages of the central nervous system (CNS) development.[13] Such specific interactions are also linked to the unique rapid and productive infiltration of GBM into healthy tissue when compared

to other types of cancer. Further evidence of the importance of tumor-microenvironment interaction is the possible correlation between tumor location and patient survival. Patients with GBM located in the deep grey matter, which is formed mainly by the neurons cell body, present longer survival that patients with GBM located in the brain lobes, formed mainly by the axonal section of the neurons and astrocytes.[108]

Brain tissue is comprised by multiple types of cells; among the most prevalent populations are astrocytes, microglia, neurons and the cells comprising the vascular network (endothelial cells and pericytes). Astrocytes are the main glial components of brain stroma.[38] Previously, astrocytes were considered only as supporters of neural function and component of the brain blood barrier, only until recently their full function in maintenance of brain homeostasis has begun to be comprehended. Astrocytes undergo astrogliosis in presence of GBM cells,[109] in a response that recapitulates their behavior after CNS injury. Reactive astrocytes increase secretion of cytokines that facilitate cell growth and migration as a response mechanism to control brain damage.[39] It has been hypothesized that GBM take advantage of astrogliosis signaling to facilitate invasion.[38,40,109,110] Among the most important signals associated with astrogliosis and involved in tumorigenesis is the up-regulation of matrix metalloproteinases (MMP) expression. MMPs are a family of proteinases able to remodel the microenvironment through degradation of multiple component of the extracellular matrix.[111] Besides being important drivers of invasion (migration, extravasation and intravasation), MMPs are also potent regulators of angiogenesis, and inflammation, all processes deregulated in cancer.[111]

MMP activity is regulated through many strategies, by repression of expression, presence of inhibitors, or secretion of an inactive isoform that will be activated by signaling cues of the microenvironment when required.[111] The delicate balance of inhibiting MMPs is fundamental to avoid undesired degradation of tissue. However, during tumorigenesis the MMP activity is up-regulated facilitating the remodeling of the tumor microenvironment and the migration of cancer cells. Greater presence of MMPs in the GBM microenvironment has been associated to two factors, increased MMPs secretion by tumor cells or activation of present MMPs induced by paracrine signaling with the microenvironment, specifically with astrocytes.

Similar to astrocytes, recruitment of endothelial cells by GBM is a driving factor that contributes to tumor migration. Cooperative interaction between endothelial cells and GBM induces expression of pro-angiogenic signals, atypical proliferation of endothelial cells and tumor neovascularization.[37] Neovascularization is a hallmark of GBM and of the most important processes that lead to the rapid progression and invasion of the tumor. Due to the rapid proliferation of the cancer cells and destabilization of the vasculature, the tumor presents hypoxic regions that express hypoxia-inducible factor (HIF) α and β. As a response to hypoxia the tumor cells up-regulate the expression of vascular endothelial growth factor (VEGF) and attracts endothelial cells to initiate the formation of new vasculature. [85] New vascular networks can acts as migration routes for invasion of the tumor into healthy parenchyma.

Despite the well-recognized reciprocal interaction between the tumor and its microenvironment, many GBM studies are performed in formats that fail to recapitulate

the main characteristics of the tumor microenvironment, namely, presence of extracellular matrix and stromal cells. Here, we use a previously developed 3D *in vitro* model that recapitulates the compositional and mechanical features of GBM ECM with incorporated astrocytes and endothelial cells to elucidate the role of different components of tumor microenvironment on the migration of GBM.

4.2 Experimental Methods

4.2.1 Standard liquid cell culture

GBM human–derived cell lines GBM10, GBM43 and MHBT32 were maintained in high-glucose DMEM (Life Technologies, Carlsbad, CA) supplemented with 10% FBS. GBM human cell line GBAM1 (CD133+ >98%) was maintained in DMEM/F12 supplemented with B27 without vitamin A (Life Technologies, Carlsbad, CA) and with growth factors EGF, bFGF (50 ng/ml each, Peprotech, Rocky hill, NJ). Human primary astrocytes from ScienCell (Carlsbad, CA) were maintained according to vendor specifications. Endothelial umbilical cord blood ECFCs from EndGenitor Technologies (Indianapolis, IN) were maintained in collagen type-I coated plates with EGM-2 medium (Lonza, Walkersville, MD) as described by Whittington (2013). All cell lines were cultured at 37°C in an atmosphere of 5% CO_2, fed with complete media every other day and passaged at 70-80% confluence. To obtained astrocyte conditioned medium, astrocytes were seeded at an initial density of 5000 cell/cm^2 and cultured according to vendor specifications for 5 days, the media was collected centrifuged at 1000rpm for 5 min to eliminate possible present cells.

4.2.2 3D Cell culture

3D matrices of collagen-hyaluronan were generated using pig skin oligomer collagen (GeniPhys, Zionsville, IN) at concentration of 2 mg/ml and sodium hyaluronate (MW 351-600) KDa (Lifecore Biomedical, Chaska, MN) was incorporated at 10 mg/ml as described previously in Chapter 2. Cells were suspended at the desired concentration in the 3D matrix prior polymerization at 37°C for 30 minutes. Complete media was added to the top of the matrix, and cells were cultured at 37°C in an atmosphere of 5% CO_2.

4.2.3 Migration on 2D surfaces

Cells were tested for viability, stained with CellTracker™ Green CMFDA dye (Life Technologies, Carlsbad, CA) for visualization and plated on glass-bottom well plates at a density of 15000 cell/cm^2 and fed with appropriate media; plates used for GBAM1 cells were coated with 1.5 μg/ml of Poly-L-lysine in water. For migration assays involving co-culture with astrocytes or with astrocytes and ECFCs, astrocytes and ECFCs were initially plated at 15000 cell/cm^2 density and cultured 24h before the addition of GBM cells to allow attachment to the plate surface. After GBM addition to the co-culture, cells were fed with media containing equal volumes of complete GBM, astrocytes and ECFC media and incubated during 4h for attachment of GBM cells and placed in an on-stage incubator chamber to perform time-lapse confocal microscopy every hour during 15h.

4.2.4 Migration in 3D brain-like matrix

GBM cells were stained with CellTracker™ Green CMFDA dye (Life Technologies, Carlsbad, CA) and embedded at a density of $1*10^6$ cells/ml within the collagen-hyaluronan matrix before polymerization. For assays involving astrocytes and/or ECFCs, all the cells were embedded at the same time in the matrix prior polymerization and at the same density ($1*10^6$ cells/ml each population). Volumes of 30 µl of matrix per well were platted in a µ-slide angiogenesis chamber (Ibidi, Germany). After matrix polymerization, 30 µl of media were added per well, co-cultured cells were fed with media containing equal volumes of GBM, astrocytes and ECFC media and maintained in incubation at 37°C in an atmosphere of 5% CO_2 for 24 h. Afterwards, cell were placed in an on-stage incubator to perform time-lapse confocal microscopy every 90 min during 15h.

4.2.5 Time-lapse confocal imaging and migration analysis

Cell migration was monitored by time-lapse microscopy using an Olympus FV1000 confocal microscope equipped with 488 nm argon laser (Figure 4.1). Optimal growth cell conditions were maintained using on-stage incubator chamber at 37°C in an atmosphere of 5% CO_2. Z-stacks of 200 µm were acquired using 12-15 µM steps; initial and final z positions were chosen to be at least 50 µm separated of the surface or the plate interface. Different areas (4 to 9 areas) were acquired per sample (each individual area of 0.0187 mm^2) to cover at least 60% of the total area of the well. Image stacks were projected as XY images for migration analysis. Trackmate plugin from FIJI was used to analyze the time-lapse images using LoG (Laplacian of Gaussian) detector, assuming a blob diameter of 10 pixels (all images were 512 pixels, 2.67 µM per pixel) and threshold of 1 pixel,

without sub-pixel localization. LAP tracker option was chosen allowing frame to frame linking and closing of 15 pixels in 3D migration experiments and 25 pixels in 2D migration experiments. Data was filtered to only account for cells visible during the total time of the experiment. Raw data from Trackmate was analyzed using the Chemotaxis tool plugin for ImageJ (Ibidi, Germany) to obtain accumulated distance, net distance and directionality (ratio of net to accumulated migration distance). Accumulated distance represents all the distance travelled by the cell while net distance only represents the distance between the initial and final position of the cell. Migration velocity was calculated by dividing accumulated distance by total time of migration. Directionality as evaluated here makes reference to intrinsic directionality and represents the degree of persistence of movement of a cell in the absence of a directional stimulus.

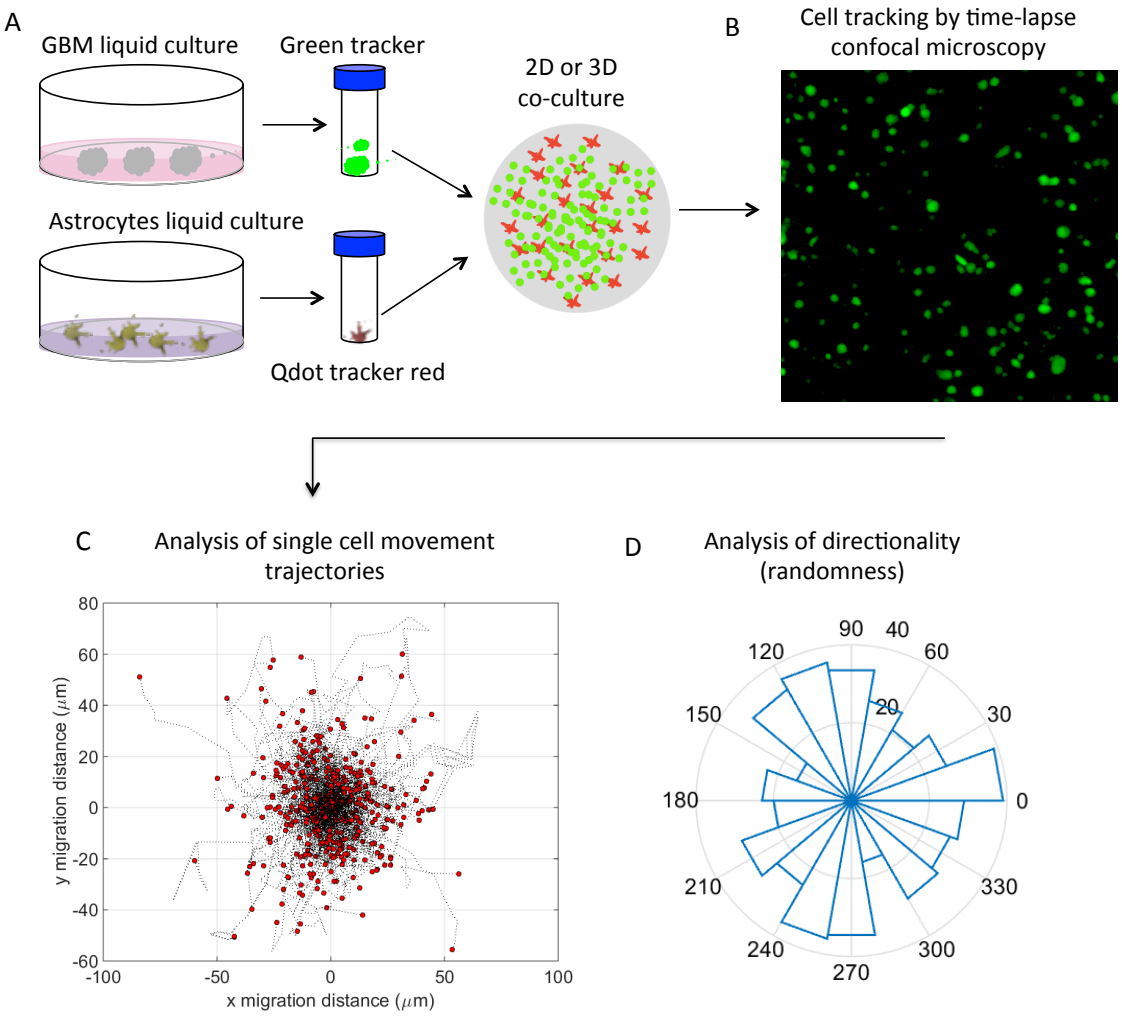

Figure 4.1 Experimental setup to analysis GBM migration in co-culture with stromal cells. A. Cell populations are expanded in liquid culture, recovered and labeled with different fluorophores for movement tracking. B. Individual cells are tracked over time every 1.5h by confocal microscopy. C. Images generated are analyzed to obtain the position of every cell on time and calculate the displacement trajectories. D. Initial and final position of the cells are used to evaluate the directionality of movement.

4.2.6 Modified 3D co-culture culture method for protein extraction

GBM cells were embedded in collagen-hyaluronan matrices at a density of $3.5*10^5$ cells in 200 µl of matrix and platted in 48 multi-well plates for polymerization. To achieve 3D co-culture of astrocytes and GBM that allowed protein extraction of the different populations, the polymerized matrix containing the GBM cells was recovered and placed in the center of a well in a 24 multi-well plate. Subsequently 200 µl of collagen matrix with $3.5*10^5$ astrocytes were pipetted to the surroundings to form a concentric ring with the astrocytes layer in the outside and the GBM layer inside. The matrices were incubated during 30 min at 37°C to allow complete polymerization. Media containing equal amounts of astrocyte and GBM media were added to the culture. Cells were maintained at 37°C in an atmosphere of 5% CO_2 for 72 h. For protein extraction the concentric ring was separated to obtain the layers containing each of the cell populations.

4.2.7 Western Blot analysis

Cells in 3D culture were washed with ice-cold PBS and incubated with RIPA buffer supplemented with 1X Halt™ protease and phosphatase inhibitor cocktail (ThermoFisher Scientific, Waltham, MA) at 4°C for 3 h with constant agitation followed by centrifugation at 12000 rpm during 20 min to recover the supernatant. Total protein concentration was quantified by Pierce BCA protein assay (ThermoFisher Scientific, Waltham, MA). Equal amounts of protein samples were denaturalized and loaded in 4-20% polyacrylamide gels (Biorad, Hercules, CA). Samples were transfer to PVDF membranes (ThermoFisher Scientific, Waltham, MA). Membranes were blocked with Odyssey blocking solution TBS (Licor, Cambridge, UK) at room temperature for 1 h and

incubated with primary antibody diluted in blocking solution during 12 h at 4°C. Afterwards, membranes were washed three times for 3 min each with TBS-T buffer (0.075% Tween-20) and incubated with secondary antibody 1 h at room temperature. Prior to visualization, membranes were washed 3 times 3 min each with TBS-T buffer. Primary antibodies used were β-actin (dilution 1:1000), MMP-9 (1:1000) from Cell Signaling (Danvers, MA), and MMP-2 (1:1000), MMP-14 (1:1000) from Abcam (Cambridge, UK). Secondary antibodies IRDye800CW anti-rabbit and IRDye680RD anti-mouse (Licor, Cambridge, UK) were used at a dilution 1:2000. Visualization was performed in Odyssey Clx System (Licor, Cambridge, UK). Quantification of western blot band intensity was performed in ImageJ.

4.2.8 Statistical analysis

All measurements are expressed as mean ± SE unless otherwise stated. Statistical analysis was performed in Origin. Comparisons between treatments were made using two samples t-test or one-way analysis of variance (ANOVA) with Tukey-Kramer mean comparison. Statistical significance was evaluated at $\alpha = 0.05$.

4.3 Results

4.3.1 GBM migration in 3D brain-like matrix is slower and more directional than in 2D rigid surfaces

Despite the increasingly recognized influence of the 3D microenvironment on cell adhesion and migration, cell migration is usually evaluated in 2D rigid or semirigid platforms by scratch assay or Transwell migration assays. To identify and quantify the differences of migration in 2D liquid culture and a 3D matrix platforms we compared distance, velocity and directionality (persistence) of migration of three different GBM cell lines (GBM10, GBM43 and GBAM1) when cultured on a rigid culture dish (standard 2D liquid culture) and within a 3D matrix of collagen-hyaluronan that recapitulates composition and mechanical properties of GBM ECM. All GBM cell lines studied showed greater accumulated migration distance in 2D culture compared to culture in 3D Col-HA matrix (Fig 4.2). However, comparison among cell lines showed that non-stem GBM lines GBM43 and GBM10 exhibited higher migration distances on 2D platforms compared to the stem cell line GBAM1. Interestingly, cell line GBM10 that reached the greatest migration distance in 2D exhibited very low migration distances when cultured in the 3D matrix. A similar trend was observed for net migration distances, where 2D platforms offered a more permissive migration platform compared to the 3D matrix. Analysis of directionality of migration showed that directionality of GBAM1 and GBM43 was higher in 3D culture compared to 2D culture, this was to be expected given the presence of extracellular matrix promotes protrusion stabilization during migration.[80]

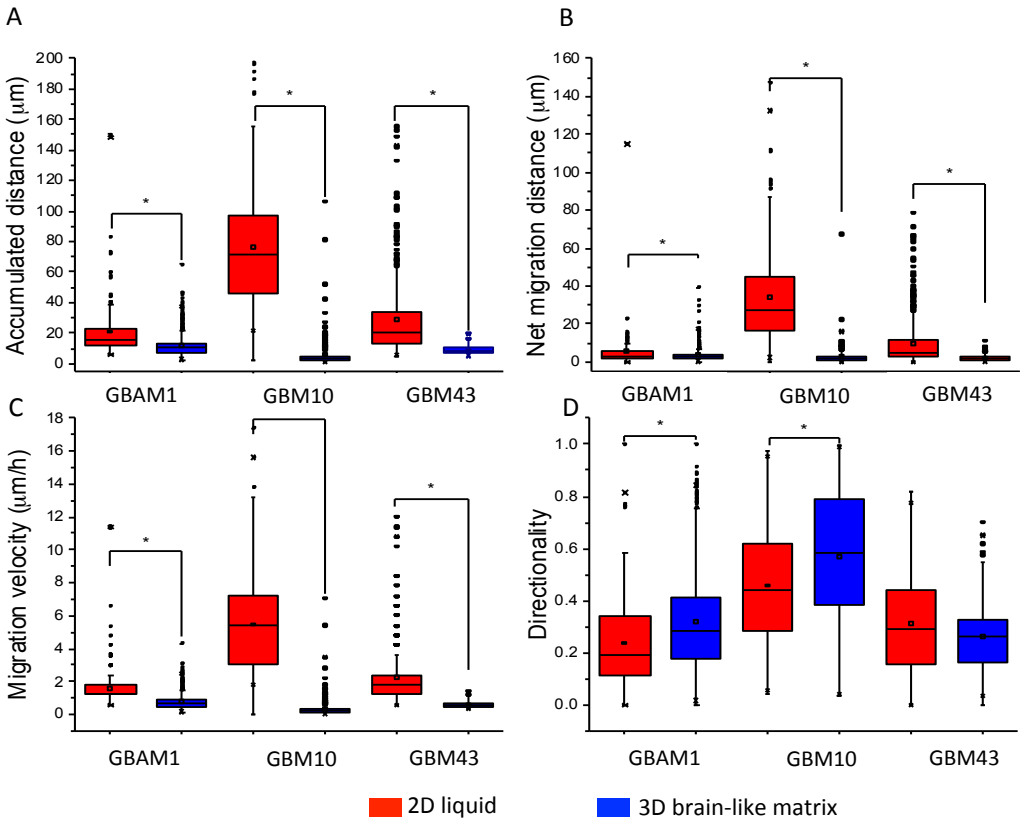

Figure 4.2 Migration of GBM in a 3D matrix presents short accumulated and net migration distance and higher intrinsic directionality. A. Accumulated distance of migration in 15h. B. Migration distance between initial (0 h) and final migration point (15 h). C. Migration velocity calculated as accumulated distance over total time. D. Directionality of migration (accumulated/net distance). Data represent n=400-1500 individual cells and is presented as boxes indicating first, second and third quartile and outliers. * Represents statistical difference at α=0.05.

4.3.2 Interaction with astrocytes increases GBM migration in 2D culture

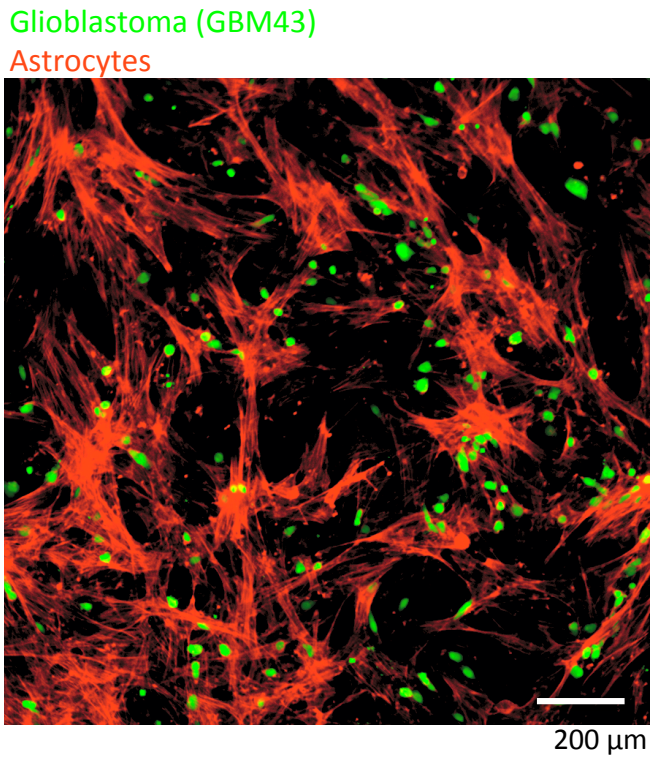

Figure 4.3 Astrocytes and GBM cells in 2D co-culture have direct physical contacts. Astrocytes present a more extended morphology that covers almost completely the 2D surface compared to the GBM cells despite been present at the same density.

As demonstrated, clear differences between migration on 2D surfaces and in 3D matrices exist. To gain further insight into differences between 2D and the 3D matrices we next tested the effect of astrocytes on GBM migration. We generated a layer of astrocytes on a rigid surface and seeded GBM cells on the astrocyte layer. With this experiment we attempted to corroborate that astrocytes have the same effect on 3D migration of non-stem GBM cells as what has been previously observed on GBM stem-like cell migration. Observations of the two cell populations in 2D culture, showed a marked difference in the morphology of the astrocytes and GBM cells. Despite been present at the same

density, the astrocytes extended their body covering a considerable part of the whole surface culture, while the GBM cells presented a predominantly rounded morphology with occasionally spindle-like deformation during movement, and could be seen spaciously distributed on the surface (Figure 4.3). Migration analysis of all the GBM cell lines studied showed that presence of an astrocyte layer increases GBM migration. GBM cells were able to reach almost 2-fold greater migration distances (both accumulated and net) in presence of astrocytes than cultured alone (Fig 4.4 A, B). To further determine the mechanism involved in increased GBM migration due to presence of astrocytes, we evaluated migration of GBM cells cultured with astrocyte-conditioned media (ACM). Presence of ACM did not increase migration. GBM cells cultured with ACM presented similar migration distances to GBM cultured alone in normal media (Fig 4.4 A, B), suggesting the dynamic interaction between the two populations caused a greater migratory behavior of GBM cells.

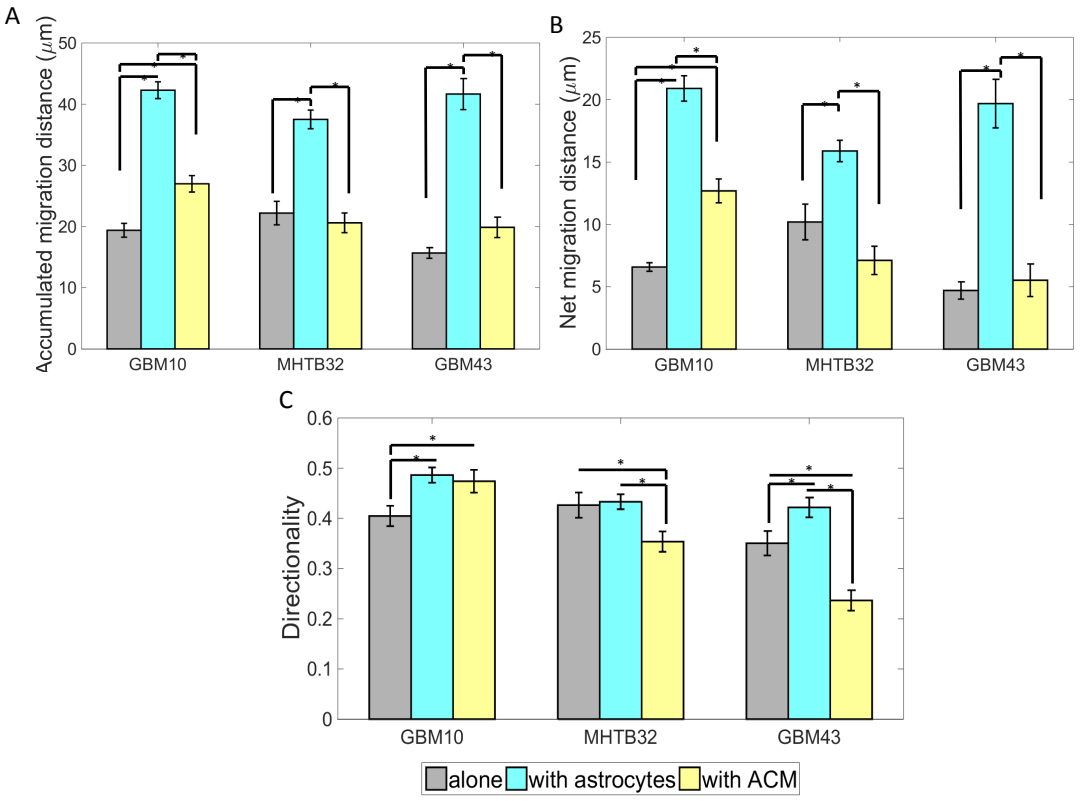

Figure 4.4 Presence of astrocytes but not astrocyte conditioned media increases GBM cell migration. **A**. Accumulated distance of migration during 15 h. **B**. Net migration distance between initial (0 h) and final points of migration (15 h). C. Directionality of migration (accumulated over net distance). Bars indicate Mean ± SE from a population of **400-1500** individual cells. * Represents statistical difference at α=0.05

4.3.3 Presence of astrocytes increases GBM migration in 3D brain-like model

Given the effect of astrocytes presence on 2D GBM migration we further tested whether the same effect was observed during 3D culture in a matrix that represents the physical and compositional characteristics of the extracellular matrix (ECM) present in the GBM microenvironment. Equal numbers of human astrocytes and GBM cells were incorporated into the 3D matrix prior polymerization and GBM migration in 3D was

analyzed. Similar to what was observed in liquid culture, presence of astrocytes increased the 3D accumulated and net migration distance of all the GBM cell lines studied (Fig 4.5).

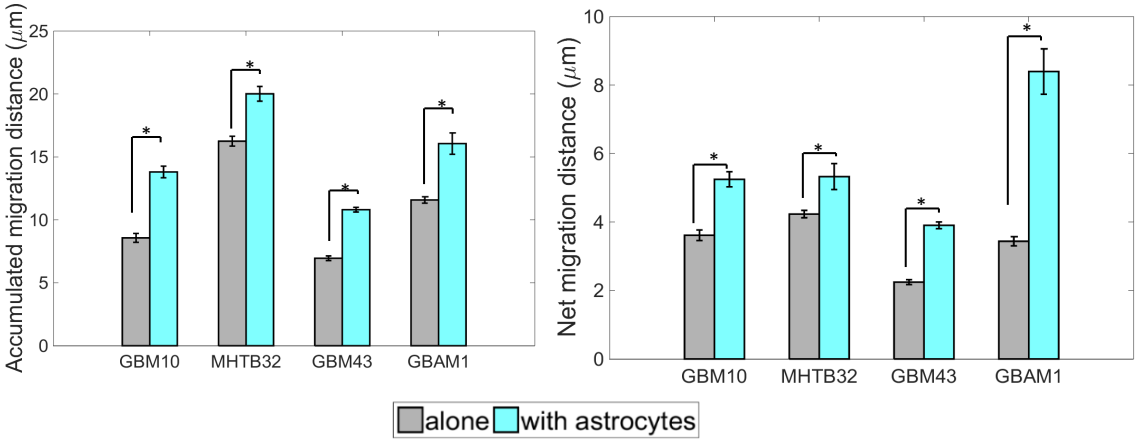

Figure 4.5 Presence of astrocytes increase migration of all GBM cultured in a 3D-brain-like model of collagen-hyaluronan. **A**. Accumulated distance of migration during 15 h. **B**. Net migration distance between initial (0 h) and final points of migration (15 h). Bars indicate Mean ± SE from a population of 400-1500 individual cells, from at least 2 independent repetitions * Represents statistical difference at α=0.05

In both cases, 2D liquid culture and in 3D-culture, presence of astrocytes increased GBM migration. However, is important to note that direct physical contact between the two population was certain in 2D (Figure 4.3) culture but not in 3D culture (Figure 4.6). In the 3D matrix, GBM and astrocytes were seeded at a concentration in which direct physical contact although probable was not predominant. Attempts to increase cell concentration to maximize contact as occurs *in vivo*, resulted in rapid matrix contraction and detachment of the constructa from the plates (data not shown).

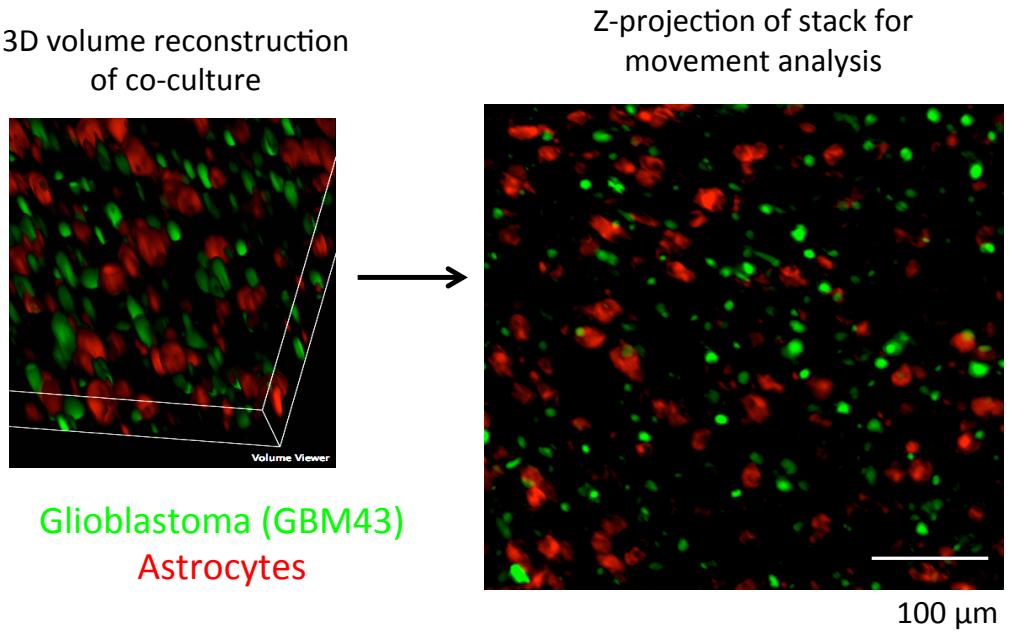

Figure 4.6 Co-culture of Astrocytes and GBM cells in a 3D-matrix. Both cell populations are homogeneously distributed within the matrix. At the cell density used for 3D culture studies the cells generally do not present physical contact with each other. GBM cells appear in green and astrocytes in red. Reconstruction of a volume of study with dimensions z: 80 µm x: 460 µm y: 460 µm.

4.3.4 3D co-culture of astrocytes and GBM cells affects GBM expression of matrix metalloproteinases (MMPs)

Increased GBM migration due to presence of astrocytes has been associated to physical interaction between the two cell populations and communication through gap junctions.[23,112] However, having observed that in 3D co-culture physical contact was not predominant, still the migration was higher in presence of astrocytes than during only-GBM culture, we hypothesized that astrocytes could affect GBM 3D migration by increasing the production of proteinases required for ECM degradation. Thus, we tested the effect of astrocyte presence on the GBM expression of MMP-2, and MMP-9, both

previously linked to GBM migration. Co-culture with astrocytes in the 3D model increased GBM production of MMP-9 but has a differential effect on the expression of MMP-2 (Fig 4.7). Presence of astrocytes slightly increased GBM10 expression of MMP-2 (both pro-enzyme at 72 kDa and activated enzyme 66 kDa). In contrast MMP-2 expression decreased in GBM43 cells in the presence of astrocytes.

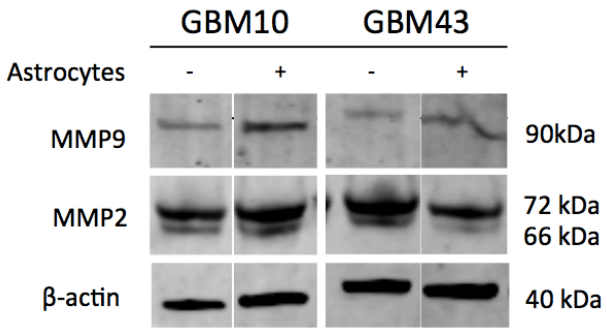

Figure 4.7 Presence of astrocytes during co-culture with GBM cells in a 3D brain-like model increases expression of MMP-9 and has a differential effect on MMP-2 expression (MMP-2 pro-enzyme: 72 kDa, MMP-2 active isoform: 66 kDa). 14µg of total protein were loaded form each sample.

4.3.5 Dual presence of endothelial colony forming cells (ECFC) and astrocytes increases GBM migration on 2D surfaces

The two principal structures used by GBM to migrate across healthy brain parenchyma are axonal tracks and blood vessels.[56] To evaluate the effect of vasculature-forming cells on the migration of GBM we co-cultured endothelial colony forming cells (ECFCs) and GBM cells at a ratio 1:1 as a monolayer on 2D surfaces and compared GBM migration when cultured alone and when cultured with ECFCs. We observed that presence of

ECFCs increased the accumulated and net migration of all GBM cell lines. The greatest effect of ECFCs on migration was observed in the stem-like cell line GBAM1 where presence of ECFCs increased accumulated migration more than 5-fold (Figure 4.8).

Given the increase of GBM migration observed due ECFCs and astrocytes as previously shown, we incorporated astrocytes and ECFCs in the same culture with GBM cells (ratio 1:1:1) to determine a possible synergistic effect of both cell populations on GBM migration. Dual presence of ECFCs-astrocytes further increased 2D GBM migration of all GBM cell lines evaluated compared to cultures with only presence of ECFC and GBM.

Differential effect of ECFCs on migration of different GBM cell lines, suggests that presence of only ECFCs has a greater effect on the migration of the stem-like cell line GBAM1 compared to non-stem cell lines GBM10 and GBM43. In contrast, migration of non-stem GBM cells is visibly increased by combined presence of ECFCs and astrocytes but not significantly affected by the presence of ECFCs only (Figure 4.8).

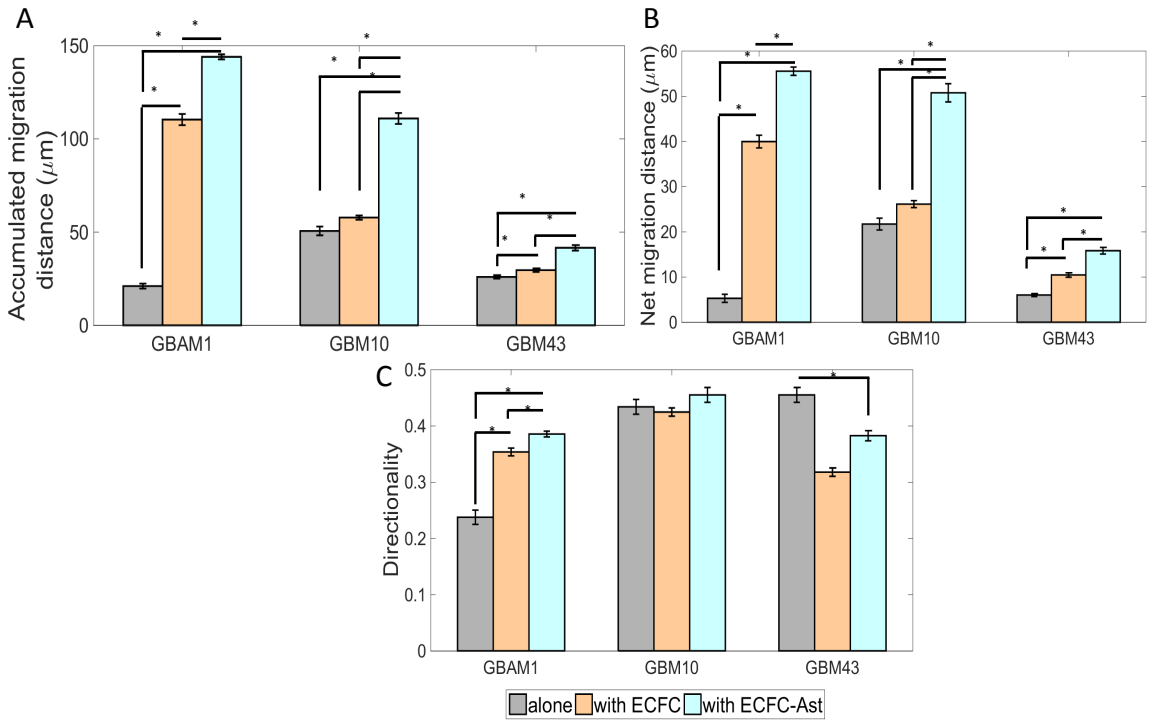

Figure 4.8 Co-culture with Endothelial colony forming cells (ECFCs) and astrocytes drastically increases overall migration of GBM on 2D rigid surfaces. Dual co-culture of GBM with ECFCs has great effect on GBAM1 migration but minimal influence on migration of GBM10 or GBM43. **A**. Accumulated distance of migration during 15 h. **B**. Net migration distance between initial (0 h) and final points of migration (15 h). **C**. Directionality of migration (accumulated / net distance). Bars indicate Mean ± SE from a population of 400-1500 individual cells. * Represents statistical difference at α=0.05.

4.3.6 Presence of ECFCs and astrocytes has an opposite effect on 3D migration of stem-like and non-stem GBM cells

To corroborate that presence of ECFCs and combined astrocytes - ECFCs had a similar effect in conditions more similar to *in vivo* settings; we used the 3D model of GBM ECM to analyze GBM migration in presence of ECFCs and astrocytes - ECFCs. Similar to what was observed in 2D, presence of ECFCs and dual presence of ECFCs and astrocytes

increased the accumulated migration of the non-stem cell lines GBM10 and GBM43, however, these co-culture conditions had the effect on the migration of stem-like cell line GBAM1 (Figure 4.9). Analysis of net migration shows that in 3D culture, presence of ECFCs or ECFC-astrocytes had no effect on the net distance covered by GBAM1; suggesting that GBAM1 in co-culture migrates shorter distances but with more directionality/persistence. Combined presence of ECFCs and astrocytes increased net migration distance of the non-stem cells similar to what was observed in 2D culture.

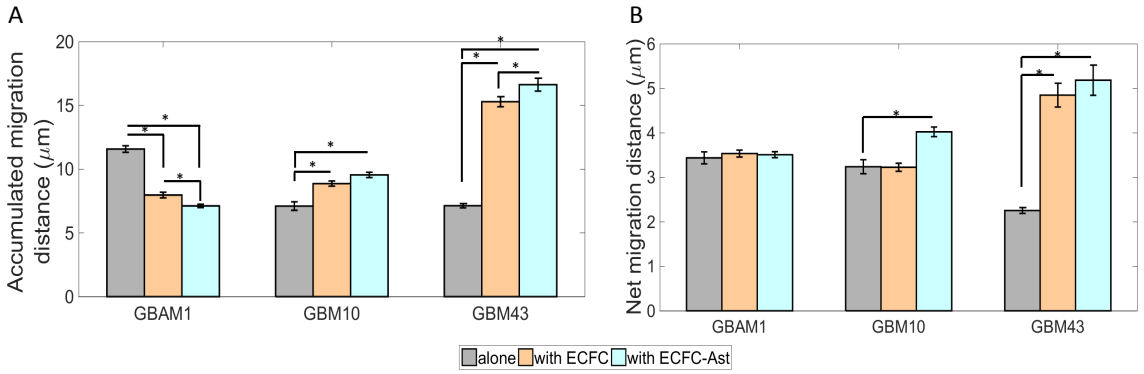

Figure 4.9 Dual presence of astrocytes and ECFCs increases accumulated migration distance of non-stem GBM cells (GBM10, GBM43), but decreases migration of the stem-like GBM cell line GBAM1. **A**. Accumulated distance and B of migration during 15 h. **B**. Net migration distance between initial (0 h) and final points of migration (15 h). Bars indicate Mean ± SE from a population of **400-1500** individual cells. * Represents statistical difference at α=0.05.

4.3.7 Presence of stromal cells increases directionality of GBM stem-like cells but decreases directionality of non-stem cells during 3D migration

Directionality or persistence of migration is a fundamental characteristic of migration that describes the real net migration achieved by the cell and involves how the cell respond to

multiple environmental and intrinsic signals to stabilize or generate more protrusions towards specific directions. Analysis of the directionality of migration in 3D culture indicated that non-stem GBM cell lines decreased directionality (greater random migration) in presence of stromal cells such as astrocytes, ECFCs or combination of both (Fig 4.10). However, presence of stromal cells increased considerably the directionality of the stem-like GBAM1 cells in the co-cultures evaluated (Fig 4.10). Given that in all conditions the properties of the extracellular matrix and the distribution of the stromal cells was homogeneous within the matrix, we suggest that presence of stromal cells increases intrinsic directionality of GBM stem-like cells but has the contrary effect on non-stem GBM cells.

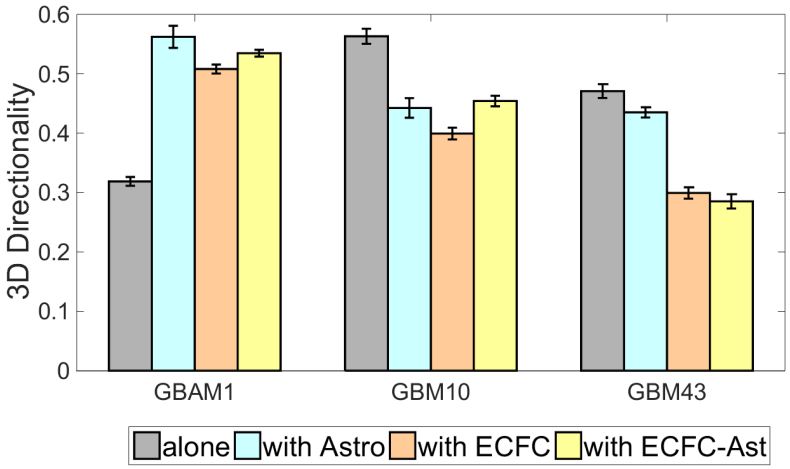

Figure 4.10 Presence of stromal cells in a 3D model increases migration directionality of GBM stem-like cells (GBAM1) but increases randomness of movement of non-stem GBM cells. Bars indicate Mean ± SE from a population of 400-1500 individual cells. * Represents statistical difference at α=0.05

4.4 Discussion

Aggressive and diffuse invasion across healthy brain parenchyma is characteristic of GBM. Despite the great efforts to surgically remove all the tumor cells, in many cases residual tumor cells are left in the tissue, mainly due to the impossibility to differentiate them from the peritumoral edema present at the margins tumor mass.

During tumor progression, cancer cells develop a dynamic relationship with the microenvironment and alter normal brain cellular functions to form a niche that supports tumor growth and expansion.[30,53,104,106,113] Here, we investigated the role of different components of the microenvironment such as presence of a GBM-like extracellular matrix and presence of astrocytes and endothelial cells, on GBM migration. Our results indicate that in a 3D environment GBM decreases the overall migration compared to standard liquid culture. Moreover, presence of stromal cells in a 3D *in vitro* tumor model increases the migration of non-stem GBM cell lines.

The majority of migration studies have used conventional migration assays on rigid surfaces to study cancer cell migration, however tumor cells exist in a 3D environment in presence of stromal cells and surrounded by ECM. Comparison of GBM migration when cultured in 2D rigid surfaces and within a 3D model of GBM ECM shows that presence of a 3D ECM reduces the migration of all GBM cell lines studied and increases the intrinsic directionality of the cells. Morphology and cell adhesion have been found to be different for cells cultured in 2D surfaces and within 3D matrices.[114–116] Differences in the mechanical and chemical clues provided by 2D or 3D platforms modulate in a

different fashion the cellular processes involved in migration and ultimately affect migration mode, velocity and directionality.

Stromal cells are fundamental components of the tumor microenvironment and synergistically interact with cancer cells during tumor progression. Incorporation of astrocytes in 2D monolayer culture increased migration distance and velocity of GBM. Previous studies by Rath (2013)[110] showed that astrocytes and astrocyte conditioned media increase migration of GBM stem-like cells in a Transwell assay, but have no effect on non-stem GBM cells. In contrast, we observed that presence of only astrocyte conditioned media had no effect on increasing migration of non-stem GBM cells but direct contact of the populations on a 2D surfaces increased GBM migration. It has been recognized that direct communication between astrocytes and GBM through gap junctions, and specifically through Connexin 43 (Cx43) increases migration.[23,112] Nevertheless, our results showed that in the 3D model of GBM ECM where cells are homogenously distributed and physical contact is not prevalent, incorporation of astrocytes also increased GBM migration, suggesting that formation of heterocellular gap junctions is not necessary for astrocytic effect on GBM migration.[24]

Regulation of GBM migration has been directly linked to astrocyte signaling through either direct secretion of MMPs[40,117] or secretion of neurotropic factors that induce cancer MMPs expression. Studies by Le (2003)[117] and Wang (2013)[40] showed that astrocyte expression of pro MMP-2 and pro MMP-9 increased GBM migration. Furthermore, presence of glial derived-cell neurotrophic factor (GDNF), normally secreted by glial

cells including astrocytes, enhances migration of cancers like human squamous cell carcinoma,[118] pancreatic cancer[119] and GBM,[21] possibly through up-regulation of tumor MMP-9 expression. Yet, these studies have been performed in 2D liquid cultures, where MMPs expression and activation are affected by the absence of a 3D ECM. We showed that presence of astrocytes during 3D culture increases expression of GBM MMP-9. Combining our observations with results by Okada (2003),[119] we suggest that higher expression of MMP-9 by GBM can be linked to astrocytic-secreted GDNF.

The role of endothelial cells in GBM progression has mainly being studied in the context of tumor neovascularization through tumor expression of VEGF. However, the link between neovascularization and VEGF has been proven to be more complex than initially recognized, and extends to multiple tumor processes beyond vascularization. For instance, vascular networks are used by GBM as migration highways; however, presence of VEGF directly decreases GBM invasion[120] and prolonged inhibition of VEGF cause ultimate enhanced GBM migration as was observed in patients treated with Bevacizumab.[121] Inhibition of interaction between the tumor and the endothelial cells, as well as inhibition of angiogenesis through VEGF-A blockade by Bevacizumab can led to tumor invasion and metastasis. The mechanism by which direct blockade of VEGF increases GBM invasion is related to the hepatocyte growth factor (HGF) and its receptor MET. MET/HGF interaction has been known to activate cell migration, however presence of VEGF antagonizes MET/HGF interaction.[120] Blockade of VEGF enhances MET/HGF interaction and GBM cells display higher invasiveness.

Interaction between tumor and endothelial cells has repercussions in multiple tumor processes. Despite the fundamental role of endothelial cells as main components of the tumor microenvironment, few studies have physically incorporated them into *in vitro* models to study their effect on cancer cell behavior.[122] Here, we demonstrated that dual presence of endothelial cells and astrocytes increases the migration of non-stem GBM cells on 2D and 3D platforms but decreases migration of stem-like GBM cells in a 3D model of GBM ECM. Stem-like GBM cells, similar to neural progenitors reside in a specific perivascular niche closely associated with blood vessels and endothelial cells.[8,35] Although, stem-like GBM cells can present high migratory potential in other contexts as we and others have shown,[26,50] we suggest that in presence of an environment that mimics the perivascular niche, they present reduced migration as the microenvironment provides supportive and maintenance cues. In the same context, presence of stromal cells increases the directionality of stem-like GBM cells, but decreases directionality of non-stem GBM cells. Differences in directionality can be attributed to differential intrinsic response of stem-like GBM cells to external guidance cues provided by microenvironment that regulates the cellular polarity machinery and stabilizes the cell leading edge during migration to achieve directionality.[80]

4.5 Summary

We investigated the role of the microenvironment in terms of presence of an ECM and stromal cells like astrocytes and endothelial cells on migration of stem-like and non-stem GBM cells. Our results demonstrate that presence of a 3D GBM-like ECM decreases migration velocity, and distance and increases intrinsic directionality of GBM cells. Presence of stromal cells either in dual or triple co-culture with GBM increases the overall migration of GBM cells on 2D rigid surfaces. When dimensionality and stromal cell are combined to evaluate their effect on GBM migration, presence of stromal cells increases migration of non-stem GBM cells, however only astrocytes alone and not ECFCs or ECFCs-astrocytes increase migration of stem-like GBM cells. This suggests a direct role of endothelial cells on migration inhibition of stem-like GBM cells in a 3D culture. In the same line, stromal cells present in a 3D environment decrease the directionality of non-stem GBM cells but increase intrinsic directionality of stem-like GBM cells. Incorporation of multiple components of the GBM microenvironment in an *in vitro* controllable platform presents a powerful tissue-engineering tool to understand how individual and combined factors modulate GBM behavior, and specific process that are characteristic to GBM such as rapid migration.

CHAPTER 5. THE 3D MICROENVIRONMENT REGULATES STAT3 ACTIVATION AND RESPONSE TO DRUG INHIBITION IN GLIOBLASTOMA

5.1 Introduction

The activity of STAT3, a member of the Signal Transducer and Activator of Transcription (STAT) family is modulated by the microenvironment. STAT3 regulates multiple cellular processes such as proliferation, survival, angiogenesis and migration (Fig 4.1).[123] In normal cells, STAT3 is present in the cytoplasm as a non-phosphorylated monomer and undergoes transient phosphorylation as a response to intracellular activators as EGFR, Src and ERK, as well as extracellular signaling through direct interaction with members of the Janus–activated kinases.[123–125] Phosphorylation of STAT3 can occur in Tyr-705 or Ser-727, however, the majority of STAT3 functions are directly related to Tyr-705 phosphorylation. Phosphorylated STAT3 forms active homodimers via interaction through the SH2 domains that translocate to the nucleus and regulate the expression of multiple genes.

STAT3 has lately attracted interest as a potential cancer target due to its location as the convergence point of multiple oncogenic pathways and constitutive activation in more than 70% of all cancers.[126] Gain of function mutation of STAT3 has not yet been reported. STAT3 constitutive activation is usually due to a mutation in an upstream regulator.[124 127]

In GBM basal STAT3 activation is widely variable; previous studies found that 9 to 83% of GBM human tumors evaluated exhibited constitutive phosphorylated STAT3.[125] The role of STAT3 in gliomagenesis involves multiple cellular processes with survival and migration being two of the most intensively studied. Constitutive activation of STAT3 directly upregulates expression of anti-apoptotic proteins Mcl-1, Bcl-2 and Bcl-XL and increases survival.[123,124] Likewise, constitutive activation of STAT3 has been linked to the conversion of non-stem cells to stem-like cells in breast cancer[128] as well as increased self-renewal of GBM stem-like cells.[129] Effect of STAT3 in migration is linked to regulation of cell adhesion and cytoskeletal rearrangement mediated by RhoGTPases. STAT3 association with NF-kB mediates glioma migration through the adhesion molecule ICAM-1.[130] Furthermore, inhibition of STAT3 expression has been shown to inhibit the activity of RhoA and reduce phosphorylation of the focal adhesion protein FAK as well reduce expression of MMPs.[131]

Constitutive STAT3 activation in cancers occurs as a response to deregulated cytokine and chemokine signaling from the tumor microenvironment. STAT3 activation in cancer can in turn be propagated to other stromal and immune cells via expression of signals such as vascular endothelial growth factor (VEGF) and interleukin-10 (IL-10).[41] Likewise, the presence of the ECM modulates the cell response to soluble signals,[132] and increases expression of adhesion molecules such as β1-integrin that induces STAT3 activation.[133] Despite the fundamental role exerted by the microenvironment on STAT3, the majority of studies that have evaluated STAT3 oncogenic function were performed in platforms that do not recapitulate the fundamental aspects of the tumor microenvironment.

STAT3 inhibition has been increasingly considered as possible route for GBM treatment. Given the great effect that the microenvironment exerts on STAT3 activation, we suggest that the use of *in vitro* models that recapitulate the characteristics GBM microenvironment are one of the most appropriate platforms for the initial assessment of drug treatments aimed to target STAT3 in GBM. In this study we investigated the impact of the 3D microenvironment comprised by a GBM-like ECM and astrocytes on the basal phosphorylation of STAT3, as well as the effect of the STAT3 inhibitor SH-4-54 on viability and migration of patient-derived GBM cells.

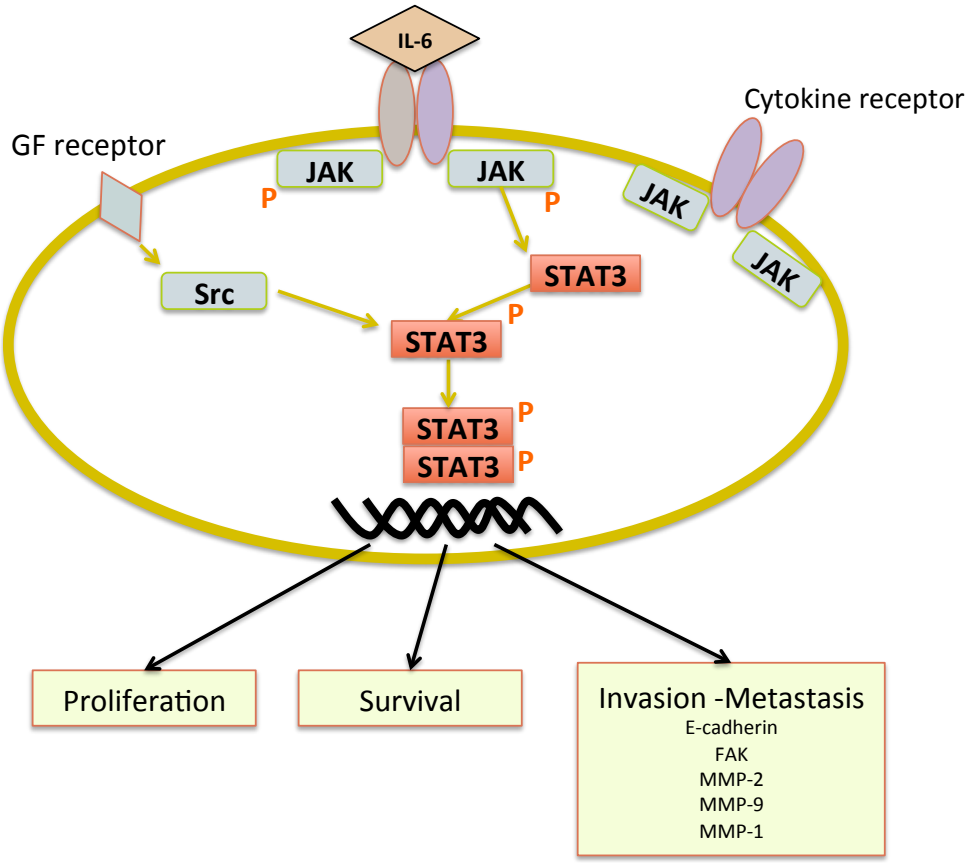

Figure 5.1 STAT3 regulates multiple pathways involved in cancer progression.

5.2 Experimental Methods

5.2.1 Standard liquid cell culture

GBM human–derived cell lines GBM10, GBM43 and MHBT32 were maintained in high-glucose DMEM (Life Technologies, Carlsbad, CA) supplemented with 10% FBS. GBM human cell line GBAM1 (CD133+ >98%) was maintained in DMEM/F12 supplemented with B27 without vitamin A (ThermoFisher Scientific, Waltham, MA) and with growth factors EGF, bFGF (50 ng/ml each, Peprotech, Rocky hill, NJ). Human primary astrocytes (ScienCell, Carlsbad, CA) were maintained according to vendor specifications. All cell lines were cultured at 37°C in an atmosphere of 5% CO_2, fed with complete media every other day and passaged at 70-80% confluence.

5.2.2 Synthesis of 3D brain-like matrix and 3D cell culture

3D matrices of collagen-hyaluronan were generated using pig skin oligomer collagen (GeniPhys, Zionsville, IN) at concentration of 2 mg/ml and sodium hyaluronate (MW 351-600) KDa (Lifecore Biomedical, Chaska, MN) was incorporated at 10 mg/ml as described previously. Cells were suspended at the desired concentration in the 3D matrix prior polymerization at 37°C for 30 minutes. Complete media was added to the top of the matrix, and cells were cultured at 37°C in an atmosphere of 5% CO_2. For 3D co-culture of GBM and astrocytes, GBM cells were embedded in collagen-hyaluronan matrix at a density of $3.5*10^5$ cells in 200 µl of matrix, following polymerization $3.5*10^5$ astrocytes suspended in 200 µl of collagen matrix were pipetted to form a concentric ring as described in Chapter 4.

5.2.3 Drug treatment and cell viability analysis

GBM cells were cultured for 24h (in liquid medium or within the 3D Col-HA matrix) in a 96-well plate at 5000 cells/well with 100 µl of complete media prior addition of SH-4-54 inhibitor in DMSO vehicle. All treatments were normalized to control DMSO volume. Viability of GBM cells cultured in liquid media and 3D collagen-hyaluronan matrix was assessed by Alamar blue assay (ThermoFisher Scientific, Waltham, MA). After drug treatment, cells were incubated with Alamar blue reagent during 3 h and absorbance was measured at 570nm. Cells treated only with DMSO served as controls. Absorbance readings were normalized to DMSO controls to calculate viability percentages.

5.2.4 RNA interfering assays

GBM43 and GBM10 were transfected by reverse transfection with STAT3 siRNA (Santa Cruz Biotechnology, Dallas, TX). Briefly, 10 pmol of siRNA were diluted in 50 µl of OptimMEM medium (ThermoFisher Scientific, Waltham, MA) and mixed with 3 µl of Lipofectamine RNAimax (ThermoFisher Scientific, Waltham, MA) in 50 µl of OptiMEM media. The mix was incubated at room temperature for 15min and added to a well of a 24-well plate. Then, $1*10^5$ GBM10 or GBM43 cells suspended in OptiMEM media were deposited per well containing the mix to a final volume of 300 µl/well. Cells were incubated at 37°C in an atmosphere of 5% CO_2 during 24 h and 300 µl of normal DMEM media with 20% FBS were added to each well to stimulate cell attachment to the plate. Forty-eight hours after transfection cells were recovered by trypsin exposure and cultured accordingly for the migration assays. Negative transfection control was transfected with

control-siRNA A and positive control with siRNA FITC conjugate-A (Santa Cruz Biotechnology, Dallas, TX).

5.2.5 Western blot analysis

Cells cultured in 2D monolayer and in 3D brain-like matrix were were washed with ice-cold PBS and lysed with RIPA buffer supplemented with 1X Halt™ protease and phosphatase inhibitor cocktail (ThermoFisher Scientific, Waltham, MA) at 4°C as described in Chapter 3. For protein extraction of GBM co-cultured in 3D with astrocytes the concentric ring was manually separated to obtain the layers containing each of the cell populations. Total protein concentration was quantified and electrophoresed as described in Chapter 3. Blotting of the membranes was done with primary antibodies against STAT3-p705 (dilution 1:2000), STAT3-p727 (dilution 1:2000), STAT3 (1:1000), actin (1:1000) (Cell Signaling, Danvers, MA). Secondary antibodies IRDye800CW anti-rabbit and IRDye680RD anti-mouse (Licor, Cambridge, UK) were used at a dilution 1:2000. Visualization was performed in Odyssey Clx System (Licor, Cambridge, UK). Semiquantitative analysis of STAT3 activation was done in ImageJ. Bands corresponding to phosphorylated STAT3 and total STAT3 were normalized to a ladder band to avoid differences in multiple readings of the same membrane. STAT3 activation was quantified as phosphorylated STAT3 over total STAT3.

5.2.6 Migration on 2D surfaces

Cells were tested for viability, stained with CellTracker™ Green CMFDA dye (Life Technologies, Carlsbad, CA) for visualization and plated in a μ-slide angiogenesis chamber (Ibidi, Germany) at a density of 15000 cell/cm^2, fed with appropriate media and

incubated during 4 h for attachment. Afterwards, cells were placed in an on-stage incubator and treated with the SH-4-54 prior initiation of time-lapse confocal microscopy during 15 h every 1.5 h.

5.2.7 Migration in 3D brain-like matrix

GBM cells were stained with CellTracker™ Green CMFDA dye (Life Technologies, Carlsbad, CA) and embedded at a density of $1*10^6$ cells/ml within the collagen-hyaluronan matrix before polymerization. Volumes of 30 µl of matrix per well were platted in a µ-slide angiogenesis chamber (Ibidi, Germany). After matrix polymerization, 30 µl of media was added per well and cells were maintained at 37°C in an atmosphere of 5% CO_2 for 24 h, prior migration analysis. Drug SH-4-54 was added to the cultures 15min prior the initiation of migration analysis. During migration cells were imagined by time-lapse confocal microscopy every 1.5 h during 15 h.

5.2.8 Time-lapse confocal imaging, analysis of migration and statistical analysis

Performed as described in Chapter 4.

5.3 Results

5.3.1 Basal status of STAT3 in GBM during 2D liquid culture

Given the wide range of basal activation found in multiple GBM tumors, we initially tested the status of STAT3 on tyrosine 705 and serine 727, the two phosphorylation sites of STAT3 to check the constitutive status of STAT3. Cell lines GBM10, GBM43 and GBAM1 showed very low to absent basal phosphorylation of Tyr-705 or iSer-727, while the cell line MHBT32 presented basal phosphorylation in both active sites (Fig 5.2). Given the low basal STAT3 activity in some cells, we stimulated with interleukin-6 (IL-6), a well-recognized inducer of STAT3 activation, and checked the phosphorylation status at varied timed after stimulation to account for the transient response characteristic of STAT3. We observed that IL-6 stimulus induced Tyr-705 phosphorylation in the non-stem cell lines GBM10, GBM43 and MHBT32 but not in the stem-like line GBAM1 (Fig 5.2). As expected the activation was transient; phosphorylation occurred almost immediately after stimulus and was maintained during the first hour but considerably decreased by 2 h post stimulation. IL-6 did not cause phosphorylation of STAT3 on Ser-727 in GBM10 or GBAM1, and had very slight effect on GBM43 and MHBT32 (Fig 5.2).

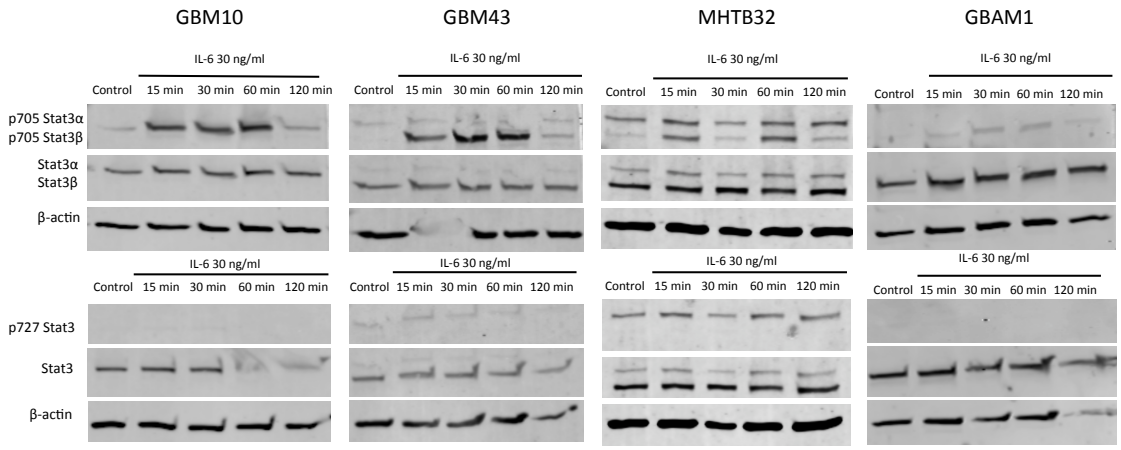

Figure 5.2 STAT3 is constitutively activated (Tyr-705 and Ser-727) in MHBT32 but not in GBM10, GBM43 and GBAM1. IL-6 stimulation caused transient phosphorylation of STAT3 in all non-stem GBM cell lines but not in the stem-like GBAM1. Upper horizontal section presents phosphorylation of Tyr-705 and lower section presents phosphorylation on Ser 727. Total protein loaded per lane 12 μg GBM10, 13 μg MHBT32 and 16 μg GBM43 and GBAM1.

5.3.2 GBM cells present constitutive STAT3 activation during culture in a 3D-model of tumor microenvironment

Following the low basal activation *in vitro* by most of the GBM cell lines studied, and based on the regulation that the microenvironment exerts on cellular behavior, we evaluated basal STAT3 status in GBM when cultured in a 3D GBM-like ECM alone or in presence of astrocytes. All GBM cells cultured in the 3D model exhibited basal activation of STAT3 although in differing degrees (Fig 5.3). GBM10, GBM43 and GBAM1 that previously displayed very low to absent STAT3 basal activity, exhibited high STAT3 activation in 3D culture. MHBT32 exhibited lower STAT3 activation and general lower total STAT3 in 3D culture compared to 2D culture, yet basal activity was

present in 3D culture. Interestingly, presence of astrocytes in the 3D-model did not significantly alter STAT3 activation in non-stem cell lines, however in the stem-like cell line GBAM1 increased basal STAT3 activation by two-fold (quantification using ImageJ); suggesting that combined effect of ECM and stromal cells drastically alters the basal status of STAT3 in GBAM1 compared to regular 2D liquid culture.

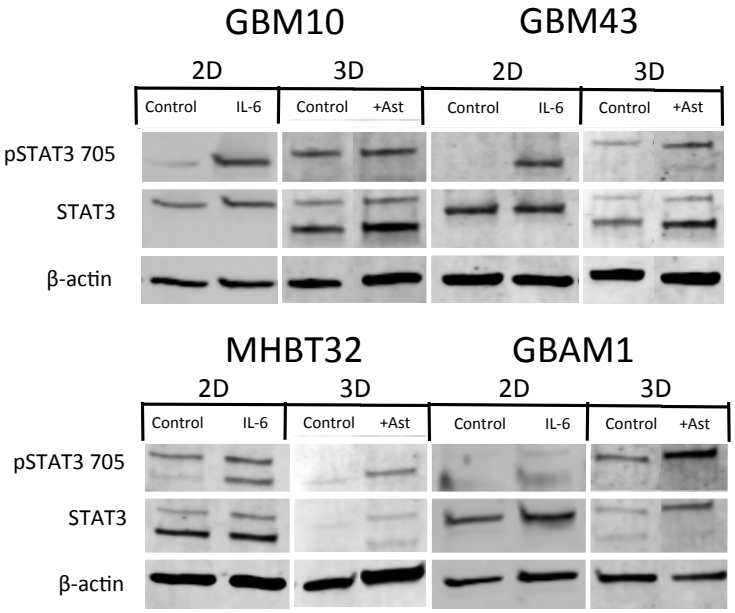

Figure 5.3 GBM exhibits basal activation of STAT3 when cultured in a 3D matrix that recapitulates characteristics of GBM ECM. Presence of astrocytes in 3D environment increases by 2X basal STAT3 phosphorylation of GBAM1 compared to 3D culture without astrocytes. Total protein loaded per lane from 2D culture: 12 µg GBM10, 13 µg MHBT32 and 16 µg GBM43 and GBAM1, from 3D culture 14 µg GBM10, GBM43, MHBT32 and 7 µg GBAM1.

5.3.3 STAT3 inhibitor SH-4-54 decreases viability of stem-like GBM cells but has minor effects on viability of non-stem GBM cells

STAT3 is involved in the regulation of multiple cell processes including apoptosis and cell proliferation. Based on our previous results that show differential basal activity of STAT3 mediated by the microenvironment, we assessed the effect of STAT3 inhibition on GBM survival, both in 2D liquid and 3D culture. To this end we treated GBM with varied concentrations of the small molecule STAT3 inhibitor SH-4-54, which binds to the SH2 domain of STAT3 preventing phosphorylation and dimerization. In liquid culture, SH-4-54 reduced cell viability of MHBT32 to 60% at concentrations as low as 5 μM, as was expected given its basal activation of STAT3 (Fig 5.4). The effect of SH-4-54 on GBM43 and GBM10, which did not present basal activation of STAT3 was minor. The drug only decreased viability of GBM43 to 65% at 25 μM and not had any effect on GBM10 viability. Interestingly, SH-4-54 was very effective in reducing viability of the stem-like line GBAM1; concentrations as low as 2 μM reduced GBAM1 viability to nearly 40%. Evaluation of the anti-STAT3 drug SH-4-54 in 3D culture showed less or similar effect on GBM viability despite the fact that all lines presented basal activity of STAT3 in 3D culture. Similar to what was observed in liquid culture, GBM10 was unresponsive to treatment. MHBT32 that exhibited high sensitivity to SH-4-54 in 2D culture presented no reduction in viability after treatment in 3D culture. Only GBM43 and GBAM1 cell lines exhibited viability decrease when treated with the inhibitor in 3D culture. Overall, anti-STAT3 treatment was very effective at low concentrations in reducing the viability of the stem-like line GBAM1 both in 2D and 3D cultures.

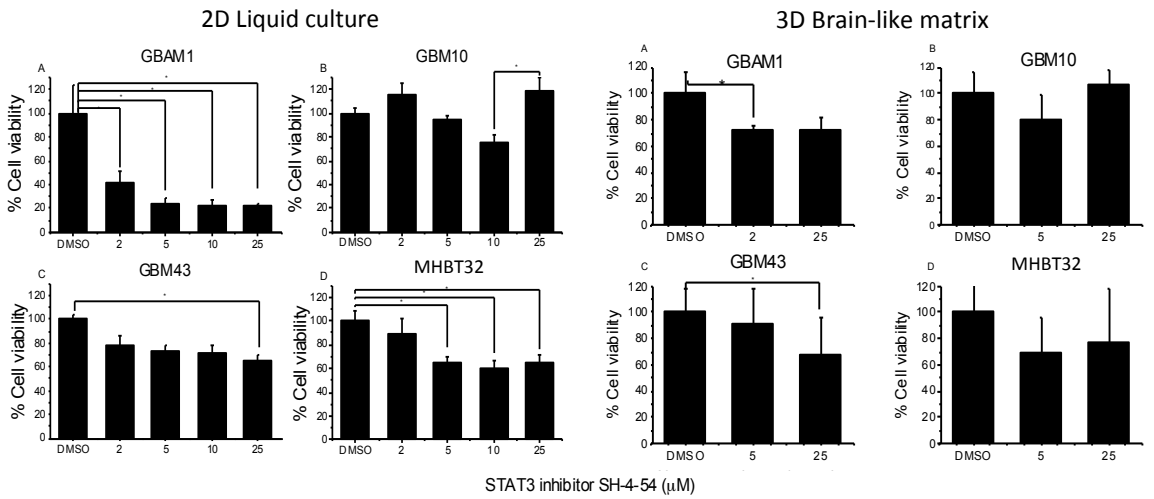

Figure 5.4. GBM viability after anti-STAT3 treatment with SH-4-54. Stem-like GBAM1 cell line exhibited the highest sensitivity to SH-4-54, however the non-stem GBM cells were less responsive to treatment, especially GBM10. Treatment in 3D was less efficient in decreasing viability compared to treatment in liquid culture.

5.3.4 Inhibitor SH-4-54 decreases STAT3 phosphorylation in GBM43 but not in GBM10

The varied results obtained when assessing the effect of SH-4-54 inhibitor on GBM viability suggested dissimilar activity of the inhibitor on the various cell lines. To corroborate that SH-4-54 was indeed inhibiting STAT3 phosphorylation, we tested the SH-4-54-resistant cell line GBM10 and the SH-4-54-sensitive cell line GBM43 by pretreating with increasing doses of SH-4-54 and subsequently stimulating STAT3 activation with IL-6. Unfortunately, testing of GBAM1 was not possible due lack of basal STAT3 activation as well as unresponsiveness to IL-6 or EGF (data not shown) stimulation. SH-4-54 did not inhibit STAT3 Tyr-705 phosphorylation in GBM10 at any concentration evaluated (2-10 μM) (Fig 5.5), agreeing with the unresponsiveness

observed in the survival tests. In contrast, the drug effectively inhibited STAT3 Tyr-705 phosphorylation in GBM43 cells and the degree of inhibition was proportional to the concentration of drug evaluated.

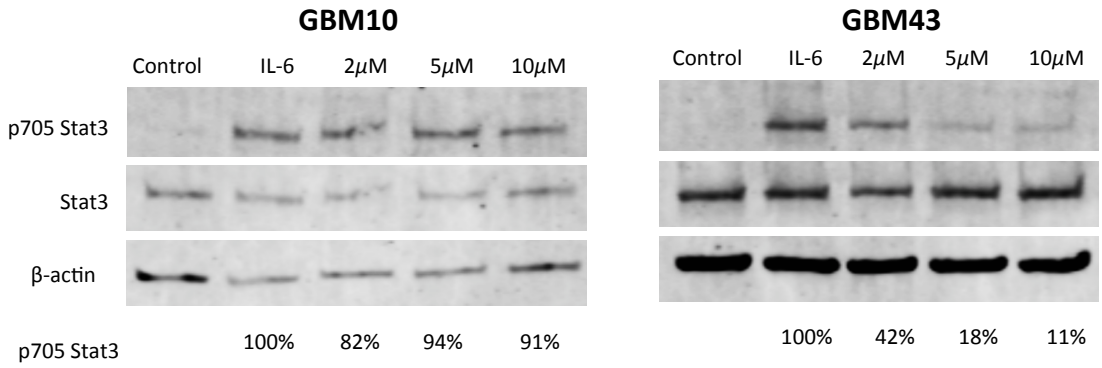

Figure 5.5 STAT3 inhibitor SH-4-54 effectively decreases STAT3 Tyr-705 phosphorylation in GBM43, but has no effect on STAT3 activity in GBM10. Total protein loaded per lane 7 μg GBM10, 14 μg GBM43.

5.3.5 Inhibitor SH-4-54 decreases STAT3 migration of GBM43 but not in GBM10 in a 3D-model of GBM microenvironment

STAT3 regulates multiple genes involved in invasion and metastasis. We therefore, tested the effect of STAT3 inhibition on migration of GBM10 and GBM43 on 2D surfaces as well as in 3D brain-like matrix. Expression of STAT3 was inhibited by siRNA in both lines as a control to validate the effect of STAT3 inhibition on migration. Analysis of GBM10 and GBM43 migration distance in 2D surfaces showed that knockdown or inhibition of STAT3 with SH-4-54 did not reduce GBM migration (Fig 5.6). In contrast, anti STAT3 treatments (STAT3 siRNA and SH-4-54) reduced the

migration of GBM43 in 3D culture. Interestingly, anti-STAT3 treatments did not the migration of GBM10 cell line in the 3D model. Although, siRNA knockdown was only 60% in GBM10, the previous unresponsiveness of this particular cell line to the SH-4-54 inhibitor combined with unaffected survival and migration after treatment suggest a possible impairment of STAT3 function. Our results show that SH-4-54 inhibitor effectively decreases STAT3 activation in the GBM43 cell line and such inhibition directly correlates with decreased survival and migration in 3D environments.

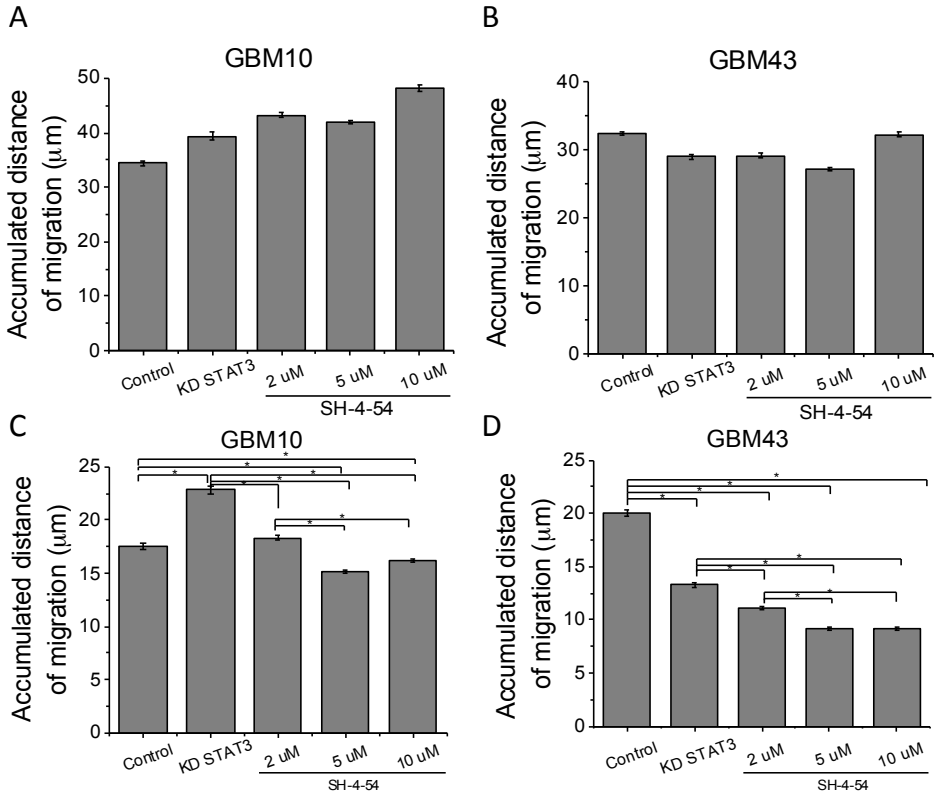

Figure 5.6 Inhibitor SH-4-54 decreases STAT3 migration of GBM43 but not of GBM10 in a 3D model of GBM microenvironment **A.B**. Targeting of STAT3 activation either using the small molecule SH-4-54 or siRNA did not affect migration of glioblastoma on 2D rigid surfaces. **C.** GBM10 migration in a 3D environment was not decreased by STAT3 targeting **D.** GBM43 decreased 3D migration after STAT3 siRNA knockdown treatment (KD STAT3) as well as after treatment with the inhibitor SH-4-54.

5.4 Discussion

STAT3 is an attractive target for GBM treatment given its convenient location as a cross point of many oncogenic pathways.[126] STAT3 activation is mediated by signaling from the microenvironment; nonetheless, the majority of STAT3 studies in GBM have been performed in liquid platforms that do not recapitulate the main features of the tumor microenvironment and might therefore lead to observations not representative of *in vivo* context. In this study we demonstrated that presence of 3D microenvironment regulates the basal activation of STAT3 in GBM and influences the effect of anti-STAT3 drug treatment on survival and migration.

Multiple studies have shown constitutive activation of STAT3 in GBM tumor samples; however, basal activation in GBM can be highly variable.[123] Evaluation of STAT3 basal activity of four patient-derived GBM cell lines showed that during culture in standard liquid platforms, the GBM cell lines GBM10, GBM43 and the stem-like cell line GBAM1 do not present constitutive phosphorylation of STAT3 in Tyr-705 or Ser-727, the two active phosphorylation sites of STAT3. Only the line MHBT32 showed constitutive activation of STAT3 in Tyr-705 and Ser-727.

STAT3 undergoes transient activation as a response to microenvironment signals such IL-6 family cytokines and certain growth factors as endothelial growth factor (EGF). Non-stem cell GBM lines were responsive to IL-6 stimulation and underwent transient phosphorylation in Tyr-705, but not in Ser-727. STAT3 phosphorylation triggered by IL-6 stimulation can occur in both active sites but through different signaling cascades.[134]

Primary association of STAT3 and regulation of main processes as survival, proliferation and invasion occurs though phosphorylation of Tyr-705, while phosphorylation of Ser-727 potentiates Tyr-705 activation and controls metabolic activity.[134,135] Differential activation of Tyr-705 and not Ser-727 can be associated with the short-lived stimulus applied that activates only the primary phosphorylation in Tyr-705 but is not sustained or strong enough to trigger phosphorylation of Ser-727 in our experimental settings.

IL-6 is the most well known activator of STAT3. Interestingly, stimulation with IL-6 did not trigger phosphorylation of STAT3 in the stem-like GBAM1. STAT3 activation has been shown essential for maintenance of stem properties of the cancer stem-like population through direct repression of genes involved in differentiation.[136] Furthermore, studies by Wang (2009)[137] showed that direct stimulation of GBM stem-like neurospheres with IL-6 increases activation of STAT3. IL-6 stimulation of the stem-like line GBAM1 did not induce STAT3 activation as expected, however many factors could have influence such outcome, for instance the lack of expression of IL-6 receptor. Further studies are needed to understand the characteristics of this cell line in terms of STAT3 activation.

STAT3 functions as a signal transducer and is responsive to signals from the microenvironment. In agreement, with previous studies regarding the fundamental role of the microenvironment in STAT3 activation in cancer, incorporation of GBM cells in a 3D model that recapitulates the properties of the brain extracellular matrix induced STAT3 basal activation. Further incorporation of astrocytes into the 3D ECM model increased STAT3 phosphorylation of the stem-like line GBAM1. These results show that the

recapitulation of the tumor microenvironment induces GBM basal STAT3 activation, however, when the cells are isolated from their niche, as happens during standard 2D culture, STAT3 basal activations is lost, and only GBM cells that harbor a mutation in an upstream regulator show constitutive STAT3 activity.

Effect of inhibition of STAT3 phosphorylation by the small molecule SH-4-54 has been effective to reduce survival of brain tumor initiating cells, both in liquid culture and in *in vivo* models.[90] Our observations corroborate the effectiveness of SH-4-54 reducing viability of the stem-like line GBAM1 both in 2D liquid culture and in 3D culture, despite the lack of basal activation in 2D culture previously observed. These results, validate STAT3 inhibition as an effective treatment for targeting stem-like GBM populations regardless of the basal activation status of STAT3. Our results also agree with previous studies that emphasize the importance of STAT3 on proliferation and survival of GBM stem-like cells. STAT3 function is essential non only for maintenance of stem embryonic cells[138] but also for survival of GBM stem-like cells.[99,129,139] Nevertheless, SH-4-54 was less efficient in decreasing viability of non-stem GBM cells.

GBM viability after treatment with the inhibitor SH-4-54 showed that the effect of the drug was greater in liquid culture despite the lack of basal STAT3 phosphorylation of most of the cell lines studied. Interestingly, SH-4-54 showed less efficiency in decreasing the viability of GBM cells in 3D culture despite the fact that all GBM cell lines showed basal activation of STAT3 during 3D culture. The varied response of non-stem cells to SH-4-54 was explained by the functionality of the molecule inhibiting STAT3

phosphorylation. Our results showed that SH-4-54 effectively inhibits Tyr-705 STAT3 phosphorylation in GBM43 but not GBM10, suggesting that is potential as GBM treatment is cell line dependent.

STAT3 regulation not only regulates survival and proliferation but also migration. Activation of STAT3 in cancer cells induces up-regulation of p21, RhoA, matrix metalloproteinases (MMPs) and phosphorylated FAK,[131] all modulators of cancer invasion. Previous studies have shown that silencing of STAT3 impairs migration of gastric carcinoma cells[131] and GBM cells.[136,140] In our studies, knockdown of STAT3 with siRNA and treatment with SH-4-54 migration of GBM43 in 2D. In contrast, the same anti-STAT3 treatments reduced the migration of GBM43 cells in a 3D environment, supporting previous studies that have shown a reduction of 3D GBM migration after STAT3 targeting.[141] The differential effect of anti-STAT3 treatment on 2D and 3D migration can be related to different basal STAT3 activation exhibited by GBM when cultured in different platforms. We suggest that in 2D platforms targeting of STAT3 has no visible effect given the lack that basal phosphorylation, while in 3D environments STAT3 is constitutively active and direct targeting of STAT3 visibly reduces the ability of GBM to migrate.

5.5 Summary

STAT3 is activated by signaling from the microenvironment and regulates various cellular processes implicated in gliomagenesis. Nevertheless, STAT3 function is usually studied in absence of the main components of the tumor environment. In this study, we investigated the effect of the 3D microenvironment on the basal activation of STAT3 and the effect of anti-STAT3 drug treatment on survival and migration of GBM. Our results demonstrate that presence of a 3D ECM induces GBM basal activation of STAT3 in cells lines that do not show constitutive STAT3 activation during 2D culture. Treatment of GBM cells with the STAT3 inhibitor SH-4-54 greatly reduces viability of stem-like GBM cells but has a weaker effect on reducing viability of non-stem cell lines. Further exploration of SH-4-54 function revealed that this drug effectively inhibits phosphorylation of the non-stem GBM line GBM43 but has no visible effect on GBM10. Evaluation of the STAT3 inhibition revealed that anti-STAT3 treatment decreases the migration in 3D environments for the SH-4-54-responsive line GBM43 but not for the SH-4-54-resistant line GBM10. Our results demonstrate the importance of the 3D microenvironment on basal status of STAT3 in GBM. As a consequence, STAT3 inhibition has different effects on survival and migration when evaluated in 2D surfaces compared to 3D matrices.

CHAPTER 6. CONCLUSIONS AND FUTURE WORK

In this study we explored the influence of the 3D extracellular matrix and stromal cells on the regulation of glioblastoma migration and drug response. Initially we addressed the effect of the extracellular matrix properties of the migration characteristics of glioblastoma neurospheres during 3D culture. By developing a composite matrix of hyaluronan structurally supported by a collagen I oligomer that simulates the brain-tumor extracellular matrix composition and comparing with standard, Matrigel and collagen type-I monomer matrices, we showed that glioblastoma cells altered their migration mode and velocity depending on the matrix composition and mechanical properties. Compositional characteristics of the extracellular matrix as presence of hyaluronan reduced velocity and number of migratory cells, and physical features such as stiffness or presence of topographical cues modulated the migration mechanisms adopted by the cells. Further efforts to increase the complexity of the developed brain-tumor extracellular matrix towards a more similar platform to *in vivo* tissues, showed that incorporation of stromal cells (astrocytes and endothelial cells) modulate glioblastoma behavior. Presence of astrocytes reduced the cytotoxic effect of temozolomide on glioblastoma stem cells compared to liquid culture only-GBM 3D culture. Combined presence of astrocytes and endothelial cells in the 3D model of brain-tumor microenvironment increased the migration of non-stem GBM cells. However,

presence of endothelial cells (ECFCs) decreased the migration ability of GBM stem-like cells suggesting a possible role of endothelial cells on signalining cues to decrease the migration activity stem-like GBM cells.

Use of the 3D model of brain-tumor microenvironment showed that the microenvironment induced basal activation of STAT3 in glioblastoma that was not evident during standard 2D culture. Therefore, making the 3D model of GBM microenvironment a more appropriate platform for the analysis of anti-STAT3 drug treatments. Moreover, presence of the extracellular matrix decreased the cytotoxicity of STAT3 inhibition on glioblastoma and allowed a more mechanistic evaluation of the effects of STAT3 inhibition on 3D glioblastoma migration.

The unique, multiparameter understanding of the 3D tumor microenvironment has revealed striking aspects on cancer migration ranging from highlighting the importance of ECM composition and physical properties to the modulation of GBM migration mode and drug-response in the presence of stromal cells. Further steps building on the 3D tumor microenvironment model present an exceptional opportunity for the generation of effective therapies that can keep the pace of the challenges imposed by the always-evolving cancerous cells.

LIST OF REFERENCES

LIST OF REFERENCES

1. Sledge, G. The Challenge and Promise of the Genomic Era--Presidential Address of George Sledge , MD. *ASCO Connect.* (2011).
2. Dolecek, T. a, Propp, J. M., Stroup, N. E. & Kruchko, C. CBTRUS statistical report: primary brain and central nervous system tumors diagnosed in the United States in 2005-2009. *Neuro. Oncol.* **14 Suppl 5,** v1–v49 (2012).
3. Lima, F. R. S. *et al.* Glioblastoma: therapeutic challenges, what lies ahead. *Biochim. Biophys. Acta* **1826,** 338–49 (2012).
4. Cheng, L. *et al.* Glioblastoma stem cells generate vascular pericytes to support vessel function and tumor growth. *Cell* **153,** 139–52 (2013).
5. Shaifer, C. a, Huang, J. & Lin, P. C. Glioblastoma cells incorporate into tumor vasculature and contribute to vascular radioresistance. *Int. J. Cancer* **127,** 2063–75 (2010).
6. Ricci-Vitiani, L. *et al.* Tumour vascularization via endothelial differentiation of glioblastoma stem-like cells. *Nature* **468,** 824–8 (2010).
7. Filatova, A., Acker, T. & Garvalov, B. K. The cancer stem cell niche(s): the crosstalk between glioma stem cells and their microenvironment. *Biochim. Biophys. Acta* **1830,** 2496–508 (2013).

8. Schonberg, D. L., Lubelski, D., Miller, T. E. & Rich, J. N. Brain tumor stem cells: molecular characteristics and their impact on therapy. *Mol. Aspects Med.* **39**, 82-101 (2014).

9. Singh, S. K. *et al.* Identification of a Cancer Stem Cell in Human Brain Tumors Identification of a Cancer Stem Cell in Human Brain Tumors. *Cancer Res.* **63,** 5821–5828 (2003).

10. Beier, D., Schulz, J. B. & Beier, C. P. Chemoresistance of glioblastoma cancer stem cells--much more complex than expected. *Mol. Cancer* **10,** 128 (2011).

11. Wang, R. *et al.* Glioblastoma stem-like cells give rise to tumour endothelium. *Nature* **468,** 829–33 (2010).

12. Ricci-Vitiani, L. *et al.* Mesenchymal differentiation of glioblastoma stem cells. *Cell Death Differ.* **15,** 1491–8 (2008).

13. Cuddapah, V. A., Robel, S., Watkins, S. & Sontheimer, H. A neurocentric perspective on glioma invasion. *Nat. Rev. Neurosci.* **15,** 455–65 (2014).

14. Giese, a, Bjerkvig, R., Berens, M. E. & Westphal, M. Cost of migration: invasion of malignant gliomas and implications for treatment. *J. Clin. Oncol.* **21,** 1624–36 (2003).

15. Huijbers, I. J. *et al.* A role for fibrillar collagen deposition and the collagen internalization receptor endo180 in glioma invasion. *PLoS One* **5,** e9808 (2010).

16. Payne, L. S. & Huang, P. The pathobiology of collagens in glioma. *Mol. Cancer Res.* **11** (10) 1129-1140 (2013).

17. Westhoff, M.-A. *et al.* Inhibition of NF-κB signaling ablates the invasive phenotype of glioblastoma. *Mol. Cancer Res.* **11,** 1611–23 (2013).

18. Smith, H. W. & Marshall, C. J. Regulation of cell signalling by uPAR. *Nat. Rev. Mol. Cell Biol.* **11,** 23–36 (2010).

19. Markovic, D. S., Glass, R., Synowitz, M., Rooijen, N. Van & Kettenmann, H. Microglia stimulate the invasiveness of glioma cells by increasing the activity of metalloprotease-2. *J. Neuropathol. Exp. Neurol.* **64,** 754–762 (2005).

20. Yeh, W.-L., Lu, D.-Y., Liou, H.-C. & Fu, W.-M. A forward loop between glioma and microglia: Glioma-derived extracellular matrix-activated microglia secrete IL-18 to enhance the migration of glioma cells. *J. Cell. Physiol.* **227,** 558–568 (2012).

21. Lu, D.-Y., Leung, Y.-M., Cheung, C.-W., Chen, Y.-R. & Wong, K.-L. Glial cell line-derived neurotrophic factor induces cell migration and matrix metalloproteinase-13 expression in glioma cells. *Biochem. Pharmacol.* **80,** 1201–1209 (2010).

22. Caspani, E. M., Crossley, P. H., Redondo-Garcia, C. & Martinez, S. Glioblastoma: A Pathogenic Crosstalk between Tumor Cells and Pericytes. *PLoS One* **9,** e101402 (2014).

23. Oliveira, R. *et al.* Contribution of gap junctional communication between tumor cells and astroglia to the invasion of the brain parenchyma by human glioblastomas. *BMC Cell Biol.* **6,** 7 (2005).

24. Aftab, Q., Sin, W.-C. & Naus, C. C. Reduction in gap junction intercellular communication promotes glioma migration. *Oncotarget* **6,** 11447–11464 (2015).

25. Nguyen-Ngoc, K.-V. *et al.* ECM microenvironment regulates collective migration and local dissemination in normal and malignant mammary epithelium. *Proc. Natl. Acad. Sci. U. S. A.* **109,** E2595–604 (2012).

26. Herrera-Perez, M., Voytik-Harbin, S. & Rickus, J. L. Extracellular matrix properties regulate the migratory response of glioblastoma stem cells in 3D culture. *Tissue Eng. Part A* **21**, 19-20, 2572-2582 (2015)

27. Petrie, R. J., Gavara, N., Chadwick, R. S. & Yamada, K. M. Nonpolarized signaling reveals two distinct modes of 3D cell migration. *J. Cell Biol.* **197,** 439–455 (2012).

28. Mertsch, S., Oellers, P., Wendling, M., Stracke, W. & Thanos, S. Dissecting the Inter-Substrate Navigation of Migrating Glioblastoma Cells with the Stripe Assay Reveals a Causative Role of ROCK. *Mol. Neurobiol.* **48,** 169–179 (2013).

29. Mertsch, S. & Thanos, S. Opposing Signaling of ROCK1 and ROCK2 Determines the Switching of Substrate Specificity and the Mode of Migration of Glioblastoma Cells. *Mol. Neurobiol.* **49,** 900–915 (2014).

30. Hanahan, D. & Coussens, L. M. Accessories to the crime: functions of cells recruited to the tumor microenvironment. *Cancer Cell* **21,** 309–22 (2012).

31. Bellail, A. C., Hunter, S. B., Brat, D. J., Tan, C. & Van Meir, E. G. Microregional extracellular matrix heterogeneity in brain modulates glioma cell invasion. *Int. J. Biochem. Cell Biol.* **36,** 1046–69 (2004).

32. Robel, S., Berninger, B. & Götz, M. The stem cell potential of glia: lessons from reactive gliosis. *Nat. Rev. Neurosci.* **12,** 88–104 (2011).

33. Abbott, N. J., Rönnbäck, L. & Hansson, E. Astrocyte-endothelial interactions at the blood-brain barrier. *Nat. Rev. Neurosci.* **7,** 41–53 (2006).

34. Calabrese, C. *et al.* A perivascular niche for brain tumor stem cells. *Cancer Cell* **11,** 69–82 (2007).

35. Filatova, A., Acker, T. & Garvalov, B. K. The cancer stem cell niche(s): the crosstalk between glioma stem cells and their microenvironment. *Biochim. Biophys. Acta* **1830,** 2496–508 (2013).

36. Bar, E. E. Glioblastoma, cancer stem cells and hypoxia. *Brain Pathol.* **21,** 119–29 (2011).

37. Onishi, M., Ichikawa, T., Kurozumi, K. & Date, I. Angiogenesis and invasion in glioma. *Brain Tumor Pathol.* **28,** 13–24 (2011).

38. Placone, A. L., Quinones-Hinojosa, A. & Searson, P. C. The role of astrocytes in the progression of brain cancer: complicating the picture of the tumor microenvironment. *Tumor Biol.* **37**, 61-69 (2016).

39. Ridet, J. L., Malhotra, S. K., Privat, A. & Gage, F. H. Reactive astrocytes: Cellular and molecular cues to biological function. *Trends Neurosci.* **20,** 570–577 (1997).

40. Wang, L. *et al.* Astrocytes directly influence tumor cell invasion and metastasis in vivo. *PLoS One* **8,** (2013).

41. Yu, H., Kortylewski, M. & Pardoll, D. Crosstalk between cancer and immune cells: role of STAT3 in the tumour microenvironment. *Nat. Rev. Immunol.* **7,** 41–51 (2007).

42. Yang, I., Han, S. J., Kaur, G., Crane, C. & Parsa, A. T. The role of microglia in central nervous system immunity and glioma immunology. *J. Clin. Neurosci.* **17,** 6–10 (2010).

43. Ananthanarayanan, B., Kim, Y. & Kumar, S. Elucidating the mechanobiology of malignant brain tumors using a brain matrix-mimetic hyaluronic acid hydrogel platform. *Biomaterials* **32,** 7913–23 (2011).

44. Pedron, S., Becka, E. & Harley, B. a C. Regulation of glioma cell phenotype in 3D matrices by hyaluronic acid. *Biomaterials* **34,** 7408–17 (2013).

45. Yang, Y. *et al.* Influence of chondroitin sulfate and hyaluronic acid on structure, mechanical properties, and glioma invasion of collagen I gels. *Biomaterials* **32,** 7932–40 (2011).

46. Rao, S. S. *et al.* Glioblastoma behaviors in three-dimensional collagen-hyaluronan composite hydrogels. *ACS Appl. Mater. Interfaces* **5,** 9276–84 (2013).

47. Kaufman, L. J. *et al.* Glioma expansion in collagen I matrices: analyzing collagen concentration-dependent growth and motility patterns. *Biophys. J.* **89,** 635–50 (2005).

48. Magee, J. a, Piskounova, E. & Morrison, S. J. Cancer stem cells: impact, heterogeneity, and uncertainty. *Cancer Cell* **21,** 283–96 (2012).

49. Ruiz-Ontanon, P. *et al.* Cellular Plasticity Confers Migratory and Invasive Advantages to a Population of Glioblastoma-Initiating Cells that Infiltrate Peritumoral Tissue. *Stem Cells* **31,** 1075–1085 (2013).

50. Cheng, L. *et al.* Elevated invasive potential of glioblastoma stem cells. *Biochem. Biophys. Res. Commun.* **406,** 643–648 (2011).

51. Persano, L., Rampazzo, E., Basso, G. & Viola, G. Glioblastoma cancer stem cells: role of the microenvironment and therapeutic targeting. *Biochem. Pharmacol.* **85,** 612–22 (2013).

52. Lathia, J. D., Heddleston, J. M., Venere, M. & Rich, J. N. Deadly teamwork: neural cancer stem cells and the tumor microenvironment. *Cell Stem Cell* **8,** 482–5 (2011).

53. Friedl, P. & Alexander, S. Cancer invasion and the microenvironment: plasticity and reciprocity. *Cell* **147,** 992–1009 (2011).

54. Carey, S. P., Kraning-Rush, C. M., Williams, R. M. & Reinhart-King, C. a. Biophysical control of invasive tumor cell behavior by extracellular matrix microarchitecture. *Biomaterials* **33,** 4157–65 (2012).

55. Willis, a L., Sabeh, F., Li, X.-Y. & Weiss, S. J. Extracellular matrix determinants and the regulation of cancer cell invasion stratagems. *J. Microsc.* **251,** 250–60 (2013).

56. Gritsenko, P. G., Ilina, O. & Friedl, P. Interstitial guidance of cancer invasion. *J. Pathol.* **226,** 185–99 (2012).

57. Motegi, H., Kamoshima, Y., Terasaka, S., Kobayashi, H. & Houkin, K. Type 1 collagen as a potential niche component for CD133-positive glioblastoma cells. *Neuropathology* **133,** (2014).

58. Mourad, P. D., Farrell, L., Stamps, L. D., Chicoine, M. R. & Silbergeld, D. L. Why are systemic glioblastoma metastases rare? Systemic and cerebral growth of mouse glioblastoma. *Surg. Neurol.* **63,** 511–9; discussion 519 (2005).

59. Vehlow, A. & Cordes, N. Invasion as target for therapy of glioblastoma multiforme. *Biochim. Biophys. Acta - Rev. Cancer* **1836,** 236–244 (2013).

60. Baker, B. M. & Chen, C. S. Deconstructing the third dimension: how 3D culture microenvironments alter cellular cues. *J. Cell Sci.* **125,** 3015–24 (2012).

61. Kreger, S. T. *et al.* Polymerization and matrix physical properties as important design considerations for soluble collagen formulations. *Biopolymers* **93,** 690–707 (2010).

62. Yang, Y., Motte, S. & Kaufman, L. J. Pore size variable type I collagen gels and their interaction with glioma cells. *Biomaterials* **31,** 5678–88 (2010).

63. Benton, G., Kleinman, H. K., George, J. & Arnaoutova, I. Multiple uses of basement membrane-like matrix (BME/Matrigel) in vitro and in vivo with cancer cells. *Int. J. Cancer* **128,** 1751–7 (2011).

64. Rao, S. S. *et al.* Inherent interfacial mechanical gradients in 3D hydrogels influence tumor cell behaviors. *PLoS One* **7,** e35852 (2012).

65. Levental, I., Georges, P. C. & Janmey, P. a. Soft biological materials and their impact on cell function. *Soft Matter* **3,** 299 (2007).

66. Bailey, J. L. *et al.* Collagen oligomers modulate physical and biological properties of three-dimensional self-assembled matrices. *Biopolymers* **95,** 77–93 (2011).

67. Rowe, R. G. & Weiss, S. J. Breaching the basement membrane: who, when and how? *Trends Cell Biol.* **18,** 560–74 (2008).

68. Poincloux, R. *et al.* Contractility of the cell rear drives invasion of breast tumor cells in 3D Matrigel. *Proc. Natl. Acad. Sci. U. S. A.* **108,** 1943–8 (2011).

69. Wolf, K. *et al.* Physical limits of cell migration: control by ECM space and nuclear deformation and tuning by proteolysis and traction force. *J. Cell Biol.* **201,** 1069–84 (2013).

70. Engler, A. *et al.* Substrate Compliance versus Ligand Density in Cell on Gel Responses. *Biophys. J.* **86,** 617–628 (2004).

71. Peyton, S. R. & Putnam, A. J. Extracellular matrix rigidity governs smooth muscle cell motility in a biphasic fashion. *J. Cell. Physiol.* **204,** 198–209 (2005).

72. Pathak, A. & Kumar, S. Independent regulation of tumor cell migration by matrix stiffness and confinement. *Proc. Natl. Acad. Sci. U. S. A.* **109,** 10334–9 (2012).

73. Delpech, B. *et al.* Hyaluronan and hyaluronectin in the extracellular matrix of human brain tumour stroma. *Eur. J. Cancer* **29A,** 1012–7 (1993).

74. Park, J. B., Kwak, H. & Lee, S. Role of hyaluronan in glioma invasion. *Cell Adh. Migr.* **2,** 202–207 (2008).

75. Bourguignon, L. Y. W. Hyaluronan-mediated CD44 activation of RhoGTPase signaling and cytoskeleton function promotes tumor progression. *Semin. Cancer Biol.* **18,** 251–9 (2008).

76. Wang, C., Tong, X. & Yang, F. Bioengineered 3D Brain Tumor Model To Elucidate the E ff ects of Matrix Sti ff ness on Glioblastoma Cell Behavior Using PEG-Based Hydrogels. *Mol. Pharm.* 2115–2125 (2014).

77. Kreger, S. T. & Voytik-Harbin, S. L. Hyaluronan concentration within a 3D collagen matrix modulates matrix viscoelasticity, but not fibroblast response. *Matrix Biol.* **28,** 336–46 (2009).

78. Hirata, E. *et al.* In vivo fluorescence resonance energy transfer imaging reveals differential activation of Rho-family GTPases in glioblastoma cell invasion. *J. Cell Sci.* **125,** 858–68 (2012).

79. Watkins, S. *et al.* Disruption of astrocyte-vascular coupling and the blood-brain barrier by invading glioma cells. *Nat. Commun.* **5,** 4196 (2014).

80. Petrie, R. J., Doyle, A. D. & Yamada, K. M. Random versus directionally persistent cell migration. *Nat. Rev. Mol. Cell Biol.* **10,** 538–49 (2009).

81. Johnson, J. *et al.* Quantitative analysis of complex glioma cell migration on electrospun polycaprolactone using time-lapse microscopy. *Tissue Eng. Part C. Methods* **15,** 531–40 (2009).

82. Friedl, P., Locker, J., Sahai, E. & Segall, J. E. Classifying collective cancer cell invasion. *Nat. Cell Biol.* **14,** 777–83 (2012).

83. Breslin, S. & O'Driscoll, L. Three-dimensional cell culture: the missing link in drug discovery. *Drug Discov. Today* **18,** 240–9 (2013).

84. Klemm, F. & Joyce, J. A. Microenvironmental regulation of therapeutic response in cancer. *Trends Cell Biol.* **25,** 198–213 (2014).

85. Soda, Y., Myskiw, C., Rommel, A. & Verma, I. M. Mechanisms of neovascularization and resistance to anti-angiogenic therapies in glioblastoma multiforme. *J. Mol. Med. (Berl).* **91,** 439–48 (2013).

86. Hu, Y.-L. *et al.* Hypoxia-induced autophagy promotes tumor cell survival and adaptation to antiangiogenic treatment in glioblastoma. *Cancer Res.* **72,** 1773–83 (2012).

87. Thoma, C. R., Zimmermann, M., Agarkova, I., Kelm, J. M. & Krek, W. 3D cell culture systems modeling tumor growth determinants in cancer target discovery. *Adv. Drug Deliv. Rev.* **69-70,** 29–41 (2014).

88. Villalonga-Planells, R. *et al.* Activation of p53 by nutlin-3a induces apoptosis and cellular senescence in human glioblastoma multiforme. *PLoS One* **6,** (2011).

89. Moran, D. M. & Maki, C. G. Nutlin-3a induces cytoskeletal rearrangement and inhibits the migration and invasion capacity of p53 wild-type cancer cells. *Mol. Cancer Ther.* **9,** 895–905 (2010).

90. Haftchenary, S. *et al.* Potent Targeting of the STAT3 Protein in Brain Cancer Stem Cells: A Promising Route for Treating Glioblastoma. *ACS J. Med. Chem. letters*, **4**, 1102-1107**,** (2013).

91. Carlson, B., Pokorny, J., Schroeder, M. & Sarkaria, J. Establishment, maintenance and in vitro and in vivo applications of primary human glioblastoma multiforme xenografts models for trasnaltional biology studies and drug discovery. *Curr. protocosl Pharmacol.* **52,** 1–14 (2011).

92. Pickl, M. & Ries, C. H. Comparison of 3D and 2D tumor models reveals enhanced HER2 activation in 3D associated with an increased response to trastuzumab. *Oncogene* **28,** 461–8 (2009).

93. Chen, L. *et al.* The enhancement of cancer stem cell properties of MCF-7 cells in 3D collagen scaffolds for modeling of cancer and anti-cancer drugs. *Biomaterials* **33,** 1437–44 (2012).

94. Hongisto, V. *et al.* High-Throughput 3D Screening Reveals Differences in Drug Sensitivities between Culture Models of JIMT1 Breast Cancer Cells. *PLoS One* **8,** 1–16 (2013).

95. Gurski, L. a, Jha, A. K., Zhang, C., Jia, X. & Farach-Carson, M. C. Hyaluronic acid-based hydrogels as 3D matrices for in vitro evaluation of chemotherapeutic drugs using poorly adherent prostate cancer cells. *Biomaterials* **30,** 6076–85 (2009).

96. Dhiman, H. K., Ray, A. R. & Panda, A. K. Three-dimensional chitosan scaffold-based MCF-7 cell culture for the determination of the cytotoxicity of tamoxifen. *Biomaterials* **26,** 979–986 (2005).

97. Fernandez-Fuente, G., Mollinedo, P., Grande, L., Vazquez-Barquero, A. & Fernandez-Luna, J. L. Culture dimensionality influences the resistance of glioblastoma stem-like cells to multikinase inhibitors. *Mol. Cancer Ther.* **13,** 1664–72 (2014).

98. Villalonga-Planells, R. *et al.* Activation of p53 by nutlin-3a induces apoptosis and cellular senescence in human glioblastoma multiforme. *PLoS One* **6,** (2011).

99. Sherry, M. M., Reeves, A., Wu, J. K. & Cochran, B. H. STAT3 is required for proliferation and maintenance of multipotency in glioblastoma stem cells. *Stem Cells* **27,** 2383–2392 (2009).

100. Rahaman, S. O. *et al.* Inhibition of constitutively active Stat3 suppresses proliferation and induces apoptosis in glioblastoma multiforme cells. *Oncogene* **21,** 8404–8413 (2002).

101. Horning, J. L. *et al.* articles 3-D Tumor Model for In Vitro Evaluation of Anticancer Drugs. **5,** 849–862 (2008).

102. Li, L. & Lu, Y. Optimizing a 3D Culture System to Study the Interaction between Epithelial Breast Cancer and Its Surrounding Fibroblasts. *J. of Cancer **2, 458-466*** (2011).

103. Chen, W. *et al.* Glioma cells escaped from cytotoxicity of temozolomide and vincristine by communicating with human astrocytes. *Med. Oncol.* **32,** 487 (2015).

104. Bonavia, R., Inda, M.-M., Cavenee, W. K. & Furnari, F. B. Heterogeneity maintenance in glioblastoma: a social network. *Cancer Res.* **71,** 4055–60 (2011).

105. Hoelzinger, D. B., Demuth, T. & Berens, M. E. Autocrine factors that sustain glioma invasion and paracrine biology in the brain microenvironment. *J. Natl. Cancer Inst.* **99,** 1583–93 (2007).

106. Charles, N. a, Holland, E. C., Gilbertson, R., Glass, R. & Kettenmann, H. The brain tumor microenvironment. *Glia* **59,** 1169–80 (2011).

107. Fang, H. & Declerck, Y. a. Targeting the tumor microenvironment: from understanding pathways to effective clinical trials. *Cancer Res.* **73,** 4965–77 (2013).

108. Ramnarayan, R., Dodd, S., Das, K., Heidecke, V. & Rainov, N. G. Overall survival in patients with malignant glioma may be significantly longer with tumors located in deep grey matter. *J. Neurol. Sci.* **260,** 49–56 (2007).

109. Lu, K. V, Jong, K. a, Rajasekaran, A. K., Cloughesy, T. F. & Mischel, P. S. Upregulation of tissue inhibitor of metalloproteinases (TIMP)-2 promotes matrix metalloproteinase (MMP)-2 activation and cell invasion in a human glioblastoma cell line. *Lab. Investig.* **84,** 8–20 (2003).

110. Rath, B. H., Fair, J. M., Jamal, M., Camphausen, K. & Tofilon, P. J. Astrocytes enhance the invasion potential of glioblastoma stem-like cells. *PLoS One* **8,** e54752 (2013).

111. Kessenbrock, K., Plaks, V. & Werb, Z. Matrix metalloproteinases: regulators of the tumor microenvironment. *Cell* **141,** 52–67 (2010).

112. Zhang, W. *et al.* Direct Gap Junction Communication between Malignant Glioma Cells and Astrocytes. *Cancer Res.,* **59** 1994–2003 (1999).

113. Weber, C. E. & Kuo, P. C. The tumor microenvironment. *Surg. Oncol.* **21,** 172–7 (2012).

114. Harunaga, J. S. & Yamada, K. M. Cell-matrix adhesions in 3D. *Matrix Biol.* **30,** 363–8 (2011).

115. Hakkinen, K. M., Harunaga, J. S., Doyle, A. D. & Yamada, K. M. Direct Comparisons of the Morphology, Migration, Cell Adhesions, and Actin Cytoskeleton of Fibroblasts in Four Different Three-Dimensional Extracellular Matrices. *Tissue Eng. Part A* **17,** 713–724 (2011).

116. Charras, G. & Sahai, E. Physical influences of the extracellular environment on cell migration. *Nat. Rev. Mol. Cell Biol.* **15,** 813–824 (2014).

117. Le, D. M. *et al.* Exploitation of Astrocytes by Glioma Cells to Facilitate Invasiveness : A Mechanism Involving Matrix Metalloproteinase-2 and the Urokinase-Type Plasminogen Activator – Plasmin Cascade. **23,** 4034–4043 (2003).

118. Chuang, J.-Y. *et al.* Glial cell line-derived neurotrophic factor induces cell migration in human oral squamous cell carcinoma. *Oral Oncol.* **49,** 1103–12 (2013).

119. Okada, Y., Eibl, G., Duffy, J. P., Reber, H. A. & Hines, O. J. Glial cell-derived neurotrophic factor upregulates the expression and activation of matrix metalloproteinase-9 in human pancreatic cancer. *Surgery* **134,** 293–299 (2003).

120. Lu, K. V *et al.* VEGF inhibits tumor cell invasion and mesenchymal transition through a MET/VEGFR2 complex. *Cancer Cell* **22,** 21–35 (2012).

121. Pàez-Ribes, M. *et al.* Antiangiogenic therapy elicits malignant progression of tumors to increased local invasion and distant metastasis. *Cancer Cell* **15,** 220–31 (2009).

122. Correa de Sampaio, P. *et al.* A heterogeneous in vitro three dimensional model of tumour-stroma interactions regulating sprouting angiogenesis. *PLoS One* **7,** e30753 (2012).

123. Siveen, K. S. *et al.* Targeting the STAT3 signaling pathway in cancer: role of synthetic and natural inhibitors. *Biochim. Biophys. Acta* **1845,** 136–54 (2014).

124. Kim, J. E., Patel, M., Ruzevick, J., Jackson, C. M. & Lim, M. STAT3 activation in glioblastoma: Biochemical and therapeutic implications. *Cancers (Basel).* **6,** 376–395 (2014).

125. Luwor, R. B., Stylli, S. S. & Kaye, A. H. The role of Stat3 in glioblastoma multiforme. *J. Clin. Neurosci.* **20,** 907–11 (2013).

126. Zammarchi, F. *et al.* Antitumorigenic potential of STAT3 alternative splicing modulation. *Proc. Natl. Acad. Sci.* **108,** 17779–17784 (2011).

127. Lee, H. J. *et al.* Drug resistance via feedback activation of stat3 in oncogene-addicted cancer cells. *Cancer Cell* **26,** 207–221 (2014).

128. Kim, S. Y. *et al.* Role of the IL-6-JAK1-STAT3-Oct-4 pathway in the conversion of non-stem cancer cells into cancer stem-like cells. *Cell. Signal.* **25,** 961–969 (2013).

129. Kim, E. *et al.* Phosphorylation of EZH2 Activates STAT3 Signaling via STAT3 Methylation and Promotes Tumorigenicity of Glioblastoma Stem-like Cells. *Cancer Cell* **23,** 839–852 (2013).

130. Kesanakurti, D., Chetty, C., Rajasekhar Maddirela, D., Gujrati, M. & Rao, J. S. Essential role of cooperative NF-κB and Stat3 recruitment to ICAM-1 intronic consensus elements in the regulation of radiation-induced invasion and migration in glioma. *Oncogene* **32,** 5144–55 (2013).

131. Wei, Z. *et al.* STAT3 interacts with Skp2/p27/p21 pathway to regulate the motility and invasion of gastric cancer cells. *Cell. Signal.* **25,** 931–938 (2013).

132. Lee, Y. & Streuli, C. H. Extracellular Matrix Selectively Modulates the Response of Mammary Epithelial Cells to Different Soluble Signaling Ligands Extracellular Matrix Selectively Modulates the Response of Mammary Epithelial Cells to Different Solub. *J. Biol. Chem.* **274,** 22401–22408 (1999).

133. Shain, K. H. *et al.* B1 integrin adhesion enhances IL-6-mediated STAT3 signaling in myeloma cells: Implications for microenvironment influence on tumor survival and proliferation. *Cancer Res.* **69,** 1009–1015 (2009).

134. Schuringa, J. J., Jonk, L. J., Dokter, W. H., Vellenga, E. & Kruijer, W. Interleukin-6-induced STAT3 transactivation and Ser727 phosphorylation involves Vav, Rac-1 and the kinase SEK-1/MKK-4 as signal transduction components. *Biochem. J.* **347 Pt 1,** 89–96 (2000).

135. Demaria, M., Camporeale, A. & Poli, V. STAT3 and metabolism: How many ways to use a single molecule? *Int. J. Cancer* **135,** 1997–2003 (2014).

136. Senft, C. *et al.* Inhibition of the JAK-2/STAT3 signaling pathway impedes the migratory and invasive potential of human glioblastoma cells. *J. Neurooncol.* **101,** 393–403 (2011).

137. Wang, H. *et al.* Targeting interleukin 6 signaling suppresses glioma stem cell survival and tumor growth. *Stem Cells* **27,** 2393–2404 (2009).

138. Tai, C.-I., Schulze, E. N. & Ying, Q.-L. Stat3 signaling regulates embryonic stem cell fate in a dose-dependent manner. *Biol. Open* **3,** 958–65 (2014).

139. Wu, N. *et al.* Cardamonin induces apoptosis by suppressing STAT3 signaling pathway in glioblastoma stem cells. *Tumor Biol.* **36**(12) 9667-9676. (2015).

140. Priester, M. *et al.* Infiltration and Tumor Growth. *Neuro. Oncol.* **15,** 840–52 (2013).

141. Agudelo-garcia, p. a *et al.* glioma cell migration on three-dimensional nanofiber scaffolds is regulated by substrate topography and abolished by inhibition of STAT3 signaling. *Neoplasia* **13,** 831–40 (2011).

VITA

VITA

R. Marisol Herrera-Perez was born in Malaga, Colombia in 1988. She obtained her bachelor degree in Chemical Engineering from the National University of Colombia-Bogota in 2009. In 2012 she received her degree of Master of Science in Chemical Engineering from the National University of Colombia- Bogota and in 2016 her Doctor of Philosophy degree in Agricultural and Biological Engineering from Purdue University.

PUBLICATIONS

PUBLICATIONS

Herrera-Perez, M. Voytik-Harbin, S.L., Rickus J.L. **2015**. Extracellular matrix properties regulate the migratory response of glioblastoma stem cells in 3D culture. *Tissue Engineering Part A*, 21 (19-20).

Jaroch, D.B., Lu, J., Madangopal, R., Stull, N.D., Stensberg, M., Shi, J., Kahn, J., **Herrera-Perez**, R. *et al.* **2013.** Mouse and human islets survive and function after coating by biosilicification. *American Journal of Physiology - Endocrinology and Metabolism*, 305, 1230-1240.